PHOTOGRAPH THIS SHEET

A995186

DTIC ACCESSION NUMBER

LEVEL

INVENTORY

WT-71

DOCUMENT IDENTIFICATION

Sept. 1951

DISTRIBUTION STATEMENT A

Approved for public release;
Distribution Unlimited

DISTRIBUTION STATEMENT

ACCESSION FOR		
NTIS	GRA&I	☒
DTIC	TAB	☐
UNANNOUNCED		☐
JUSTIFICATION		
(Sept. 1951)		
BY		
DISTRIBUTION /		
AVAILABILITY CODES		
DIST	AVAIL AND/OR SPECIAL	
A		

DISTRIBUTION STAMP

Released

DTIC
ELECTE
SEP 21 1983
S D
D

DATE ACCESSIONED

UNANNOUNCED

83 09 21 002

DATE RECEIVED IN DTIC

PHOTOGRAPH THIS SHEET AND RETURN TO DTIC-DDA-2

DTIC FORM OCT 79 70A

DOCUMENT PROCESSING SHEET

[redacted]

[redacted]

UNCLASSIFIED

SHORT TITLE WT-71

Copy 1 A

AD A995186

REGRADED UNCLASSIFIED

BY AUTHORITY OF A6 23/74 (AC6 G

BY [illegible]

OPERATION GREENHOUSE

SCIENTIFIC DIRECTOR'S REPORT

ANNEX 4.6 ATMOSPHERIC CONDUCTIVITY

[redacted]

NUCLEAR EXPLOSIONS

1951

Statement A
Approved for public release;
Distribution unlimited

~~Classification (Cancelled) (Changed to ~~

By Authority of JT Bev Doe(DNA) & DOD(DNA)

By [illegible] Date 30 Aug 83

[redacted]

UNCLASSIFIED [redacted]

[redacted]

UNCLASSIFIED

This document consists of 96 plus 4 pages
(counting preliminary pages)

No. 1 of 150 copies, Series A

Scientific Director's Report of Atomic Weapon Tests at Eniwetok, 1951

Annex 4.6

Atmospheric Conductivity

[redacted]

UNCLASSIFIED

[redacted]

FC/0951001

[redacted]

UNCLASSIFIED

Distribution

	Copy
DEPARTMENT OF DEFENSE	
Armed Forces Special Weapons Project (Sandia)	1–3
Armed Forces Special Weapons Project (Washington)	4–15
ARMY	
Army Field Forces	16
Assistant Chief of Staff, G-3	17
Assistant Chief of Staff, G-4	18–19
Chief Signal Officer	20–23
Chief of Engineers	24–25
Chief of Ordnance	26–27
Operations Research Office (Johns Hopkins University)	28–29
NAV[redacted]	
Bureau of Aeronautics	30
Bureau of Ships	[redacted]
Chief of Naval Operations	[redacted]
Chief of Naval Research	[redacted]
AIR FORCE	
Air Force Cambridge Re[redacted] Center	[redacted]
Air Research and Develop[redacted] Command	35–38
Air Targets Division, Dir[redacted] of Intelligence (Phys. Vul[redacted])	39–40
Assistant for Atomic Energy	41–42
Assistant for Development Planning	43
Assistant for Materiel Program Control	44
Deputy Chief of Staff for Development (AFDRD)	45

	Copy
AIR FORCE	
Director of Operations (Operations Analysis Division)	46
Director of Plans (AFOPD-P1)	47
Director of Requirements	48–49
Director of Research and Development	50–51
Eglin Air Force Base, Air Proving Ground	52–53
Ent Air Force Base, Air Defense Command	54–55
Kirtland Air Force Base, Special Weapons Center	56–58
Langley Air Force Base, Tactical Air Command	59–60
Maxwell Air Force Base, Air [redacted]	61–62
[redacted] Air Force Base, Strategic [redacted]	63–65
[redacted] apons Squadron	66
Rand Corporation	67–68
[redacted] Air Force Base, Air Training Command	69–70
Wright Air Development Center	71–73
[redacted] iel Command	74–75
ATOMIC ENERGY COMMISSION	
Atomic Energy Commission, Washing[redacted]	76–78
Los Alamos Scientific Laboratory, Report Library	79–83
Sandia Corporation	84–85
Technical Information Service, Oak Ridge (surplus)	86–149
Weapon Test Reports Group, TIS	150

UNCLASSIFIED [redacted]

[redacted]

UNCLASSIFIED

ATMOSPHERIC CONDUCTIVITY

by

SAMUEL C. CORONITI
Geophysics Research Division
Air Force Cambridge Research Center

G. R. WAIT
Carnegie Institution

A. J. PARZIALE
Geophysics Research Division
Air Force Cambridge Research Center

Assisted by

LT COL J. B. McKENZIE, A. NAZAREK, G. A. FAUCHER, and LT F. KNAUSS
Atmospheric Electricity Section, Atmospheric Physics Laboratory
Air Force Cambridge Research Center

Approved by: PETER H. WYCKOFF
Director, Program 4

Approved by: ALVIN C. GRAVES
Scientific Director

Air Force Cambridge Research Center
Cambridge, Massachusetts
September 1951

UNCLASSIFIED

[redacted]

[redacted]

UNCLASSIFIED

UNCLASSIFIED

[redacted]

UNCLASSIFIED

Acknowledgments

The scientific instruments used on this Project were installed in the two B-50 and two L-13 aircraft by the Component and System Division of Wright-Patterson Air Force Base, Dayton, Ohio. The military personnel associated with the operation and maintenance of the B-50A aircraft came from Griffiss Air Force Base, Rome, N. Y. The military personnel associated with the L-13 aircraft came from Task Group 3.4.

UNCLASSIFIED

UNCLASSIFIED

UNCLASSIFIED

[redacted]

UNCLASSIFIED

CONTENTS

	Page
ACKNOWLEDGMENTS	v
ABSTRACT	1
CHAPTER 1 INTRODUCTION	3
1.1 Purpose	3
1.2 Historical Background	3
1.3 Basic Theory	3
1.3.1 Scientific Data	3
1.3.2 Relation between Units	5
1.3.3 Military Data	5
1.3.4 Summary of Problems	6
CHAPTER 2 EXPERIMENTAL PROCEDURE	7
2.1 Method	7
2.1.1 Conductivity Measurements in and around Radioactive Clouds	7
2.1.2 Ground-contour Measurements	7
2.2 Description of Apparatus	8
2.2.1 B-50 Aircraft	8
2.2.2 L-13 Aircraft	10
CHAPTER 3 TEST RESULTS	11
3.1 Disposition of Radioactive Material in the Cloud	11
3.2 Minute Particles from Combustion Processes	12
3.2.1 Ratio of Charged to Uncharged Particles from Combustion Processes	13
3.2.2 Minute Particles Produced in an Atomic Explosion	13
3.2.3 Minute Radioactive Particles Produced by an Atomic Explosion	13
3.2.4 Multiply Charged Large Ions in a Radioactive Cloud	14
3.3 Filter Efficiency	15
3.3.1 Efficiency Derived from Conductivity Values and Filter-paper Counts	15
3.3.2 Increase in Filter Efficiency with Time	16
3.3.3 Filter Efficiency beyond Boundaries of Radioactive Cloud	17
3.4 Over-all Movement of the Cloud	17

UNCLASSIFIED

[redacted]

CONTENTS (Continued)

Page

3.5 Magnitude of Fall-out from an Atomic Cloud at and near the Shot Islands . . . 19
3.5.1 Comparison between Conductivity and Radiac Values . . . 20
3.5.2 Dog Shot . . . 20
3.5.3 Easy Shot . . . 22
3.5.4 George Shot . . . 25
3.6 Shot-island Survey . . . 28
3.7 Decay Rates of Accumulated Fall-out and Increased Radiation . . . 29

CHAPTER 4 CONCLUSIONS . . . 33

ILLUSTRATIONS

CHAPTER 2 EXPERIMENTAL PROCEDURE

2.1 Location of the Three Main Electrometer Amplifiers . . . 35
2.2 Three Brown Electronik Recorders . . . 36
2.3 The Field-meter Brush Recorder . . . 37
2.4 B-50 Main Control Junction Panel Showing Location of Air-meter Indicators . . . 38
2.5 Location of the Statham Transducers . . . 39
2.6 The Consolidated Recording Oscillograph . . . 40
2.7 Junction Box for the Consolidated Recorder . . . 41
2.8 Particle Filter . . . 42
2.9 L-13 Conductivity Chamber . . . 43

CHAPTER 3 TEST RESULTS

3.1 Measured Values of Large Ions per Cubic Centimeter, N; Small Ions per Cubic Centimeter, n; and Calculated Values of Ions per Cubic Centimeter per Second, q (Easy Shot, 1031–1041 and 1026–1036 Hours) . 44
3.2 Measured Values of Large Ions per Cubic Centimeter, N; Small Ions per Cubic Centimeter, n; and Calculated Values of Ions per Cubic Centimeter per Second, q (Easy Shot, 1049–1059 and 1039–1049 Hours) . 45
3.3 Measured Values of Large Ions per Cubic Centimeter, N; Small Ions per Cubic Centimeter, n; and Calculated Values of Ions per Cubic Centimeter per Second, q (Easy Shot, 1149–1159 and 1124–1134 Hours) . 46
3.4 Measured Values of Large Ions per Cubic Centimeter, N; Small Ions per Cubic Centimeter, n; and Calculated Values of Ions per Cubic Centimeter per Second, q (Easy Shot, 1346–1356 and 1208–1218 Hours) . 47
3.5 Measured Values of Large Ions per Cubic Centimeter, N; Small Ions per Cubic Centimeter, n; and Calculated Values of Ions per Cubic Centimeter per Second, q (Dog Shot, 1109–1119 and 1130–1140 Hours) . 48
3.6 Measured Values of Large Ions per Cubic Centimeter, N; Small Ions per Cubic Centimeter, n; and Calculated Values of Ions per Cubic Centimeter per Second, q (Dog Shot, 1142–1152 and 1221–1231 Hours) . 49

[redacted]

ILLUSTRATIONS (Continued)

Page

3.7 Measured Values of Large Ions per Cubic Centimeter, N; Small Ions per Cubic Centimeter, n; and Calculated Values of Ions per Cubic Centimeter per Second, q (Dog Shot, 1230–1240 and 1258–1308 Hours) . 50
3.8 Measured Values of Large Ions per Cubic Centimeter, N; Small Ions per Cubic Centimeter, n; and Calculated Values of Ions per Cubic Centimeter per Second, q (Dog Shot, 1502–1512 and 1521–1531 Hours) . 51
3.9 Measured Values of Large Ions per Cubic Centimeter, N; Small Ions per Cubic Centimeter, n; and Calculated Values of Ions per Cubic Centimeter per Second, q (Dog Shot, 1608–1618 and 1617–1627 Hours) . 52
3.10 Measured Values of Large Ions per Cubic Centimeter, N; Small Ions per Cubic Centimeter, n; and Calculated Values of Ions per Cubic Centimeter per Second, q (Dog Shot, 1242–1252 and 1354–1404 Hours) . 53
3.11 Calculated Values of Ions per Cubic Centimeter per Second, q, vs Time (Dog Shot, H+52 to H+60) 54
3.12 Plot for Obtaining K, the Quantity of Radioactive Matter per Large-ion Particle, from the Relation $KN = \alpha n^2 + 2\eta Nn = q$ (Easy Shot, 21 Apr. 51) 55
3.13 Variation with Time of Filter Efficiency Due to Agglomeration between Radioactive Particles of Micron Size and Large-ion Size 56
3.14 Flight Path for Dog Shot, H+2 to H+11 Hr 57
3.15 Flight Path for Dog Shot, H+24 to H+30 Hr 58
3.16 Flight Path for Dog Shot, H+52 to H+60 Hr 59
3.17 Flight Paths for Easy Shot 60
3.18 Cloud Positions at 25,000 Ft Predicted from Observed Winds at That Altitude (Easy Shot) 61
3.19 Cloud Positions at 35,000 Ft Predicted from Observed Winds at That Altitude (Easy Shot) 62
3.20 Predicted Cloud Positions at 25,000 Ft Assuming That Vertical Mixing Occurs within the Layer between 25,000 and 40,000 Ft (Easy Shot) 63
3.21 Predicted and Actual Cloud Positions at 25,000 Ft (Easy Shot) 64
3.22 Comparison of Conductivity and Radiac AN/PDR-T1B Counter Readings in Roentgens per Hour for George Shot 65
3.23 Fall-out, Dog Shot, H+10 Hr, Altitude 1000 Ft 66
3.24 Example of Fall-out on Pinnacle near Runit Shot Island at an Altitude of 500 Ft on D+3 Days 67
3.25 Pass through Building Cumulus Cloud, Base 1500 Ft, Height 4500 Ft, near George Shot Island at an Altitude of 3000 Ft on G-Day, H+6 Hr 68
3.26 Contour Maps of Radioactivity over Runit Shot Island at Various Altitudes on D+3 Days 69
3.27 Contour Maps of Radioactivity over Engebi Shot Island at Altitude of 500 Ft for Different Times 70
3.28 Contour Maps of Radioactivity over Shot Island at Various Altitudes on G-Day, H+6 Hr 71
3.29 Contour Maps of Radioactivity over Shot Island at Lower Altitudes on G+7 Days 72

[redacted]

[redacted]

ILLUSTRATIONS (Continued)

Page

3.30 Decline in Activity Due to Decay of Induced Radiation and Fall-out Material from Conductivity Measurements at Certain Fixed Altitudes over Shot and Adjacent Islands (Dog Shot, 1000 Ft) 73
3.31 Decline in Activity Due to Decay of Induced Radiation and Fall-out Material from Conductivity Measurements at Certain Fixed Altitudes over Shot and Adjacent Islands (Dog Shot) 74
3.32 Decline in Activity Due to Decay of Induced Radiation and Fall-out Material from Conductivity Measurements at Certain Fixed Altitudes over Shot and Adjacent Islands (Dog Shot) 75
3.33 Decline in Activity Due to Decay of Induced Radiation and Fall-out Material from Conductivity Measurements at Certain Fixed Altitudes over Shot and Adjacent Islands (George Shot) 76
3.34 Decline in Activity Due to Decay of Induced Radiation and Fall-out Material from Conductivity Measurements at Certain Fixed Altitudes over Shot and Adjacent Islands (George Shot) 77
3.35 Decline in Activity Due to Decay of Induced Radiation and Fall-out Material from Conductivity Measurements at Certain Fixed Altitudes over Shot and Adjacent Islands (George Shot) 78
3.36 Decline in Activity Due to Decay of Induced Radiation and Fall-out Material from Conductivity Measurements at Certain Fixed Altitudes over Shot and Adjacent Islands (Easy Shot, 500 Ft) 79
3.37 Decline . . Activity Due to Decay of Induced Radiation and Fall-out Material from Conductivity Measurements at Certain Fixed Altitudes over Shot and Adjacent Islands (Easy Shot, 500 Ft) 80
3.38 Decline in Activity Due to Decay of Induced Radiation and Fall-out Material from Conductivity Measurements at Certain Fixed Altitudes over Shot and Adjacent Islands (Easy Shot, 500 Ft) 81
3.39 Decline in Activity Due to Decay of Induced Radiation and Fall-out Material from Conductivity Measurements at Certain Fixed Altitudes over Shot and Adjacent Islands (Easy Shot) 82
3.40 Decline in Activity Due to Decay of Induced Radiation and Fall-out Material from Conductivity Measurements at Certain Fixed Altitudes over Shot and Adjacent Islands (Easy Shot) 83

TABLES

CHAPTER 1 INTRODUCTION

1.1 Relations Used in Calculations 5

CHAPTER 3 TEST RESULTS

3.1 Space and Time Variation of Conductivity at Edge of Cloud 12
3.2 Comparison of K Values 14
3.3 Comparison of Small-ion Production 16
3.4 Motion of Cloud at 25,000 Ft 18
3.5 Measured and Required Winds at 25,000 Ft 18

[redacted]

[redacted]

TABLES (Continued)

		Page
3.6	Fall-out, Dog Shot	21
3.7	Ground-radex Atoll Survey	23
3.8	Fall-out and Induced Radioactivity on Islands, Apr. 21, 1951, As Deduced from Conductivity Measurements at 500 Ft	24
3.9	Comparison of Radioactivity on Islands As Computed from Conductivity Q_x with That Observed with Radex Q_r	24
3.10	Fall-out, Easy Shot	26
3.11	Fall-out, George Shot	27
3.12	Relative Proportions of Components in Fall-out of Easy Shot Determined from Normal Decay Curves	31

[redacted]

Abstract

Investigations on this Project were restricted to two phases: one consisted in measurements on air conductivity (both signs) and large-ion content (one sign) of air within an atomic cloud, and the other consisted in measurements of air conductivity (one sign) above the shot island and adjacent islands.

The purposes of the first phase were to obtain information on the following points:

1. Disposition of radioactive matter in an atomic cloud, and on the physical and electrical characteristics of particles composing the cloud.

2. Over-all movement, both horizontal and vertical, of an atomic cloud.

3. Efficiency of mechanical filters for the collection of radioactive material composing an atomic cloud.

The purposes of the second phase were to obtain information concerning the following:

1. Magnitude of fall-out and its relation to the direction and velocity of the wind.

2. Rate of radioactive decay of fall-out material on adjacent islands.

Information was obtained on all these points, and a discussion of each is embodied in this volume.

[redacted]

Chapter 1

Introduction

1.1 PURPOSE

The primary purpose of the air-conductivity measurements was to obtain information on the following:

1. Disposition of radioactive material in an atomic cloud originating from an atomic explosion.
2. Characteristics, both physical and electrical, of particles composing an atomic cloud.
3. Efficiency of the mechanical filters for the collection of radioactive material composing an atomic cloud.
4. Over-all movement, both horizontal and vertical, of an atomic cloud during the first few days after formation.
5. Magnitude of fall-out from an atomic cloud at and near the shot island.
6. Pattern of fall-out in the vicinity of the shot island and the relation between such a pattern and direction and velocity of the wind.
7. Rate of radioactive decay for material.

1.2 HISTORICAL BACKGROUND

Coulomb[1] first pointed out the possibility of electrical conductivity in air. It remained, however, for Elster and Seitel[2] and for Wilson[3] to prove that this conductivity actually exists and is due to the presence of ions in the air. Ions, which are electrically charged particles, exist in the lower atmosphere in several different size groups. The group having the smallest radius (small ions) consists of air molecules, which are generally found in concentrations of less than 1000 per cubic centimeter, except at increased altitudes or under unusual circumstances. Another important group (large or Langevin ions) consists of the well-known condensation nuclei (radius 10^{-6} cm) with an electric charge. These ions are found over land in concentrations of several thousand per cubic centimeter, particularly in regions of considerable industrial activity, since they are copiously produced by any combustion or vaporization process. Observations on the concentrations over the ocean areas are almost lacking, but based on observations of the concentration of condensation nuclei and the electrical conductivity of the lower atmosphere, carried out by the Carnegie Institution of Washington,[4] concentrations of more than a few hundred large ions per cubic centimeter are seldom present at the lowest altitudes over the ocean. There are generally other groups of ions present in the atmosphere but ordinarily in relatively small concentrations, and thus they play a minor role in the determination of the total conductivity of the air.

1.3 BASIC THEORY

1.3.1 Scientific Data

The conductivity of the air due to any particular group of ions is equal to the product of the total electronic charge per ion, the mobility (velocity due to a unit electric field), and the ionic concentration. The unipolar conductivity λ is given by the equation

$$\lambda = nek \tag{1.1}$$

where n is the number of ions per cubic centimeter in this group, k is the mobility in centimeters per second per unit field intensity, and

[redacted]

[redacted]

e is the electronic charge per ion. At normal temperature and pressure the value of k for small ions is around 1.5 cm/sec/volt/cm, while that for the large ion is about 3×10^{-4} cm/sec/volt/cm. In order to contribute as much to the conductivity as the small ions, the large ions would thus need to be 5000 times as numerous as the small ions. This is never the case except under very exceptional circumstances which need not be discussed at this time.

Any factor which affects the small-ion content of the atmosphere will produce a corresponding effect on the conductivity of the air, as indicated by the relation shown in Eq. 1.1. In any volume of air, particularly during normal fair-weather conditions, the number of small ions per cubic centimeter in the atmosphere will depend on the two factors: the rate of production and the rate of destruction. Small ions are produced in the atmosphere by cosmic rays and by radiations from radioactive matter in the soil and in the air. These ions are destroyed principally in three ways: by recombination with a small ion of opposite sign; by combination with a large ion of opposite sign, which results in an uncharged condensation nucleus; and by combination with uncharged condensation nuclei, which results in the formation of a large ion of that particular sign. This matter appears to have been considered first by McClelland and Kennedy[5] and somewhat later by Schweidler.[6] Further considerations were made by Nolan, Boylan, and de Sachy[7] and by Nolan and de Sachy.[8] This matter has been discussed in considerable detail by Gish.[9]

For equilibrium conditions between production and destruction of small ions in the atmosphere and on the basis of certain simplifying assumptions,[8,9] the relation between the rate of production and the rate of destruction of small ions is given by the equation

$$q = \alpha n^2 + 2\eta N n \qquad (1.2)$$

where q = the rate of small-ion production (rate of ionization) in the atmosphere

n and N = the concentration of small and large ions of one sign, respectively, in the atmosphere

α = the coefficient of recombination between small ions of opposite sign

η = the combination coefficient between small ions and large ions

The term representing the combination process between small ions and uncharged condensation nuclei is incorporated in the last term of Eq. 1.2.

In view of the relations expressed in Eq. 1.1 between λ and n and in Eq. 1.2 between q and n, it is obvious that any increase in the ionization will result in an increase in the conductivity of the atmosphere, unless it is accompanied by an even greater increase in the value of N. Since it was well known that an increase in the radioactive content of the atmosphere will result from an atomic blast and that any increase in the radioactive content of the air will result in an increase in the rate of ionization of the air, it seemed promising to utilize conductivity determinations for obtaining estimates of the quantity of radioactive matter present. Such a project was undertaken by Gish and Wait in connection with Operation Sandstone. It was amply demonstrated in these tests that the conductivity equipment is practical for locating a radioactive cloud and for obtaining cross-sectional profiles of such a cloud. The rate of ionization q from which the quantity of radioactive matter might be deduced could be obtained in only an approximate manner, owing to the fact that no measurement of large-ion concentration was carried out. It is surmised that condensation nuclei will be formed in great abundance in the production of an atomic cloud. It therefore appeared doubtful that the large-ion concentration in such a cloud could be considered negligible in computing the rate of ionization from values of conductivity. There were disadvantages also in measuring the conductivity, one being a relatively large drift in the zero and another being the type of recording employed. It was apparent that these two disadvantages should be corrected in any instrument employed in aircraft measurement of conductivity. The required improvements were effected by the development of a stable amplifier system which would operate a pen-and-ink recorder. This was carried out[10] by the Applied Physics Corporation, 30 W. Green St., Pasadena, Calif., under AF Contract No. AF19(122)-106.

The Geophysical Research Directorate of the Air Force Cambridge Research Laboratories was requested by the Air Force Office for Atomic Energy[11] (AFOAT) to make meas-

[redacted]

urements of background atmospheric conductivity over the ocean and over land at all possible altitudes which could be reached by aircraft. For the past 2 years, members of the Atmospheric Physics Laboratory of the Air Force Cambridge Research Laboratories have been investigating these and other problems, making use of the newly improved Model 33A electrometer installed on a B-17 aircraft[12] (No. 8635). During March and April of 1950 the conductivity equipment on the B-17 was employed in tests conducted by the Los Alamos Scientific Laboratory, Los Alamos, N. Mex. The purpose of the tests was to ascertain the efficiency of the equipment in detecting and in tracking radioactive clouds produced by a simulated bomb explosion and also in measuring the fall-out of radioactive products.[13] In July of the same year,[14] tests were conducted at Los Alamos to detect gamma radiation from a 300-curie source. Results from these and other experiments support the conclusion that the instrument has military application when used under proper conditions.

1.3.2 Relation between Units

The unit employed for the measurement of gamma radiation is the roentgen (r) and is defined as the amount of gamma (or X) radiation which produces, in 0.001293 g of dry air, ions carrying 1 esu of electricity of either sign. If q_0 represents the rate of ion production (in ion pairs per cubic centimeter per second) due to gamma radiation, then the relation at NTP between the number of milliroentgens per hour (mr/hr) and the rate of ionization is given by the equation

$$\text{mr/hr} = 1.72 \times 10^{-3}\, q_0 \qquad (1.3)$$

Likewise, for equilibrium conditions of small ions there exists a definite relation between n, the number of small ions per cubic centimeter (in the absence of condensation nuclei), and the number of milliroentgens, which is given by the equation

$$\text{mr} = 2.76 \times 10^{-9}\, n^2 \qquad (1.4)$$

These and other relations which may prove useful in connection with this volume are summarized in Table 1.1 at NTP and for average conditions at 25,000 ft altitude.

TABLE 1.1 RELATIONS USED IN CALCULATIONS*

At NTP	At 25,000 Ft Altitude
$\text{mr/hr} = 1.72 \times 10^{-3}\, q_0$	$\text{mr/hr} = 4.44 \times 10^{-3}\, q$
$\text{mr/hr} = 2.76 \times 10^{-9}\, n^2$	$\text{mr/hr} = 8.89 \times 10^{-9}\, n^2$
$q_0 = 1.6 \times 10^{-6}\, n^2$	$q = 2.0 \times 10^{-6}\, n^2$
$n = 4.65 \times 10^{6}\, \lambda$	$n = 2.11 \times 10^{6}\, \lambda$
$\lambda = 2.9 \times 10^{-6}$ mv	$\lambda = 2.9 \times 10^{-6}$ mv

*Relations between milliroentgens per hour, rate of small-ion production q per cubic centimeter per second, small-ion concentration n, conductivity λ in electrostatic units of the air, and the millivolt deflection of the conductivity meter are given.

1.3.3 Military Data

In the defensive or offensive use of atomic explosions the detection, intensity, and spatial distributions of radioactive particles are of vital importance. It is necessary to know the facts concerning these in order to safeguard the health and life of civilian and military personnel.

From the discussion in Sec. 1.3.1 it is apparent that atmospheric conductivity is a measure of the concentration of small ions within a given volume of air. It is an indirect measure of the total ionization due to radioactivity. Essentially it is a measure of the effect of radioactivity. Ten seconds after an atomic detonation the emission of gamma rays accompanying fission will have ceased.[15] The fission products present will still give off beta and gamma rays, which are instrumental in the productions of ions which, in turn, are detected and counted by the conductivity meter. The size and the shape of an atomic cloud and some qualitative information on the intensity within the cloud can be determined by measuring the concentration of small and large ions. Logically, therefore, the radioactive cloud can be tracked until the intensity of radioactivity has been reduced to a value which falls below the detection capabilities of the conductivity meter. The detection is dependent on meteorological parameters such as winds, turbulence, and convection currents.

Immediately after an explosion the radioactive-contaminated dirt particles and the radioactive metallic oxides gradually fall back

[redacted]

to the earth. The distribution and strength of these fall-out particles can be determined and computed by measuring the conductivity over the area. The resolution of the contours will depend largely on the altitude at which the measurements were made. At altitudes of 50 to 200 ft the resolution will be extremely good, whereas at greater altitudes it will be poor.

The nature of the radioactive characteristics of the fall-out particles can be determined by measuring the conductivity at a fixed altitude over a given area at various intervals of time. The decrease in conductivity with time is related to the decrease of radioactivity and thence to radioactive decay.

1.3.4 Summary of Problems

The data obtained by these tests will be analyzed, and empirical relations between the various parameters will be developed. Whenever possible a mathematical theory will be developed. The problems discussed in Secs. 1.3.1 and 1.3.2 are summarized as follows:

1. Determine the small-ion and large-ion conductivity at fringes of the radioactive cloud at an altitude of 25,000 ft and at various times.
2. Compute the corresponding numbers of small and large ions and also compute the number of ions produced per cubic centimeter.
3. Determine the recombination and attachment coefficients of ions.
4. Correlate the various conductivity measurements with the size of the radioactive particles.
5. Compute the efficiency of mechanical filter paper for the collection of radioactive material.
6. Determine the fall-out pattern of radioactivity over the shot and contiguous islands.
7. At a given instant compute the intensity of radioactivity on the ground.
8. Determine the nature and characteristics of the fall-out particles.
9. Determine the diameter and shape of the ionic sheet around the cloud.

REFERENCES

1. C. A. de Coulomb, Mem. Acad. Paris, 616 (1795).
2. Elster and Seitel, Physik Z., 1: 245 (1899).
3. C. T. R. Wilson, Proc. Cambridge Phil. Soc., 11: 32 (1900).
4. Scientific Results of Cruise VII of the Magnetic-survey Yacht, 1928-1929, Carnegie Inst. Wash. Pub., 568 (1946).
5. J. A. McClelland and H. Kennedy, Proc. Roy. Irish Acad., A30: 72-91 (1912); A32: 1-6 (1913).
6. E. von Schweidler, Sitzber. Akad. Wiss. Wien, Math. naturw. Klasse, Abt. IIa, 27: 952-967 (1918).
7. J. J. Nolan, R. K. Boylan, and G. P. de Sachy, Proc. Roy. Irish Acad., A37: 1-2 (1925).
8. J. J. Nolan and G. P. de Sachy, Proc. Roy. Irish Acad., A37: 71-94 (1927).
9. J. A. Fleming, "Terrestrial Magnetism and Electricity," pp. 182-252, Dover Publications, Inc., New York, 1949.
10. Applied Physics Corporation, Instruction Manual for Vibrating Reed Electrometers, Model 33A.
11. AFOAT-1 Project No. W/62/N/AMC.
12. S. C. Coroniti et al., Report on Study of Atmospheric Conductivity, Geophysical Research Directorate, Air Force Cambridge Research Laboratories, Cambridge, Mass., Sept. 6, 1950.
13. S. C. Coroniti, Report on Atmospheric Electrical Conductivity Tests Conducted in the Vicinity of Los Alamos Scientific Laboratories, Report CRL-0014, May 26, 1950.
14. S. C. Coroniti and J. B. McKenzie, Report on Radiation Tests Conducted at Los Alamos, Report CRL-0200, July 19, 1950.
15. Los Alamos Scientific Laboratory, "The Effects of Atomic Weapons," Sec. 2.16, p. 29, U. S. Government Printing Office, Washington, 1950.

[redacted]

[redacted]

Chapter 2

Experimental Procedure

2.1 METHOD

2.1.1 Conductivity Measurements in and around Radioactive Clouds

It was originally proposed to measure both vertical and horizontal contours of the cloud. However, it was realized, after some experience, that the cloud was too extensive to permit more than horizontal contour measurements, with the time of flight limited by fuel consumption. Consequently all the information given here was obtained from measurements at an altitude of about 25,000 ft, except for background flights before and after the periods of the atomic blast. The times of measurement extend anywhere from H+4 hr up to H+80 hr.

Owing to the very irregular shape of the cloud and lack of knowledge as to its location until after the contour was completed, the manner in which the aircraft approached the cloud depended mainly on the instantaneous readings of the instruments and on chance. Foremost in the mind of the operator was to avoid flying too far into regions of high radioactive intensity, which could result in contamination of the aircraft and thereby jeopardize the measurements. It was therefore established that, as soon as a certain arbitrarily chosen maximum value of conductivity was reached, the aircraft would turn out. The angle of turn-out was determined by the intensities reached during previous contacts with the cloud. The interval between contacts was such as to provide enough time to reestablish normal background readings and check the instruments' zero in a normal, clear atmosphere. This procedure was used in tracking the cloud around its edges until the available flying time of the aircraft was consumed. In one or two instances it was possible to encircle the cloud or patch of cloud that was contacted. In general the flights were separated by 24-hr intervals with the first starting at H+4 hr. The flights numbered no more than three for each atomic explosion and lasted from 6 to 10 hr each. The reader should keep in mind the fact that what is referred to as the "cloud" in this volume is the first large patch of radioactivity encountered in each flight. The location of the cloud was predicted before each flight from winds and previous contacts. It was known that usually more than one large patch, or cloud, existed at any given altitude. However, there was sufficient time to cover only one large patch in a single flight.

2.1.2 Ground-contour Measurements

An L-13 single-engine aircraft was used for measurement of ground contours, i.e., radioactive intensity on the ground as determined by measurements of air conductivity. The aircraft traveled at a speed of about 90 mph. Measurements were made by a conductivity meter mounted under the wing of the aircraft away from the tip of the propeller.

The type of pattern flown varied with the island. Orthogonal grids spaced about 400 to 500 yd from each other were flown over the shot islands. This same pattern was repeated at various altitudes ranging from 50 to 4000 ft. Over all nonshot islands a single pass at each altitude was made. The grid survey over the shot islands started at D+3 days for Dog, E+10 hr for Easy, and G+6 hr for George. Normal survey flights over the other atoll islands started from 8 to 12 hr after the time of blast,

[redacted]

[redacted]

and the same flights were repeated almost every 24 hr up to 10 days after the blast.

During George measurements a radiac training set, AN/PDR-T1, which measures gamma-ray intensities, was carried in the L-13. The readings were noted and recorded every minute. The conductivity values were recorded continuously on a Brown Electronik recorder.

2.2 DESCRIPTION OF APPARATUS

2.2.1 B-50 Aircraft

The instrumentation on B-50-017 was identical in all respects with that on B-50-023; therefore a description of the special equipment on one aircraft will be sufficient for the purpose of this volume.

All measuring apparatus on the aircraft centered about three main detection chambers. These chambers measured the positive small-ion conductivity, negative small-ion conductivity, and large-ion concentration in the air. Each of these chambers measures the above-mentioned electrical characteristics of the atmosphere by sampling the outside air in the electrostatic field between its probe and cylinder. The sampled air enters the intakes of three separate ducts leading to the three chambers. One of the intakes is located on the top of the aircraft about 12 ft forward of the engine propellers. This duct enters the aircraft at the forward nonpressurized bomb bay and continues to the small-ion chamber in the same bomb bay. The other two intakes are located on top of the fuselage between the two bomb bays and continue to the two chambers in the rear bomb bay. The length of each duct is approximately 14 ft, and the diameter of each is 2 in. Since the small-ion chambers have 4-in.-diameter openings, they require a funnel section for matching into the 2-in.-diameter duct. This change in cross-sectional areas is accomplished gradually along the length of the funnel (about 2 ft) to minimize turbulent air flow and realize conditions for measuring ohmic conductivity of the air. The large-ion chamber is preceded by a 4-in.-diameter electronic precipitator which is used to filter out all the small ions in the air before it enters the large-ion chamber for large-ion count. The output of the 4-in. precipitator, which is about 18 in. long, is matched to the 2½-in.-diameter opening with a reducer of the same type described above. A gate valve is placed at the terminating end of each 2-in. duct to shut out air flow in flight.

Each of the chambers has a preamplifier mounted on it. The preamplifier consists mainly of two high-input resistors, a vibrating-reed capacitor, and a stage of amplification. The conductivity current collected by the chamber probe registers a signal voltage across a high-input resistor. The signal is then impressed on a carrier wave by the use of the vibrating-reed capacitor. After passing through three stages of voltage amplification the signal is transmitted from the preamplifier to the main amplifier through a 30-ft cable (see Fig. 2.1).

The main amplifier, located at the operator's position in the rear pressurized cabin, uses feedback control for improved stability and a lower over-all system time constant. It also contains a phase-sensitive demodulator in cascade with its direct channel. This permits measuring either sign of conductivity while still retaining the advantages of a-c amplification. On the front panel, each amplifier has the means for switching scales through a factor of 10^6 in seven steps and also for zeroing and reversing meter readings.

A thermocouple air meter is placed at the output of each of the chambers to measure air velocity through the system. Measurement of air velocity is important for proper determination of large-ion concentration but should not be necessary for conductivity measurements if the velocity is above the critical value determined by the voltage applied to the probe. The critical value in the present case is 2½ mph. The air-meter indicators are located in the first three positions from left to right of the bottom row of meters at the operator's position as shown in Fig. 2.4. Figures 2.1 and 2.2 show the location of the conductivity electrometers and recorders, respectively.

In addition to conductivity and large-ion concentration measurements it was originally planned to obtain qualitative records of gamma-ray intensity and condensation-nuclei concentration. Instruments for measuring these, however, did not operate successfully.

With the complete instrumentation system, records of the following elements were obtained: static-air temperature, relative humid-

[redacted]

ity or water content, pressure deduced from altitude indicators, electrostatic fields resulting from precipitation charge on the aircraft and external fields, and the true air speed and manifold pressure of the aircraft. This additional information makes possible the derivation of other atmospheric characteristics and correlations known to exist among the various functions.

The electric fields are measured and recorded by two rotating field-meter heads which are mounted on the outside skin of the aircraft. Insulated plates are alternately shielded and unshielded by the rotating vanes so that an a-c signal, proportional to the field, is induced on the plates. The signal is amplified, rectified, and then recorded on a Brush pen recorder (shown at the top of Fig. 2.3) located behind the operator with its controls on the operator's panel. By using two field-meter heads the vertical component of any external field can be determined in addition to the field produced by charge accumulated on the surface of the plane.

Temperature and humidity are measured with a probe which contains a thermal resistance and a carbon cell, the resistance of which varies with moisture absorbed. These signals are amplified and recorded on an aerograph recorder. The aerograph is located directly behind the operator's position.

Visual indicators of temperature, true air speed, altitude, manifold pressure, and bottle pressure, which will be discussed later, are located in the next to the top row of instruments on the operator's panel shown in Fig. 2.4. These are connected to the aircraft lines in the same way as the pilot's instruments. The bottle-pressure indicator is used to determine the pressure of air samples in the bottles, which will be filled by a compressor. Air speed, altitude, and manifold-pressure signals are also picked up by three additional instruments. They are Statham transducers, shown in Fig. 2.5, which convert the various pressure signals to electrical signals with the use of diaphragms and strain-gauge bridges. The electrical signals are, in turn, recorded on the recording oscillograph. Temperature, in addition to being recorded on the aerograph, is picked up by two additional Lockheed-type temperature probes in a bridge circuit and recorded on the consolidated oscillograph.

All 13 functions mentioned above are recorded simultaneously on a single consolidated recording oscillograph located behind the operator's seat as shown in Fig. 2.6. This recorder has 18 recording channels and 3 reference channels. It makes use of a small galvanometer for each channel. The final signals are in the form of moving light beams which are recorded on a moving photosensitive paper. Impedance-matching circuits, filters, and zero-setting controls for the various functions going into the oscillograph are located in a junction box mounted directly above the oscillograph, as shown in Fig. 2.7. One of the reference channels is used to record the timing pulses from the r-f timing system used to control the complete Greenhouse operation. This timing pulse is also indicated visually on a lamp which is located on the left-hand side of the operator's control panel.

An auxiliary synchronizing system is used for the aircraft's special instrumentation. It consists of a synchronous motor-driven timer which supplies a signal every minute to mark all records simultaneously. The Brown recorders use a relay-controlled marker pen to receive this signal and mark a pip on the edge of the chart. The field-meter recorder picks up the timing signal in its main signal channel since the pen assembly has a very fast time response. The recording oscillograph receives the signal on a special timing lamp which projects a grid line across the width of the photosensitive chart. In addition to the automatic pulses generated every minute the motor-driven timer can be excited manually by a momentary switch at the bottom of the operator's control panel. A coding system will be established for the manual control by which various anomalies can be noted on all records simultaneously.

In addition to instantaneous measurements of atmospheric characteristics, specimens of the atmosphere were taken in flight. This was done in two ways: by filtering out a sample of the larger particles in the air and by obtaining samples of the air in bottles. The larger particles were obtained by allowing the air to pass through filter papers in flight. The particular paper used was furnished by AFOAT-1, 1712 G St., Washington, D. C. The paper is held in place by metal grids located in a large scoop mounted on top of the aircraft as shown in Fig.

[redacted]

2.8. The air samples are compressed into five large metal bottles. A motor-driven pump and the bottles are assembled on a bomb-bay cargo rack, and the rack is mounted in the forward bomb bay of the aircraft.

2.2.2 L-13 Aircraft

The instrumentation on the L-13 aircraft consists of one conductivity chamber and recorder. The conductivity chamber, without housing of any kind, is mounted under the right wing, just above the wing strut of the aircraft as shown in Fig. 2.9. The probe-and-chamber axis is parallel with the normal line of flight of the aircraft and is located 3 to 4 ft away from the propeller extremities.

[redacted]

[redacted]

Chapter 3

Test Results

3.1 DISPOSITION OF RADIOACTIVE MATERIAL IN THE CLOUD

It has been previously mentioned that the approach to the cloud was mainly dependent on chance. To put measurements from different contacts on exactly the same comparative basis would require that all approaches be made at the same angle with the edge of the cloud, that they be made simultaneously, that they extend the same distance into the cloud, that they be correlated with aircraft speed, etc. Such a procedure would obviously have been impractical. However, a comparison of the data, as taken, will give a fair picture of the gradients and peak values of radioactivity with their variations to be expected in the cloud.

The variation of radioactivity with time and distance is shown in Figs. 3.1 to 3.4 for the first day of Easy and in Figs. 3.5 to 3.7 for the first day of Dog Shot for the various contacts with the cloud. On the same graphs are shown the simultaneous variations in large-ion and small-ion concentrations. The correlation between the increase of large and small ions is readily noticeable.

Under normal conditions an increase in large-ion concentration causes a corresponding decrease in small-ion concentration.[1,2] The reason for this lies in the strong tendency for small ions to combine with the large. This additional destructive process causes the number of small ions to diminish until a new equilibrium is reached with the production rate from normal sources. At 25,000 ft the main source of ion production normally is cosmic radiation. From the results obtained in a radioactive cloud it seems that additional sources of ion production are closely associated with the large ions in sufficient quantity not only to replenish the loss of small ions due to their combination with large ions but also to cause an increase in their concentrations. This point will be discussed in greater detail later.

Figure 3.8 and the upper graph of Fig. 3.9 show the normal inverse relation between large and small ions in an atmosphere of very low radioactive intensity. These samples were taken from the flight through the cloud on the third day of Dog Shot. The radioactive intensity during this flight averaged only about 50 per cent above the normal background due to cosmic radiation. The lower graph of Fig. 3.9 and the upper graph of Fig. 3.10 show samples of the flight where inverse and proportional relations between large and small ions directly follow each other. These correspond to intervals when the aircraft passed from a region containing normal large ions to a region containing radioactive large ions.

Graphs of the calculated rate of small-ion production (rate of ionization) will naturally follow the variations in small and large ions, since the values were computed from Eq. 1.2 of Chap. 1. The peak value of activity encountered as derived from rate of ionization was about 2.4 mr/hr, as shown in the upper graph of Fig. 3.2. This is the activity at about 10 miles in from the edge of the cloud on the first day of Easy Shot, where the edge of the cloud was detected by means of the conductivity apparatus, and the activity corresponded to increases of 10^{-2} mr/hr above background. Since the cloud is at least 100 miles deep, much higher values of activity could be expected near its center.

The value of the leading slope of each peak is a measure of the gradient of radioactive intensity on the edge of the cloud. The maximum

[redacted]

gradient encountered showed an increase of 3.54 mr/hr per mile, or 0.33 mr/hr per second, for a true air speed of 335 mph. The minimum turning radius of B-50-type aircraft is about 1 mile, which means that it travels an additional mile in the original direction into the cloud after the time the pilot begins turning out. A list of the gradients and peak values of the more prominent contacts is given in Table 3.1.

TABLE 3.1 SPACE AND TIME VARIATION OF CONDUCTIVITY AT EDGE OF CLOUD

Gradient (mr/hr/mile)	Gradient (mr/hr/sec)	Peak (mr/hr)
1.32	0.12	3.85
1.04	0.10	1.60
1.32	0.12	4.10
2.00	0.19	6.10
3.25	0.30	9.60
1.77	0.17	5.50
0.09	0.01	1.70
3.54	0.33	6.70
1.43	0.13	4.45
2.22	0.21	3.50

From Table 3.1 it is apparent that the peak reading was increased by 30 to 50 per cent before the turn could be completed.

In Figs. 3.1 to 3.10 several instances are noted where minor peaks occur before and after the main peaks. During times on either side of the main peak the aircraft is flying a straight-line course into or out of the cloud. The minor peaks therefore give a fair representation of the small patches of radioactive clouds that exist along the edges of the main cloud. These patches were estimated to vary from 2 to 20 miles or greater in width with peak intensities up to 2 mr/hr. To obtain data on the disposition of radioactive material within the cloud was difficult since these particular measurements were made on the first day of the blast and since it was still too soon to fly through the cloud without the aircraft becoming contaminated. It was possible to fly directly through the cloud on the third day of Dog Shot, however.

A graph of radioactive intensity vs time for the whole flight of the third day of Dog Shot is shown in Fig. 3.11. The small patches of high radioactive intensity no longer exist. The results imply that these patches have diffused and blended to yield extensive regions, as much as 600 to 1000 miles long, over which the intensity is slightly above background. The normal background in this area was found to correspond to a small-ion-production rate between 15 to 20 ions/cc/sec or from 0.067 to 0.09 mr/hr at 25,000 ft. On the third day the intensity reached a peak of 0.25 mr/hr, while the average level in the cloud is about 0.04 mr/hr above normal background.

3.2 MINUTE PARTICLES FROM COMBUSTION PROCESSES

Minute particles of matter are produced in any combustion process. From a study of charged particles formed in this manner it appears that the particles, on being produced, may show a rapid increase in size in some cases because of the condensation of water vapor on the particle. The subsequent increase is thereafter slow and occurs because of recombination processes between oppositely charged particles. The recombination rate is proportional to the product of the number of particles per unit volume of each sign or to the number squared if the positive and negative ions are equal in number. Small-sized particles, because of the relatively large recombination coefficient associated with them, will recombine rapidly as long as they are numerous and small. If not produced continuously, they soon tend to become stabilized in both size and number per unit volume. The diminishing rate of recombination with size will tend to prevent the particle from attaining the 1-μ radius. The following example will illustrate the manner in which the recombination rate of particles and consequently the rate of growth is affected by particle size. The time required for particles to be reduced to 1 per cent of the original number, say from 10^6 to 10^4 per cubic centimeter, assuming zero production, is given below. In the case of ions of molecular diameter the time is 1 min; for ions of 10^{-6} cm diameter the time is 9 hr; and for ions of 1 μ diameter the time is 120 days. In other words, the size of the particle as a result of recombination processes tends to become stabilized

within a short period at diameters considerably less than 1 μ.

3.2.1 Ratio of Charged to Uncharged Particles from Combustion Processes

In many cases electrically charged as well as uncharged particles may originate through combustion processes. In any case, however, the fraction of particles with an electric charge, assuming equilibrium conditions, will eventually be determined not by the number of charged particles originally produced but by the size of the particles. This fraction will be constant as long as the particle size remains constant. In the atmosphere under normal conditions the ratio of number of total particles (charged and uncharged) to the number of uncharged particles, as found in Washington, D. C.,[3-5] is equal to 1.4. This ratio corresponds to an average particle radius[6] of 1.5×10^{-6} cm. The ratio increases as the size of the particle increases to a value of 3.3 for particles of about 3×10^{-6} cm radius or greater.

3.2.2 Minute Particles Produced in an Atomic Explosion

It would be expected that minute particles would be produced in an atomic explosion and that the above discussion would apply equally well to them. It was planned to investigate this matter by suitably designed equipment. The condensation-nuclei content of the air was to be determined by means of a GE recording condensation-nuclei counter. The large-ion content (of a given sign) was to be obtained by means of a specially constructed large-ion apparatus. The small-ion content (both signs) was to be obtained by means of two pieces of conductivity equipment, and a gamma-ray count was to be obtained by means of a scintillation counter. The first- and last-mentioned pieces of equipment failed to function properly so that only values of large-ion and small-ion contents of the air were obtained. These, however, have provided some very useful information. The results have shown that minute particles (around 10^{-6} cm radius) exist in considerable concentrations inside an atomic cloud and must therefore have been produced by the atomic explosion.

3.2.3 Minute Radioactive Particles Produced by an Atomic Explosion

The results on large-ion and small-ion contents of the atomic cloud show not only that considerable concentrations of particles of 10^{-6} cm radius exist but that many of them are radioactive. This view is contrary to that commonly held, and hence evidence relating to this point will be presented in considerable detail.

Before discussing the evidence for the existence of very small radioactive particles, it seems desirable to indicate the diameter of particles normally caught in the large-ion apparatus. Electrically charged particles smaller than about 1×10^{-7} cm radius were not admitted since they were removed with an electrostatic precipitator immediately in front of the apparatus. When the geometry of the apparatus, the voltage applied between central electrode and surrounding cylinder, and the rate of air flow through the equipment are considered, it turns out that, at 25,000 ft altitude, all singly charged particles with a radius between 1×10^{-7} and 2×10^{-6} cm were caught on the electrode system. Only a portion of those with a larger radius will, however, be caught. On an average, 80 per cent of the particles with a radius of 4×10^{-6} cm and 98 per cent with a radius of 2×10^{-5} cm will escape. Therefore the particles caught by the apparatus lie mostly between 1×10^{-7} and 1×10^{-5} cm radius.

Normally, when the large ions are numerous, there exists a reciprocal relation between the variations in large- and small-ion contents of the air, as may be seen from Eq. 1.2. In the derivation of this equation it was assumed that the large ions (as is usually the case) act only to destroy (through combination) the small ions. If large ions were radioactive, such an equation would not be adequate without modification; the large ions would, in effect, be responsible for the production of small ions. Equation 1.2 can, however, be modified by the substitution of a quantity KN for the quantity q, where K is proportional to the average quantity of radioactive matter on each large-ion particle. In other words it represents the average number of small-ion pairs per cubic centimeter per second produced by the radioactive matter composing, or attached to, each large-ion particle.

A graphical analysis of data obtained by flying in and out of an atomic cloud (see Fig. 3.12) shows that the data are consistent with this idea and that Eq. 1.2 must be modified as indicated by

$$K(N - C) = \alpha n^2 + 2\eta Nn \qquad (3.1)$$

The constant C corresponds to a current in the apparatus equivalent to 1000 to 2000 ion pairs per cubic centimeter in the air stream. This could, however, be due to ions produced inside the apparatus by an accumulation of radioactive matter on the electrode system. An analysis of the data has shown that this explanation is correct. The accumulated radioactive matter has been examined for the presence of particles of relatively large size, say of 1 μ radius or larger, by the exposure of a photographic film to the electrode. The results showed no evidence of particles as great as 1 μ in radius, but they did show evidence of radioactive matter in a much more finely divided state. This is regarded as evidence that radioactive material in an atomic cloud may exist on particles much smaller than 1 μ in radius.

The value of the constant K has been obtained from data for three different days (two for Dog, one for Easy Shot). It was thus possible to compare the value of K for two different shots at approximately the same interval after the shot and for the same shot but for two rather widely separate time intervals after the shot. The results are summarized in Table 3.2, together with other pertinent information. The results show that the value of K may differ considerably from one shot to another.

TABLE 3.2 COMPARISON OF K VALUES

Date (1951)	Day	Time Interval	Shot	K
Apr. 8	First	H+7	Dog	0.200
Apr. 10	Third	H+56	Dog	0.017
Apr. 21	First	H+6	Easy	0.375

The value diminished by a factor of more than an order of magnitude between April 8 and 10. If particles did not combine or otherwise gain radioactive matter, a diminution would be expected, owing to the gradual radioactive decay of radioactive matter composing the particles. The rate of diminution in the value of K during these 2 days is precisely that expected because of radioactive decay. The precision with which the value of K can be determined is not high, and more checks on the rate of diminution will be required before it can definitely be concluded that radioactive large ions neither pick up nor lose additional radioactive matter after being formed.

Radioactive matter in the form of particles of a few microns in diameter are known to exist in an atomic cloud. It might be questioned therefore whether the results indicated in the graph of Fig. 3.12 could be accounted for on the basis of a variation in the number per unit volume of such particles. Such an explanation would require a comparatively high correlation between the number of such particles and the number of particles of much smaller diameters such as compose the large ions. An examination of this matter has shown that, in general, a high correlation between the variations in concentrations of these two groups of particles does not exist. On the other hand, very high correlations do exist between large-ion concentrations and between both the small-ion concentrations and ionization of the atmosphere, as may be seen, for example, from the graphs shown in Figs. 3.1 to 3.11. It is accordingly concluded that the variations in the rate of ionization in an atomic cloud cannot be fully accounted for by radioactive particles which are generally caught with a paper filter of the type commonly utilized. This is taken to mean that the rate of ionization in an atomic cloud cannot generally be fully accounted for by radioactive particles of a few microns in diameter.

3.2.4 Multiply Charged Large Ions in a Radioactive Cloud

For normal conditions in the atmosphere the uncharged condensation nuclei are gradually converted into large ions, and the large ions are converted into uncharged condensation nuclei by combining with the small ions which are present. The rate at which these two processes occur are equal when large-ion equilibrium conditions are attained. If multiply charged large ions are then introduced into the atmosphere, the time required for them to be reduced to singly charged ions, other things

being equal, will depend on a number of factors, such as the concentration of small ions of condensation nuclei and the size of the condensation nuclei at the time.

Multiply charged large ions are produced in several ways, such as combustion processes, the breaking of water drops, and triboelectric effects. Some or all of these processes may play a part in the production of multiply charged large ions in an atomic explosion. Another process will also play a part if the large-ion particle is radioactive and emits a beta particle, because the large-ion particle will then be left with a resulting positive charge. Under the circumstances it is important to examine the possibilities of the multiply charged large ions being maintained in a radioactive cloud.

There may be sufficient evidence available to indicate whether or not the multiple charges on the large ions are predominantly of a given sign, although subsequent experiments conducted by this Laboratory make this conclusion doubtful. However, if the multiple charges are almost all of one sign, then the positive and negative conductivity would no longer be equal. The large ions of the particular sign of multiple charges would more rapidly combine with the oppositely charged small ions. This would reduce the concentration of small ions and consequently the electrical conductivity of this sign, thus bringing about an inequality in the two signs of conductivity. There is no evidence from the measurement of the two signs of conductivity that the values differ by more than about 20 per cent, which is about that generally found for the atmosphere under normal conditions. From this evidence it must be concluded that, if multiply charged large ions exist, they are not confined to a given sign nor does the quantity of charge differ appreciably in the case of the two signs. It would indeed seem remarkable if multiply charged large ions exist in appreciable amounts and yet be so equally divided between the two signs. To ascertain if this is or is not the case it is necessary to examine the discharge rate of large-ion particles for the particular conditions which existed at the time the measurements were carried out.

The discharge rate of the large-ion particle will depend on the concentration of uncharged condensation nuclei, the large ions, and the positive and negative small ions, and on the size of the condensation nuclei. The concentrations of the positive and negative small ions and of the positive large ions are known from the measurements, and the value of the remaining factors may be assumed closely enough to permit calculations which will be good within an order of magnitude. The resulting calculations indicate that, on the average, the charge on each large-ion particle will be reduced from 2 to 1 in about 2 min and, since the discharge rate is relatively rapid at first, from a charge of 10 to 1 in a time considerably less than 20 min.

The condensation nuclei will be continually recharged if they are radioactive. The rate at which the recharge occurs will depend on the amount of radioactive matter on each particle. This amount can be deduced from the value of K given in Table 3.2, which represents the number of ion pairs per cubic centimeter per second produced by the radioactive matter associated with each large-ion particle. Selecting the largest value of K (0.375) given in the table and reducing this to curies, assuming that the radioactive matter is uniformly distributed throughout the atmosphere and that 3.7×10^{10} beta particles per second are given up by each curie, then each large-ion particle will be given, on the average, a positive charge each 10 hr. This charging rate is so low that it may be neglected in comparison with the relatively rapid discharge rate of the large-ion particle noted above. It may therefore be concluded that multiply charged large ions cannot persist for any great length of time in a fairly intense radioactive cloud. Since the observations were not carried out in connection with this Project until several hours after the blast, it seems safe to presume that essentially all the large-ion particles were singly charged.

3.3 FILTER EFFICIENCY

3.3.1 Efficiency Derived from Conductivity Values and Filter-paper Counts

A comparison has been made of the gamma-ray count, from radioactive matter caught on the filter paper during flight through an atomic cloud, with the value of q, the rate of small ion production for the same time interval. In general the filter paper was changed every 30 min. Whenever it was possible, integrated values of q were taken for each of the 30-min periods.

In some cases it was not possible to make a comparison because the gamma-ray intensity was too great to permit even an accurate estimate. In these cases the large-ion apparatus became so polluted with radioactive matter that accurate counts of the large ions were impossible. Comparisons are consequently available for only 3 days, and only a portion of the 30-min intervals on these 3 days can be used for comparison purposes. A summary of the results of the comparisons is shown in Table 3.3. The value of q_f was determined on the following basis: If C is the gamma-ray counts per second and W represents the total volume of air in cubic centimeters per second passing through the filter, then the average number of beta or gamma rays attributed to the radioactive matter in each cubic centimeter of air will be 2C/W, assuming that only half of the liberated rays pass through the gamma-ray counter. In deducing the rate of small-ion production, it is assumed that the beta- or gamma-ray energy is equal to 1 Mev and hence is capable of producing 3×10^4 ion pairs. The values of q_f must then be multiplied by a factor F to compensate for the failure to take into full account the ionizing effects of gamma rays and beta particles from the collected radioactive matter and other effects. The value of F is uncertain but probably lies between 10 and 20. In deriving values of q_f it was assumed that the value of F was equal to 20.

From the values given in Table 3.3 it is obvious that in many cases there was not sufficient radioactive matter of a form which could be collected on the filter paper to maintain the observed small-ion content of the air in an atomic cloud. There were five cases, as noted from the values in Table 3.3, in which there appeared to be more than sufficient radioactive matter of a form that could be collected on the filter paper to maintain the small-ion content of the air. Such a situation is, of course, impossible, since radioactive matter present in any form must ionize the air and consequently increase the conductivity of the air. It seems possible that on these occasions the filters may have received radioactive matter from sources other than the surrounding air, such as might result from material being blown off adjacent parts of the airplane or from contamination in handling of the filter paper.

TABLE 3.3 COMPARISON OF SMALL-ION PRODUCTION*

Shot	Hour	Mean Values of q from Filter Paper (q_f)	Mean Values of q from N and n (q)	Number of Cases for Which $q_f > q$	Number of Cases for Which $q > q_f$
Dog	H+0	0	13	0	10
Dog	H+52	18	8	5	9
Easy	H+0	2	97	0	9

*The rate of small-ion production by radioactive matter on filter paper (q_f) is compared with the rate calculated (q) on the basis of small-ion and large-ion content.

3.3.2 Increase in Filter Efficiency with Time

There is evidence pointing to a greater rate of collection of radioactive matter on the filter several days after the shot. The rate of small-ion production as deduced from the conductivity measurements tends to vary after the shots in a reverse manner. Such a situation raises the question as to whether or not the radioactive particle of micron diameter may not increase in radioactive content through agglomeration with the much smaller radioactive particles of the dimensions of large ions. The larger particles thus tend to become compensated for the decay effect of radioactive matter, whereas the smaller particles have no means of recuperating from the decay effect, assuming that no smaller radioactive particles exist. In any case the quantity of radioactive matter per

particle in the case of smaller particles would be too slight to allow the large-ion-size particles to recuperate to a large extent.

The rate at which the number N per cubic centimeter of large-ion-size particles vary because of their agglomeration with 1-μ-size particles is given by the equation

$$\frac{dN}{dt} = -LPN \qquad (3.2)$$

where P is the number of particles per cubic centimeter of 1-μ dimension and L represents the coefficient of combination between the two sets of particles. Upon integration this equation becomes

$$\log N_t = \log N - LPT \qquad (3.3)$$

where N and N_t represent the initial number of large ions and the number at time t, respectively. A more or less average value of N may be estimated from the large-ion measurements, owing to allowance being made for the presence of uncharged particles and to the fact that only one sign of large ions was measured. The value of L may be estimated[7] from a consideration of the size of the two sets of particles, and a fair estimate of the value of P may be made from examination of photographic film exposed to the filter papers. The following values are accordingly assumed to hold as a basis of calculations: $N = 1.3 \times 10^4$, $P = 4 \times 10^{-4}$, and $L = 1 \times 10^{-4}$. On the basis of these assumptions it appears that the loss of radioactive large-ion-size particles from the air is relatively slow, requiring about 7 months to be reduced to half value. On the other hand, the acquisition of large-ion-size particles by the micron-size particles is relatively rapid. Each of the larger particles, on the average, acquires a smaller particle in about 1 sec. If it is assumed that the quantity of radioactive matter per particle varies as the volume of the particle, then it is possible to compute the increase in radioactive content of the large particles through agglomeration with the smaller particles at various times after the shot. It is found that the radioactive content per particle (neglecting radioactive decay) is doubled in about 9 days. Taking into account radioactive decay (assumed to be on the basis of $A_t = A_0 t^{-1.2}$), the resulting filter efficiency may be computed. Two curves of filter efficiency (initial efficiency 10 and 50 per cent) plotted against time (in days) are given in Fig. 3.13. From these curves it is seen that the efficiency increases rather rapidly at first and then relatively slowly.

3.3.3 Filter Efficiency beyond Boundaries of Radioactive Cloud

If an atomic cloud with sharp boundaries exists, then the gamma rays from the radioactive matter will increase the conductivity of the air by penetrating the air beyond the boundaries. No radioactive matter, however, will be received by the filter paper from such an area. The resulting effect is to reduce the apparent efficiency of the filter for the collection of radioactive matter as derived from the comparison of conductivity values with counts from the filter paper. The question then arises as to the magnitude of such an effect. To simplify the consideration of this question, assume that the boundary of the cloud is a vertical wall of infinite extent. The rate of ionization q beyond the boundary is given by Eq. 3.4. The value of q should vary by a factor of 20 for each 3000 ft traversed (assuming $\mu = 3.3 \times 10^{-5}$ per centimeter) in a straight line perpendicular to the cloud. It is thus possible to compare this rate of variation with that observed while pulling into and out of atomic clouds. Such a comparison will indicate the maximum effect to be expected either because the edge of the cloud is not sharp or because the cloud is not of infinite extent. If the cloud can be regarded as a point source, the effect is further reduced by the factor of $1/x^2$, where x is the distance from the center of the cloud and is accordingly relatively small for practically all circumstances. An examination of a number of cases indicates that for clouds of moderate intensities the mean (computed rate of variation in q attributed to gamma rays beyond the cloud divided by the observed rate of variation) is around 6 per cent. Clouds of very weak intensities may show an effect around two times the above value. In any case, however, the effect seems sufficiently small that it can be neglected for most considerations.

3.4 OVER-ALL MOVEMENT OF THE CLOUD

Figures 3.14 to 3.17 show the flight paths covered for the 3 days of Dog Shot and 2 days

of Easy Shot. The solid portions in Figs. 3.14, 3.15, and 3.17 indicate places where the aircraft was in contact with the cloud. The figures to the side of the lines give the times for various positions along the flight paths.

A summary of the information obtained during these flights is given in Tables 3.4 and 3.5.

The position of the cloud at 25,000 ft was usually predicted by winds at that altitude together with information on its location at given times. The wind data used were scattered since they consisted mainly of a few wind readings taken by aircraft in the area of the cloud and by a ground station at Eniwetok. In Table 3.5 are listed the required winds and directions to move the cloud to the point at which it was found during definite time intervals after the blast. These are compared with navigator's wind readings during the same periods. For Dog Shot it may be seen how the available wind data at 25,000 ft happened to be sufficient for a fair prediction of cloud location, except for the third period listed. During that interval, from H+11 to H+27 hr, the winds were high and variable owing to a heavy storm in that area. How-

TABLE 3.4 MOTION OF CLOUD AT 25,000 FT

Time (hr)		North-South Dimension (miles)	East-West Dimension (miles)	Position of Cloud Front from Point Zero (miles)
Dog	6	200	140	225 east
	11	240	150	400–450 east
	27	180	150	500–550 southeast
	57	300	550	1000 east-southeast
Easy	4	150	180	150 east
	8	170	250	300 east
	30	330	420	660 east

TABLE 3.5 MEASURED AND REQUIRED WINDS AT 25,000 FT

Interval over Which Winds Act (hr)		Required Winds (average)		Navigator's Winds (average)	
		Rate (mph)	Direction (deg)	Rate (mph)	Direction (deg)
Dog	0–6	37.5	270	35.0	270
	6–11	39.0	270	32.0	300
	11–27	9.0	315	26.0	220
	27–57	24.0	270	26.0	260
Easy	0–4	37.5	270	7.0	325
	4–8	37.5	270	7.0	325
	8–30	16.5	270	Low variable	345

The cloud front at 25,000 ft for Dog Shot reached a position 1000 miles away from the point of detonation in 57 hr. The cloud at the same time was about 550 miles long and 300 miles wide. For Easy Shot at the end of 30 hr the front traversed 660 miles, and the cloud dimensions were 420 by 330 miles. The cloud front was determined as the edge of the cloud farthest away from point zero. The dimensions of the cloud were determined by extreme north-south and east-west edges.

ever, on examination of the data for Easy Shot the disagreement found between required and measured winds shows that the wind information was not complete enough for good prediction. The several hundred miles traversed during the periods in question could not be explained by the relatively low winds at 25,000 ft. Fall-out was a possible explanation for the distant patches over so short a period. The clouds for these tests were known to reach an altitude of about 60,000 ft at the time of blast. The winds between 30,000 and 50,000 ft were also known to have the proper amplitudes and direction for carrying the cloud to its geographical location at 25,000 ft. The cloud could have traversed most of the distance at about 30,000 ft, and particles from it could have fallen out gradually to appear as a radioactive cloud at 25,000 ft. The fallacy in this argument is that the largest radioactive particles, which have diameters of 0.05 μ and which seem to carry most of the activity, collected by the large-ion chamber fall about 3 ft in 40 days. Moreover, this figure for the fall-out rate due to gravity is high since particles of that size are seriously affected by Brownian motion. Therefore, it does not seem likely that the cloud could fall to 25,000 ft under the influence of gravity alone.

Another and a more plausible explanation was that vertical mass-air motions carried the cloud from the higher altitudes, where horizontal wind velocities are high, down to 25,000 ft. This idea was suggested by C. E. Palmer of the University of California at Los Angeles, who later explained some of the mechanics of this behavior with data that he obtained in that particular area of the Pacific and at that particular time.

Figure 3.18 illustrates the predicted motion and growth of the cloud with time for Easy Shot at 25,000 ft. This result was obtained by using wind data for 25,000 ft and assuming that there was no vertical motion toward or away from the 25,000-ft plane. Comparison of Fig. 3.18 with Fig. 3.21 shows that the 25,000-ft prediction accounts for only a small portion of the findings at the southwestern end of the cloud at H+8½ hr. Figure 3.19 illustrates the same type of prediction made for the 35,000-ft level. When this same predicted position is projected vertically to the 25,000-ft plane, it can be seen how it can account for the northwestern portion of the cloud found at 25,000 ft.

If large eddy air currents are assumed to exist between horizontal planes in addition to the horizontal wind velocities measured at the various altitudes, a spreading of the cloud would occur. It would be very similar to the predicted cloud that would be obtained by projecting the single-altitude predicted positions of the cloud at higher altitudes down to the 25,000-ft plane. Figure 3.20 shows the prediction obtained if the individual predictions for single-altitude winds are taken for three separate altitudes between 25,000 and 40,000 ft and then assumed to be mixed by eddy air currents between those extremes.

The actual cloud locations as measured by the conductivity equipment for Easy Shot are shown in Fig. 3.21. The predicted cloud, assuming eddy air currents, is superimposed on the same graph. Close agreement between the predicted and actual locations at times 2.5 and 8.5 hr after the blast can be seen. Owing to unfortunate circumstances the prediction data for the cloud at 26.5 hr after the blast were not available for positions farther east than 168 deg at the time this chapter was written. However, the trend of the predicted cloud, as shown in Figs. 3.19 and 3.20, does indicate it to be very close to the actual cloud at 26.5 hr after the blast.

The contours of the cloud are extremely irregular compared to the contours that might be predicted. The degree of irregularity in its shape would be made more pronounced by eddy air currents. There is little doubt that most of the details about the shape and distribution of the cloud were lost in the prediction. This was brought about mainly by the lack of facilities for obtaining more extensive prediction data and the lack of time for analyzing the data more thoroughly.

3.5 MAGNITUDE OF FALL-OUT FROM AN ATOMIC CLOUD AT AND NEAR THE SHOT ISLANDS

It was mentioned in Chap. 2 that orthogonal flight paths were flown over the shot islands from H+6 hr to D+10 days. These flights were repeated at various altitudes ranging from 50 to 4000 ft.

The conductivity survey for fall-out over the islands began at approximately 6 hr after each shot and was repeated for D+10 days. The peak

values in milliroentgens per hour above background values were tabulated for each shot. The values measured ranged from a low of 0.005 mr/hr to a high of 55,000 mr/hr.

The following equations were used to calculate the radioactive intensities at the ground from ionization rates obtained from conductivity readings in the air and survey-meter values at the ground.[8]

$$q = \frac{KQe^{-\mu x}}{x^2} \quad \text{(for point source)} \qquad (3.4)$$

$$q = 2\pi KQ_A e^{-\mu x} \quad \text{(for extended source)} \qquad (3.5)$$

where q = ion production per unit volume
K = Eve's constant and is equal to 4.6×10^9 determined for gamma rays in air
μ = the absorption coefficient in air
x = distance from the point source
Q = number of curies at the point source
Q_A = number of curies per square centimeter uniformly distributed at the ground surface

It will be shown by actual computations that Eq. 3.4 is applicable to these measurements, provided, however, that the distance x is greater than 500 ft. The maximum deviation in the computed values for different distances of x will be shown to be 25 per cent. Equation 3.5 assumes that the distribution of radioactive material is uniform on the ground.

3.5.1 Comparison between Conductivity and Radiac Values

A radiac training set, AN/PDR-T1, was installed in the L-13 aircraft used in the conductivity survey measurements. It was thus possible to obtain a correlation between values with the two instruments. The conductivity values were recorded continuously on a Brown recorder, whereas the peak readings of the radiac were made by an observer. The results are shown in Fig. 3.22, in which the values in roentgens per hour as obtained from the conductivity are plotted as ordinates. The slope of the straight line is 2.16, which indicates that the values obtained from the conductivity are approximately twice those obtained from the radiac observations. This large discrepancy might be attributed to a movement of small ions into the regions from areas of greater concentration since the conductivity depends on the total number of small ions per unit volume. This movement of small ions would occur from upward movement of air since the small-ion concentration falls off rapidly with altitude. It must be remembered, however, that the number contributed from this source would vary with the distance from the source or ground. At a height x the small-ion content would be reduced over that near the ground by a factor proportional to 1/x. Assuming equal vertical velocities at various altitudes under consideration, it can be shown that this cannot be the explanation of the lack of agreement in the two methods of deducing the values of milliroentgens per hour cited above.

In the discussion so far it is assumed that no radioactive material is present in the sampled air. This assumption is considered valid since background conductivities when removed from the islands were normal.

Mention should be made that radiac values were made by an observer. An effort was made to record peak readings. The deflection of the meter lasted only about 1 or 2 sec. It is therefore likely that the observer would be inclined to underestimate this deflection and record values which were too low, possibly by a factor of ½. Using the background conductivity data at 1000 ft before Dog Shot, a value of q equal to 1.57 ion pairs/cc/sec is computed. This value is within a few per cent of that derived from cosmic-ray data.

3.5.2 Dog Shot

The first survey measurements of conductivity were made at approximately H+10 hr. These measurements were made at an altitude of 1000 ft, and none were made over the shot point. However, traverses were made over Runit airstrip and east and west of Runit. Above the airstrip 2.5 r/hr was recorded, whereas east and west of Runit the values were, respectively, 0.013 and 0.5 mr/hr. The normal background value at 1000 ft was 0.005 mr/hr. The ratio of the value over the airstrip to background value is 5×10^5.

Table 3.6 shows the values of conductivity over some of the islands at various times and altitudes. Since the wind direction on shot day was toward the southwest, the greater amount

[redacted]

TABLE 3.6 FALL-OUT, DOG SHOT

(D = Apr. 8, 1951)

Island	Direction from Point Zero (deg)	Altitude (ft)	Conductivity (mr/hr) D	D+1	D+2	D+3	D+4	D+10	D+12
Rigili	249	1500				0.013			
		1000	2.92	1.55	0.506	0.102		0.014	
		500				1.30		0.042	0.091
		200				8.30		0.61	0.506
Giriinien	225	1000	2.45	0.61	0.47	0.11			
		500				1.0		0.094	
		200							0.173
Ribaion	222	1000	1.38	0.56	0.28	0.02			
		500				0.46		0.029	
		200							0.2
Pokon	218	1000	2.23	0.92	0.45	0.03			
		500				0.92		0.04	
		200							0.153
Mui	215	1000	1.78	0.73	0.34	0.087			
		500				0.86		0.05	
		200							0.18
Igurin	210	1000	0.99	0.28	0.16	0.022			
		500				0.032		0.024	
		200							0.07
Parry	192	1000	0.56	0.21	0.003				
		500			0.688		0.085	0.02	
		200	16.4			1.36	0.27		0.04
Japtan	165	1000	0.28	0.20	0.092	0.019	0.003		
		500			0.92	0.34	0.12	0.12	
		200				1.56	0.72	0.078	
Runit	0	1000				911	293	26.8	
		500				4,311*	1518	145	
		200				20,240			

*Flew over crater.

of fall-out occurred on Rigili, Giriinien, Ribaion, Pokon, Mui, Igurin, Japtan, and Parry. The conductivity value obtained over all the atoll islands north of Runit was approximately equal to normal background.

By comparing the values at a given altitude for successive days an understanding of the decay rate is obtained. This feature will be discussed later. The largest amount of fall-out occurred on Rigili. The conductivity value at 1000 ft was 0.506 mr/hr as late as D+2.

Figure 3.23 is a graphical variation of conductivity at an altitude of 1000 ft. Rigili was approached from the north. It is interesting to note that peak and minimum values were obtained over the islands and over the water, respectively. Between Rigili and Giriinien there is a coral reef, a part of which protrudes above the water. The conductivity over the visible area approximated 4.30 mr/hr, whereas the submerged section yielded 0.5 mr/hr. When the coral was completely submerged by the

[redacted]

[redacted]

tide, the value of conductivity dropped to a value only slightly greater than background.

The Rad-Safe monitors had measured the activity on the ground on part of the islands. Their data are shown in Table 3.7. By using the radex and conductivity data on and above an island, the amount of contamination, expressed in curies, on the ground can be computed. The values obtained should agree. Consider one of the values obtained on Rigili on April 9. From Table 3.6 the conductivity value at 1000 ft is 1.55 mr/hr, and from Table 3.7 the radex value is 180 mr/hr. Using Eqs. 3.4 and 3.5, the values Q = 1460 and 1400 curies are computed. In performing these computations, the milliroentgens per hour must be converted into ions per cubic centimeter (consult Table 1.1 for the conversion factors).

The conversion equations are discussed in Sec. 1.3. These formulas can be used to calculate the amount of activity on the ground. From the above fall-out discussion, it is apparent that wind direction on Dog Shot was south to southwest. It would therefore be assumed that various coral pinnacles would trap some of the radioactive particles. Figure 3.24 is a copy of a conductivity record made at D+3 at 500 ft over Runit and over the lagoon. The flight began northeast of Runit, crossed the west end of Runit airstrip, and proceeded 2¼ miles out over the lagoon. A peak conductivity value of 0.125 mr/hr was observed at this point. A map of Eniwetok Atoll shows that a small coral-reef pinnacle is located at this particular spot. It must be remembered that this pinnacle is periodically submerged by water, at which time the conductivity value as observed at 500 ft was equal to the normal background value. Comparing this value with the corresponding one (0.102 mr/hr) over Rigili, it is clear that the radioactivity resulting from fall-out over the pinnacle was approximately 25 per cent greater. Furthermore a successive submerging by tidal motions seemed not to affect the amount of radioactive material trapped within the coral.

At D+12, survey flights were made over the crater of Runit and over a nearby sand pit. These flights were made at an altitude of 200 ft. Over the crater the value of conductivity was an equivalent 340 mr/hr, and over the sand pit it was an equivalent 76 mr/hr. The same survey was repeated on E+10, and respective values were 200 mr/hr and 32 mr/hr. Again, it must be noted that repeated washing of the sand pit did not remove any of the radioactive material which must have become embedded in the sand or been induced at the time of detonation.

3.5.3 Easy Shot

The conductivity surveys were initiated at H+10 hr, and the flights were made at altitudes of 1000 and 500 ft. The results considered on these surveys will be limited to islands in the northern half of the atoll. The results have been summarized in Table 3.8, using only the values obtained at 500 ft. The intensity on the islands nearest point zero on Engebi is low, thus indicating that induced radioactivity resulting from the blast was relatively unimportant. The values of conductivity obtained over the various islands indicate that the fall-out was not solely in response to Stokes' law but was considerably influenced by meteorological factors, especially wind direction and force. The islands to the southeast of point zero on Engebi show but very slight intensity, whereas those islands to the west received the greatest amount of fall-out. The direction and velocity of the wind at 4000 ft altitude was southwest (70 deg) and 10 mph. Assuming that the lower portion of the cloud drifted with the wind, then the distance from each of the islands, lying to the west of point zero on Engebi, to the center of the cloud's path can be computed. An examination of the results shows that islands lying nearest the center of the cloud's path received the greatest amount of fall-out and that the amount diminished very rapidly with distance from the path. The data relating to these matters are summarized in Table 3.9; the third column represents the intensity of fall-out in curies per square foot. All the values of radioactive intensity, except for the first, may be closely represented by the equation $\ln C = A - bD$, where C represents the intensity in curies per square foot, A and b are constants, and D is the distance in miles to the center of the cloud's path. This equation is of the same form as that required to express the rate of diffusion of particles in a gas and possibly suggests diffusion as an important factor in causing the spread of particles in the atomic cloud in its early stages.

Radiac measurements on some of the fall-out islands have been carried out at various times

[redacted]

TABLE 3.7 GROUND-RADEX ATOLL SURVEY*

Island	Apr. 9	Apr. 10	Apr. 11	Apr. 12	Apr. 13	Apr. 21	Apr. 22	Apr. 23	Apr. 24	Apr. 27	Apr. 28	May 5	May 10
Parry	15	NR†	6	5	3	0	0	0.5–1					
Japtan	12	NR	6	5	3	0	0	NR					
Runit						1	4	2.8	1.6	0.5	0.4	0.6	0.2
Aomon	0.5	1	0.05	0.03	0.03	140	40	25	12	4	3.4	1.2	200
Eberiru						200	60	30	15	4	3.4		2000
Engebi	0.2	0.1	0.01	0.03	0.03	0							0.4
Bogallua	0.4	0.03	0.03	0.03	0.03	1000	1000	800	600	150	120	46	30
								1000					
Rigili	180	80	45	30	24	0	0	106	NR			1.0	1.0
Pokon	62	38	20	14	10	NR	NR	NR	NR			1.2	

*Values are in milliroentgens per hour.
†NR is the abbreviation for no readings.

TABLE 3.8 FALL-OUT AND INDUCED RADIOACTIVITY ON ISLANDS, APR. 21, 1951, AS DEDUCED FROM CONDUCTIVITY MEASUREMENTS AT 500 FT

Island	From Point Zero Engebi Direction (deg)	Distance (miles)	Distance to Cloud's Path (miles)	Radioactivity (curies/sq ft $\times 10^{-4}$)
Bogon	289	1.3	0.46	3.0
Bogairikk	281	1.7	0.50	10.7
Teiteiripucchi	278	2.0	0.49	9.9
Elugelab	272	2.6	0.49	36.9
Ruchi	261	3.7	0.35	153.6
Bogombogo	257	4.6	0.26	190.0
Bogallua	255	5.4	0.19	141.6
Aomon	118	5.6		3.7
Eberiru	119	5.1		8.5
Aitsu	124	3.8		8.9
Muzinbaarikku	134	1.2		8.4

TABLE 3.9 COMPARISON OF RADIOACTIVITY ON ISLANDS AS COMPUTED FROM CONDUCTIVITY Q_x WITH THAT OBSERVED WITH RADEX Q_r

Island	Q_x	Q_r	Date of Observation
Bogallua	14,700	21,400	4-21-51
Aomon	1,190	8,370	4-21-51
Eberiru	900	3,880	4-21-51
Engebi	126,000		4-21-51
Japtan	16	310	4-11-51
Rigili	56	280	4-11-51
Pokon	34	170	4-11-51

by the Rad-Safe Group of the Los Alamos laboratory. Air-conductivity measurements were carried out at several altitudes by the group responsible for this volume and are summarized in Table 3.10. It is possible to compare the results obtained with the two pieces of equipment for the same islands and for the same time period. For such a comparison it is necessary to reduce the data to a common basis, the unit chosen being total curies per island, assuming that the fall-out is uniformly spread over the island.

The rate of ionization q may be readily computed from the measured values of the conductivity. In so doing it was assumed that the condensation nuclei were too few to alter appreciably the measured value of the conductivity. If this is not the case, then it will be necessary to increase the determined values of q and consequently the resulting values in curies just to the extent that the condensation nuclei have lowered the conductivity. There are good reasons for believing that no large error will be introduced if the condensation-nuclei effect is neglected in most cases. The ionization of the air at an altitude of 500 ft is assumed to be entirely due to gamma rays from radioactive matter on the island over which the flight is being made. The approximate number of curies on the ground may accordingly be calculated through the application of Eve's equation (Eq. 3.4). It is appreciated that this equation can be considered only as a rough approximation but should be sufficiently precise to give the proper order of magnitude. Calculations have been carried out accordingly, and in the case of several islands the results are given in Table 3.9 under the heading Q_x. The radiac values listed as milliroentgens per hour can be readily converted to values of q, from which corresponding values of Q_A may be derived through the application of Eq. 3.5. Since these values will be in curies per unit volume, they must be multiplied by the area of the island. The final results are also listed in Table 3.9 under the heading Q_r. In view of the various assumptions which were required the comparisons are probably as close as can be expected. The assumption that the radioactive matter is uniformly distributed over the island and that the radex measurement can be regarded as a fair measure of the intensity per square foot is perhaps open to question. The fact that the value of Q_x is in all cases smaller than the corresponding value of Q_r may mean that the effect of large ions on the conductivity is not entirely negligible. The results do suggest, however, that within reasonable precision the average radioactive intensities of an island subjected to fall-out may be obtained from conductivity measurements at low altitude over the island.

3.5.4 George Shot

By the time of George Shot the operators of the L-13 were cognizant of the radiological problems involved. To avoid any accidents the Health Division installed radiac instruments in the L-13. The Health Division also supplied an operator to read the instrument. Taking all necessary precautions, the operators of the conductivity apparatus decided to fly over the crater of Eberiru at H+6 hr, first at an altitude of 3000 ft and then gradually reducing to a minimum altitude of 1000 ft.

The wind direction during the test was from the west, and the radioactive fall-out on any island except the adjacent one was practically zero. This fact is borne out by the Table 3.11. It is observed that the bulk of the activity is concentrated on Eberiru and Aomon. Furthermore Aomon is nearer to Eberiru than Rujoru. The value of conductivity at a 1000-ft altitude is 1822 and 6.8 mr/hr, respectively, for Aomon and Rujoru toward Eberiru. This is an excellent example of the effect of winds on fall-out.

The fall-out conductivity value over Runit, Engebi, and the other islands showed no additional new fall-out. This is evident from the fact that the values do not decrease appreciably with time. For instance, over Runit from G+2 hr to G+7 hr the conductivity values changed from 28 to 21.5 mr/hr, and over Engebi from H+6 hr to G+6 days the values changed from 19.2 to 15.7 mr/hr. If these decay rates are compared with those of Eberiru, the activity is seen to decrease rapidly. This decay rate should be compared with the activities over Runit and Engebi of the Dog and Easy Shots, respectively.

From the values of conductivity at H+6 hr over Eberiru the curies on the island can be computed. This was computed for altitudes of 1000, 2000, and 3000 ft, which yielded values of 179, 158, and 167 $\times 10^7$ curies, respectively.

[redacted]

TABLE 3.10 FALL-OUT, EASY SHOT

Island	Direction from Point Zero (deg)	Altitude (ft)	Conductivity (mr/hr) E* H+10 hr	E+1	E+2	E+3	E+5 – E+7	E+10
Piiraai	38	1000			0.15			
		500	5.02	3.29	1.72	0.06	0.03	
		200						0.08
Aaraanbiru	33	1000			0.18			
		500	7.5	3.5	1.8	0.37	0.06	
		200						0.13
Rojoa	30	1000			0.32			
		500	11.9	5.6	3.5	0.67	0.16	
		200						0.23
Biijiri	30	1000			0.67			
		500	18.5	7.5	4.03	1.73	0.53	
		200						0.41
Aomon	28	1000			0.88			
		500	26.6	8.5	4.93	2.12	1.38	
		200						0.73
Eberiru	29	1000			0.613			
		500	20.1	4.86	3.89	0.88	0.366	
Rujoru	38	1000			1.38			
		500	31.2	11.65	7.12	3.04	1.38	
		200						1.06
Aitsu	34	1000			1.22			
		500	29.7	10.0	5.85	2.44	1.14	
		200						1.3
Yeiri	35	1000			0.613			
		500	10.49	6.2	3.52	1.14	0.25	
		200						0.214
Bokon	38	1000			0.67			
		500	14.22	8.3	3.5	1.3	0.28	
		200						0.18
Bogon	199	1000			0.4	0.08	0.03	
		500	10.7	3.16	1.14			0.015
Kirinian	44	500	16.4	6.92	1.92	0.85	0.28	
Muzin	44	500	8.5	4.25	0.613	0.46	0.13	
Engebi	0	1000	7[illegible]8	607	359	41.4	6.98	2.02
		500	2808	2429	1087	162	41	22.3
		200						683
Bogairikk	191	1000			0.41	0.18	0.07	
		500	8.08	4.25	1.14			0.04
Teiteiripucchi	188	1000			2.56	1.06	0.32	
		500	52.7	19.5	11.18			0.73
Elugelab	182	1000			6.02	2.68	0.89	
		500	138	53.7	30.8			2.34
Ruchi	171	1000			15.58	5.67	1.83	
		500	155	125.5	85.6			3.96
		200						15.58
Bogombogo	167	1000			32.4	16.15	6.92	
		500	712	268	159			10.24
Bogallua	165	1000			18.4	10.8	3.9	0.96
		500	329	192	93.4	46	23	8
		200					34	29
		50						95

*E-day was Apr. 21, 1951.

[redacted]

TABLE 3.11 FALL-OUT, GEORGE SHOT

Island	Direction from Point Zero Eberiru (deg)	Altitude (ft)	Conductivity (mr/hr) G* H+6 hr	G+1	G+2	G+3	G+5	G+6	G+7
Parry	165	1000	0.0006			0.003			
		500				0.003		0.0015	0.0013
		200					0.008		0.007
Japtan	160	1000	0.0006						
		500			0.003	0.002	0.0018	0.0018	0.002
		200					0.012		0.005
Runit	151	1000	5.3	3.17					
		500			28	26.5	23.5	22.5	21.5
		200				127			97
		100					200		
Aomon	115	1000	1,822	445	253	114	61	45	35
		500				455	266	189	137
		200				2,682	1,012	809	582
		100					1,822	1,518	1163
		50							1450
Eberiru	0.0	3000	880	270	83	28	4.2	1.6	0.85
		2000	5,000	1,560	560	160	35	19.5	13.5
		1000	55,600	12,144	6,072	1,685	557	344	243
		500			26,800	9,209	2,934	1,872	1467
		200				29,340	9,867	7,337	5067
		100					18,216	14,674	8602
Rujoru	285	1000	6.8		5.3	3.2	0.85	0.48	0.39
		500						0.61	0.52
		100							0.[illegible]8
Aitsu	285	1000		0.21				0.036	
		500			0.75	0.60	0.18		
		200						0.18	0.15
Engebi	300	1000	19.2	18.7	18.2	16.6		15.7	
		500			114	98.7	91	66	
		200				344	248	213	183
		100					374	324	278
		50							575

*G-day was May 9, 1951.

The good agreement of these values substantiates the applicability of Eq. 3.4.

Evidence is available to show that fission products of an atomic explosion are easily trapped[9] within light cumulus rain clouds. It is not known whether or not these particles are attached to raindrops or if the particles are of the correct size to form condensation nuclei. During George Shot the conductivity and the gamma rays were measured in the cumulus cloud. On the average the strength of the gamma as measured by the radiac instrument was 3 mr/hr. The maximum and minimum values measured were 4 and 2 mr/hr, respectively. Figure 3.25 is a copy of the continuous conductivity record taken over Eberiru at approximately H+6 hr at an altitude of 3000 ft. The effect of the cloud on conductivity is shown by peaks a and b. The value of conductivity increases appreciably while in the cloud. For peak a it increases from a value of 657 to 1876 mr/hr. The question naturally arises regarding the effect that an ordinary light cumulus cloud has on the conductivity-measuring instruments. To answer this question, flights were made through numerous light cumulus clouds in the United States before and after the tests. It was found that the maximum increase in conductivity was relatively small, amounting to an equivalent of 0.5 mr/hr.

Using the average measured radiac value of 3 mr/hr, a value of q in ion pairs per cubic centimeter per second equal to 17.4×10^2 is computed. The value of q computed from the difference in conductivity values 1876 and 657 mr/hr is equal to 7060×10^2 ion pairs/cc/sec. This latter result does not take into consideration the presence of large ions within the cumulus cloud. From the equilibrium equation $q = \alpha n^2 + 2\eta Nn$ it is clear that the value of q computed is the minimum value. This large number of small ions cannot be attributed to gamma rays. Therefore they must have been produced by beta rays. The radioactive particles within the sampled cumulus cloud produce by means of their beta activity ionization within the conductivity cylindrical capacitor. If additional evidence is needed, inspection of Fig. 3.25 shows that the conductivity attains its normal value immediately after passing through the cumulus cloud. If it had been due to gamma activity, the conductivity would decrease at least as inversely as the square of the distance.

Some attempts were made to measure the conductivity during light precipitation but without success. A rapidly fluctuating record always results owing (it is believed) to the "Lenard breaking drop effect."

3.6 SHOT-ISLAND SURVEY

In conducting the conductivity measurements in an L-13 aircraft following an orthogonal pattern as previously described, invaluable data of induced radiation and radioactive deposition intensities and characteristics were obtained. Flights were made at various altitudes over the shot islands as well as over the remaining islands of the atoll. This section will be limited to a discussion of the shot-island surveys.

From the data recorded on a Brown Electronik recorder it is possible to plot contours of the intensity of radioactivity associated with the induced radiation on the shot island. This was done for all altitudes at the various times that flights were conducted over the shot island. Only the more important contour maps will be shown. Figures 3.26 to 3.29 are plotted contour maps of radioactivity in roentgens per hour over the various shot islands at specific times and altitudes.

It must be mentioned first that the radioactivity of the material on and around the immediate vicinity of the shot island was so intense as to make it almost impossible to conduct a survey of the island at low altitudes even up to H+6 hr. Only on Easy Shot was it possible to undertake a pattern flight over Engebi at 500 ft on E+10 hr; yet, a pass over point zero was not made. It was possible, however, to conduct a higher-altitude survey over point zero, provided that weather conditions (cloud cover) were favorable. For Dog and Easy Shots it was not possible. After George Shot it was possible to conduct a flight pattern on G-day above 1000 ft over ground zero successfully. The results are shown in Fig. 3.28. On several occasions, cumulus clouds were encountered. The effects of passes made through these clouds have been discussed in another section.

The results show a rather uniform symmetrical picture such as would be expected. However, there are a few interesting features which should be mentioned. In Fig. 3.26, contour maps of radioactivity over Runit shot

[redacted]

island at various altitudes are shown for D+3 days. For a more detailed distribution of radioactivity on the ground it was necessary to conduct the flight patterns at lower altitudes, as shown by the contour map at the 200-ft level. It is to be noted that the conductivity over zero point was 20.6 r/hr. An interesting fact noticeable is that of a fairly radioactive sandspit off the northwest tip of Runit with a reading of 0.89 r/hr at this altitude. On D-day at H-hour the winds were from the east-northeast at approximately 26 mph. Under such conditions it is quite obvious that fall-out would occur on the sandspit and other islands downwind, whereas a comparative absence of activity is noticeable over middle Runit near the airstrip and over lower Runit.

Figure 3.27 gives a contour picture of Easy Shot decay over Engebi at an altitude of 500 ft from E+10 hr to E+10 days. Here again, with the wind from east-northeast at 20 mph, radioactive ground contamination is practically nil (upwind) along the east coast of Engebi, a distance of approximately 3700 ft from ground zero.

Contour maps of radioactivity over George Shot island at various altitudes from 4000 to 1000 ft on G-day at H+6 hr and at lower altitudes from 500 to 50 ft on G+7 days are shown in Figs. 3.28 and 3.29, respectively. The nature of George Shot was suggestive of an extremely high radioactive count on the shot island shortly after blast time. This was verified by the high reading of 54.5 r/hr over ground zero at an altitude of 1000 ft on G-day at H+6 hr. The contour map of radioactivity at 1000 ft shows quite clearly the intense radiation associated with this shot. The contour lines over Aomon are suggestive of a large amount of induced radiation and fall-out. This becomes obvious in Fig. 3.29, in which the closed contours at lower altitudes show conclusively the large amount of radioactivity still existing on Aomon after G+7 days. This fact and the presence of a contaminated sandspit to the northeast of Eberiru, which can be seen on the contour map at 100 ft, can be explained partly by the wind conditions, which were from the southwest at 18 mph at the time of blast. Another important factor in the comparatively high radioactive contamination on Aomon can be attributed to the fission and nonfission by-products of the blast which were caught by a relatively high ridge parallel to and midway between the northwest coast and the center of Aomon directly opposite the Eberiru shot island. In comparison Rujoru, the next island to the northwest of Eberiru, has relatively little activity associated with it.

The most important fact obtained from very low flights over the shot island and ground zero is the resolution of the activity. This is evidenced by the spacings of the closed contours on the map at 50 ft. Around the north to northeast rim of the crater there exists a maximum or ridge of high radioactivity contamination of approximately 12 r/hr after G+7 days. Over the center of the crater or directly above point zero a reading of 4 r/hr is observed. This indicates that a depression or low region in activity occurs over the crater, owing to the fact that ocean water contained in the crater absorbs the rays from radioactivity. The high readings over the northeast rim of the crater formed by George Shot may be attributed to the wind conditions existing at H-hour as mentioned above.

3.7 DECAY RATES OF ACCUMULATED FALL-OUT AND INCREASED RADIATION

The ground contours of radioactivity obtained with the L-13 can be analyzed and replotted to yield time-decay rates of the accumulated fall-out and induced radiation on the islands. Several of these curves for Dog, Easy, and George Shots are shown in Figs. 3.30 to 3.40. They are plotted on semilog paper, and hence they actually represent curves of the log of radioactive intensity in milliroentgens per hour vs time.

Upon inspection it is apparent that a majority of the curves have a similar peculiarity. This fact is manifested by the hump which interrupts the smooth decay with time. For all these cases, except Engebi after Easy Shot, this hump occurs around the second day. For the Engebi shot island after Easy Shot it occurs directly after the shot. On the decay curves of Dog and George Shots in which the hump does not appear, it should be noted that there are very little, if any, data before the third day. Consequently the same feature may have existed in the decay rates of those particular islands even though data were not taken for those earlier periods. On the other hand there

[redacted]

[redacted]

are sufficient data on the Easy Shot curves to show that certain islands do not display this hump in the decay rate of the accumulated fall-out and induced radiation. Moreover these islands which do not display this characteristic lie west of Engebi, the shot island. The islands which do display the hump lie east of Engebi.

One might first question the measurements made before assuming that this peculiarity is real. The conductivity instrument could possibly have been indicating high on the second day owing to some fault. However, it is very unlikely that the same fault would occur on the second day of all three shots. Moreover, there was an instance where the same feature appeared in the data taken with a survey-type meter which was on the same aircraft. The logical conclusion then seems to be that the hump in the decay curves is real.

If the total fall-out and induced radiation consist of several isotopes, which are in equilibrium with their decay products for the purposes of this discussion, then the radioactive intensity can be expressed as

$$q = (Ae^{-\lambda_1 t} + Be^{-\lambda_2 t} + Ce^{-\lambda_3 t} + \ldots) \qquad (3.6)$$

where q, the rate of ion production at a constant altitude proportional to the number of milliroentgens per hour, and t, time, are the only variables. A, B, C, etc., are proportional to the amounts of each radioactive isotope at time zero, and λ_1, λ_2, λ_3, etc., are the respective decay constants for each isotope. Since the curves shown here are in milliroentgens per hour, the same units will be used, and the constant of proportionality can be absorbed in the constants A, B, C, etc. Actually the graphs represent the log of q vs time so that

$$\log q = \log (Ae^{-\lambda_1 t} + Be^{-\lambda_2 t} + Ce^{-\lambda_3 t}) \qquad (3.7)$$

It can be shown that the second derivative of log q with respect to time is

$$q^2\left[\frac{d^2 \log q}{dt^2}\right] = AB(\lambda_1 - \lambda_2)^2 e^{-(\lambda_1+\lambda_2)t} + BC(\lambda_2 - \lambda_3)^2 e^{-(\lambda_2+\lambda_3)t} + CA(\lambda_1 - \lambda_3)^2 e^{-(\lambda_1+\lambda_3)t} \qquad (3.8)$$

This expression will always be positive if A, B, C, etc., are positive constants. Therefore the slopes of all the curves in Figs. 3.30 to 3.40 should show no negative inflection, provided that the amount of each element remains the same as it was at time zero.

There are two means by which A, B, C, etc., might be varied to cause a decreasing slope in the decay curves. One of these is by production of the daughter decay products by the original elements. If this is the case, then the original elements were not yet in equilibrium with their decay products by the second day.[10] However, this does not explain why, for Easy Shot, the islands west of Shot island Engebi do not show the property of decreasing slope while the islands east of Engebi do. The same type of behavior in decay for both groups of islands would be expected since they are both close enough to Engebi to have the same radioactive materials in the same proportions. This fact implies that some other process is also occurring. Another means by which a decreasing slope can be brought about is the accumulation of additional fall-out. If this were the case, then winds and other meteorological conditions might conceivably have caused more fall-out (on the second day, in particular) to reach one group of islands than reached the other group. This, in effect, would make A, B, C, etc., functions of time. They would be equal to the amount of induced radiation and radiation of radioactive material left on the ground at time zero plus the integral of the rate of fall-out up to a time T, after which they would remain constant if no more appreciable fall-out occurs due to meteorological conditions. It does not seem likely that the fall-out conditions should repeat so well that the hump in decay rate should occur on the second day of each shot.

There are insufficient data available to this Laboratory on the meteorological conditions that existed and on size distribution of particles to determine the dependence of fall-out on time. Also there are insufficient data available to this Laboratory on the products of the atomic blast to determine how long the transient lasts before equilibrium between the elements and their decay products is reached. Both of these effects might cause an inflection in slope in the decay curve if these processes were taking place to some extent. However, the information at present is not enough to determine, in general, which of the two contributes most to this

[redacted]

characteristic. The curves of Fig. 3.40 for the shot island of Easy Shot have slopes that decrease in the very early stages. It appears likely that the proportions of elements are in a transient state and that the rate of fall-out would be very high at this time. Table 3.10 is a listing of the radiation intensities for two groups of islands (east and west of Engebi) for Easy Shot. It will be noticed that values are very low for the group east of Engebi compared with those for the western group. The decreasing slope in decay curves is also very prominent for the eastern group, but no such feature is detectable for the western group. A given amount of fall-out on both groups made a high percentage change in radiation intensity (as much as 100 per cent more than it would be in some cases if the activity had continued at its initial decay rate) on the group of low intensity, whereas it made no detectable change on the western group because the intensity was already quite high. Therefore the hump, at least in this case, appears to be attributable to additional fall-out at that time. If, in this case, it is due to a nonequilibrium state, the percentage change in both groups should be the same, assuming all elements to be present in the same proportions on all the islands.

An analysis was attempted on the decay curves for which the elements appeared to be in equilibrium with their decay products and fall-out appeared to be negligible (i.e., the curves for which A, B, C, etc., are constant) in order to determine the separate quantities and decay rates of the radioactive components. It was found that each could be fairly well represented by the sum of three components. These deduced data are given in Table 3.12. Decay rates much lower than those shown in the column of third components most likely exist, but they were not detectable from the total-decay curves, since data beyond the tenth day were not available. Inconsistency in the data from island to island is due to at least three causes. One of these is that the data used were obtained from the peak reading in flying over the island at a constant altitude. If the aircraft did not go directly over, but did go to one side of, the center of activity, then the peak reading obtained would be less than the peak value which existed at that altitude. However, these peaks were found to be usually very broad, and hence this source of error was not serious. Another cause of inconsistency in the data is the fact that some of the islands still had radioactive material from the previous (Dog) shot. The other reason is that fall-out may still have been continuing and equilibrium may not have yet been attained, although the analysis of subtracting out components requires the assumption that the quantities of radioactive materials are fixed from zero. The number of islands for which the analysis was made is relatively small because most of the decay curves have a region of decreasing slope. Attempting an analysis on these curves is very difficult since the dependence of rate of fall-out on time is unknown.

TABLE 3.12 RELATIVE PROPORTIONS OF COMPONENTS IN FALL-OUT OF EASY SHOT DETERMINED FROM NORMAL DECAY CURVES

Island	First Component	Second Component	Third Component
Bogallua	$350\ e^{-1.37t}$	$145\ e^{-0.5t}$	$14\ e^{-0.07t}$
Teiteiripucchi	$192\ e^{-4.3t}$	$5\ e^{-0.81t}$	$20\ e^{-0.35t}$
Bogon	$33\ e^{-3.46t}$	$0.4\ e^{-0.64t}$	$3\ e^{-0.5t}$
Bogombogo	$1682\ e^{-3.37t}$	$33\ e^{-0.47t}$	$280\ e^{-0.33t}$
Elugelab	$380\ e^{-3.35t}$	$5.3\ e^{-0.47t}$	$52\ e^{-0.31t}$

REFERENCES

1. J. A. Fleming, "Terrestrial Magnetism and Electricity," p. 182, Dover Publications, Inc., New York, 1949.

[redacted]

2. G. R. Wait, J. Wash. Acad. Sci., 36: 321, 343 (1946).
3. O. W. Torreson and G. R. Wait, Terr. Mag., 39: 47-64 (1934).
4. O. W. Torreson, Terr. Mag., 39: 65-68 (1934).
5. K. L. Sherman, Terr. Mag., 45: 191-195 (1940).
6. P. G. Nolan and P. G. Tedde, Arch. Met. Geophys. u. Bioklimatologie, A, Met. Geophys., 2(4): 374-385 (1950).
7. W. R. Harper, Phil. Mag., 18: 97 (1934); 20: 740 (1935); Proc. Cambridge Phil. Soc., 28: 219 (1932); 31: 430 (1935).
8. A. S. Eve, Phil. Mag., 22: 551 (1911).
9. Los Alamos Scientific Laboratory, "The Effects of Atomic Weapons," p. 274, U. S. Government Printing Office, Washington, 1950.
10. E. Rutherford, "Radioactive Substances and Their Radiations," pp. 410-443, G. P. Putnam's Sons, New York, 1913.

[redacted]

Chapter

Conclusions

It was found that the radioactive cloud follows the predicted direction of winds. The approximate location of the cloud could be predicted on the basis of horizontal movements of air masses, whereas the more precise position could be determined only by considering both horizontal and vertical air motions.

The clouds were found to be extremely scattered. The boundaries of these clouds were characterized by a sharp increase in radioactivity, amounting to as much as 3 mr/hr per mile for the period H+30 hr. At H+52 hr the greatest gradient encountered was found to be less than 1 per cent of the above value.

The data revealed the presence of particles having a radius of 10^{-6} cm. Some of them appear to be radioactive. The quantity of radioactive particulate matter diminished with time in accordance with the normal rate of decay.

The over-all efficiency of mechanical filters is a function of the size of the particulate matter to be filtered. From simultaneous measurement with the ion counter and the mechanical filter the efficiency was found to vary over wide limits, from zero to practically 100 per cent. As has already been shown, there is reason to believe that the low efficiency may be associated with the presence of small radioactive particles which pass through the filter. Reasons are given for believing that the efficiency of the filter may increase with time.

One of the objectives was to measure the amount of radioactive material falling out of the cloud. The fall-out in terms of curies on the two shot islands Engebi and Eberiru, according to a conductivity survey measured at H+6 hr, amounted to 1×10^5 and 1.5×10^7, respectively. No measurement was made over Runit at H+6 hr. The fall-out was found to be much greater on the downwind side. Fall-out was measured on small pinnacles jutting out of the water, coral reefs, and sandspits. From the analysis of decay curves, derived from the conductivity data over the islands, there is evidence of the presence of several radioactive isotopes.

The computed values of radioactive intensities on the ground from the simultaneous measurement made by radiac and conductivity meters were in reasonably good agreement. This fact is very important because it clearly emphasizes the possibility of substituting the air-conductivity meter for the present radiac instrument, especially for a quick and accurate determination of contamination, particularly over areas inaccessible to ground monitoring. To establish a better correlation factor, more simultaneous measurements of air conductivity and alpha, beta, and gamma counts should be made.

By measuring the air conductivity over the various shot and other islands the pattern of the fall-out was established.

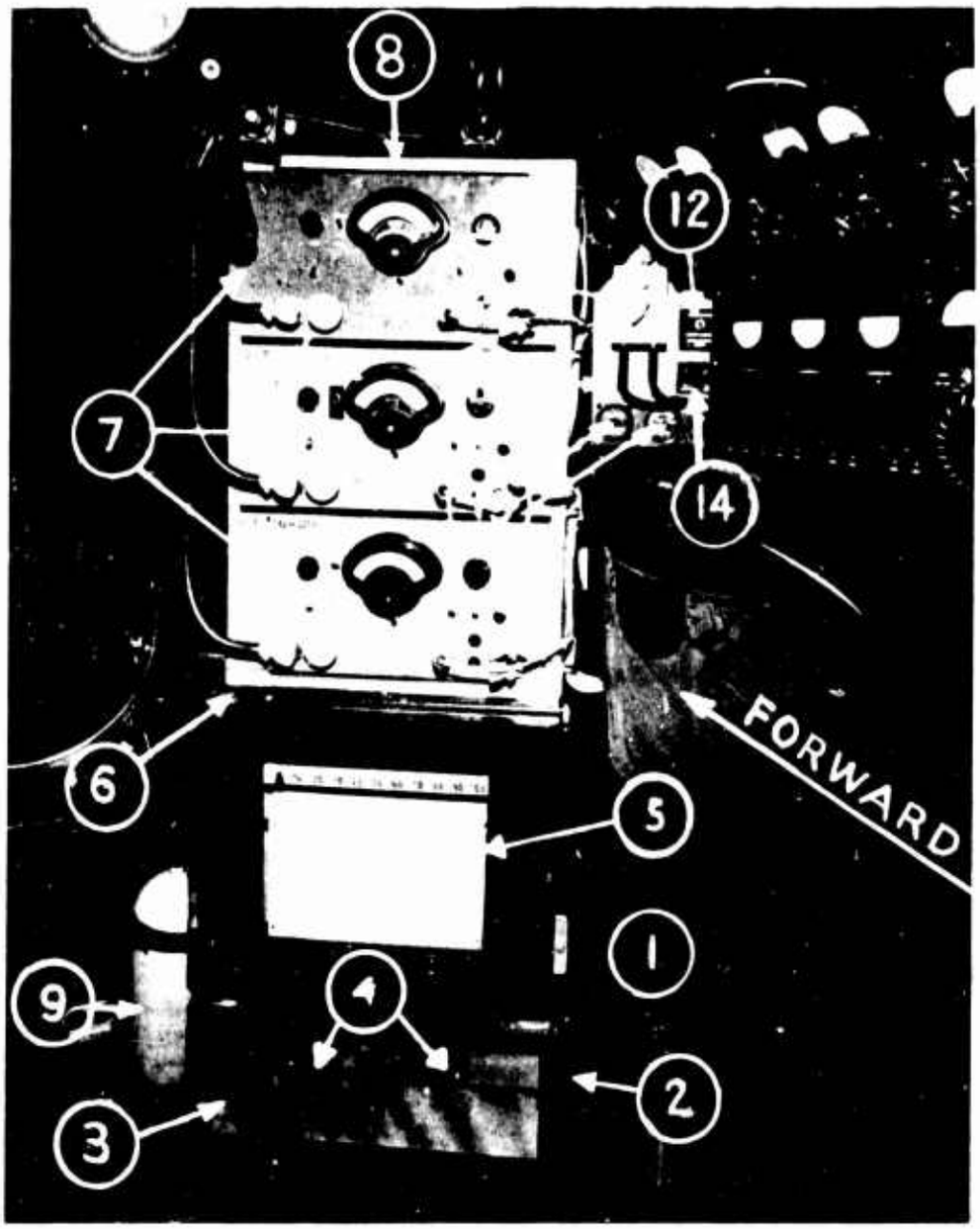

Fig. 2.1 Location of the Three Main Electrometer Amplifiers

(1) Seat assembly, type 199A
(2) Supporting rack
(3) Drawer, miscellaneous storage
(4) Drawers, lamp and fuse storage
(5) Recording potentiometer
(6) Rack assembly, 51J2326
(7) Electrometer amplifiers, three required
(8) Rack, mounting 51J2034
(9) Regulator and cylinder assemby 44D22201 with bracket assembly 44B24621
(10) Auxiliary equipment panel
(11) Jack box BC-1366-N
(12) Switch AN3021-3 with identification plate 51B2376
(13) Indicator, oxygen flow, AN6029-1, and gauge, oxygen, AN6021-1A
(14) Light assemblies AN3157-2 and AN3157-3, one each required with identification plate 51B2392

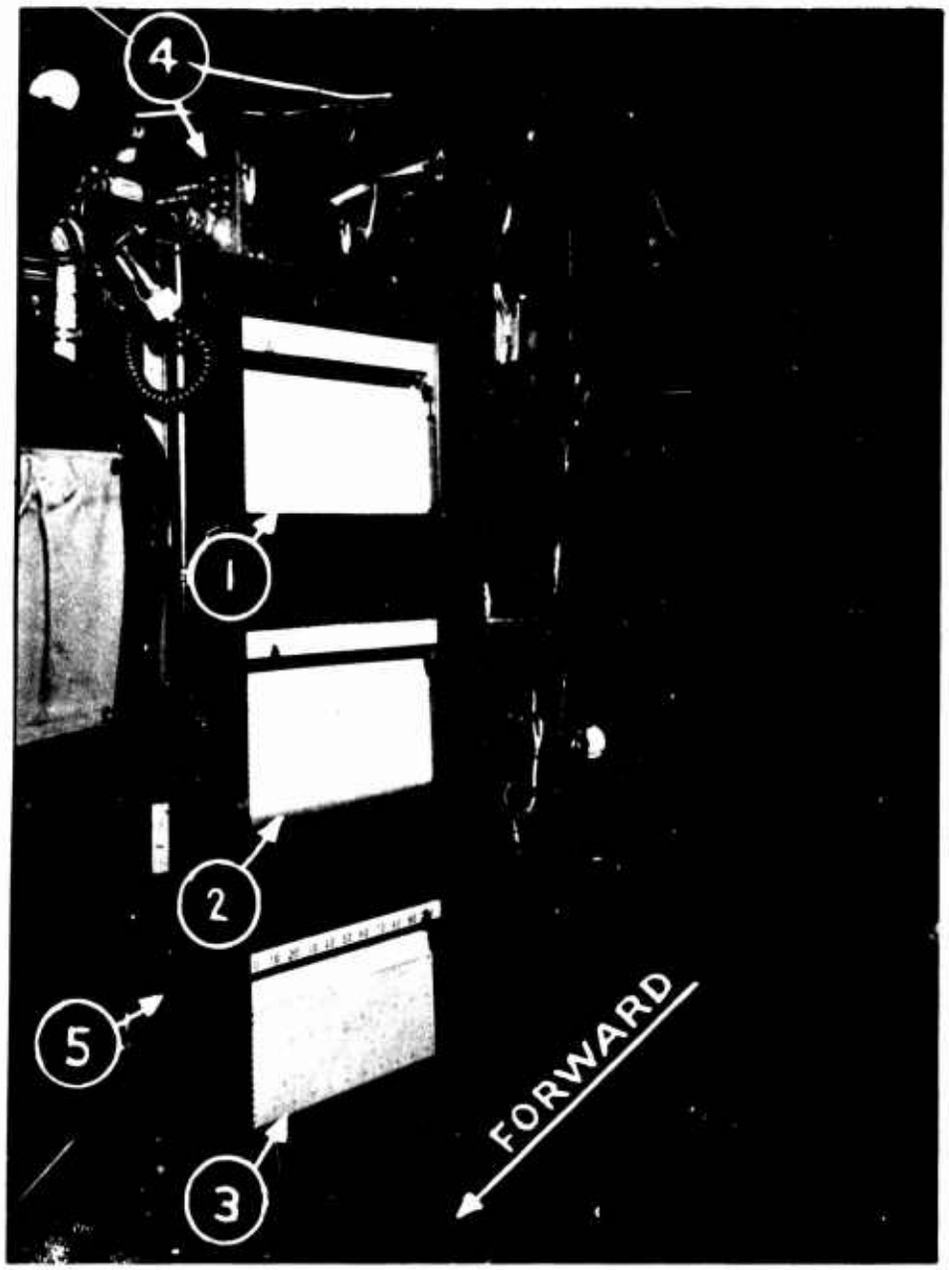

Fig. 2.2 Three Brown Electronik Recorders
(1) Recording potentiometer No. 1
(2) Recording potentiometer No. 3
(3) Recording potentiometer No. 2
(4) High-voltage battery box (3000 volts)
(5) Rack assembly, recording potentiometer 51J2325

[redacted]

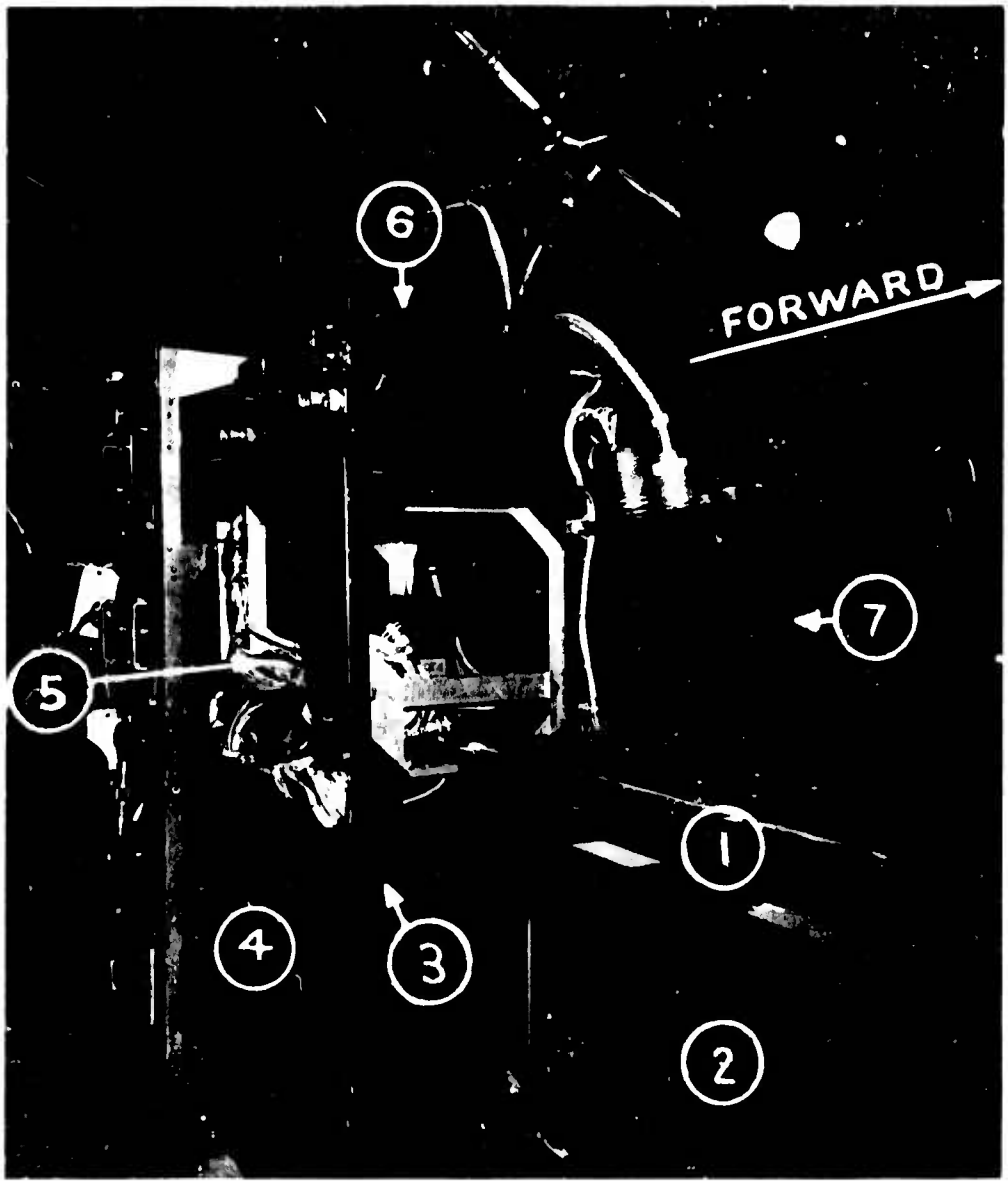

Fig. 2.3 The Field-meter Brush Recorder

(1) Recording oscillograph equipment rack
(2) Electronics unit, part of nuclei condensation detector
(3) Rack assembly, Brown recorder, double deck, 51J2091
(4) Recording potentiometer
(5) Rack, equipment adapter 51J2208
(6) Amplifier, recorder group OA-(XA-16)/ASH-1
(7) Junction Box J-106C/APQ-13A. Relocate approximately 1½ in. aft of original position

[redacted]

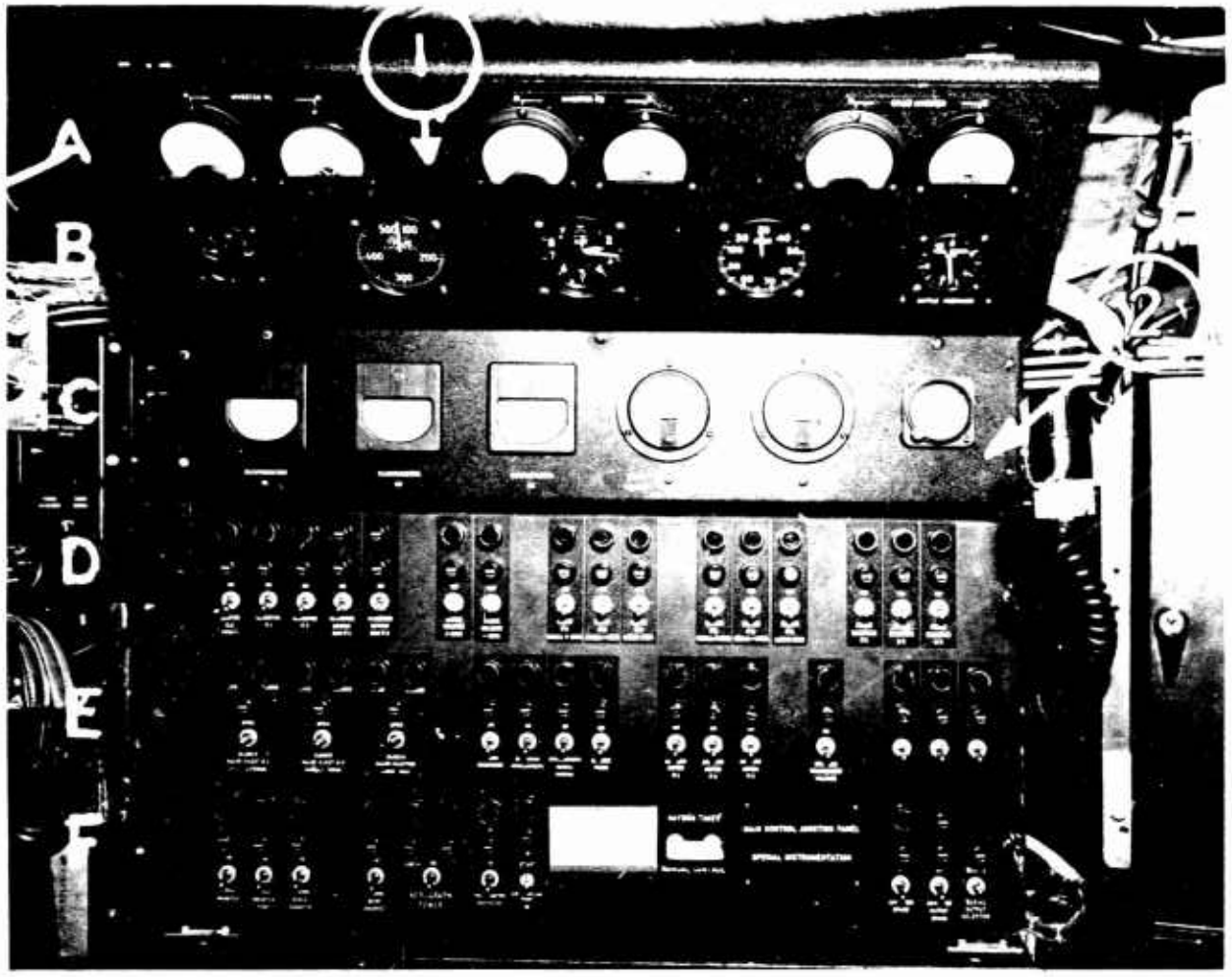

Fig. 2.4 B-50 Main Control Junction Panel Showing Location of Air-meter Indicators

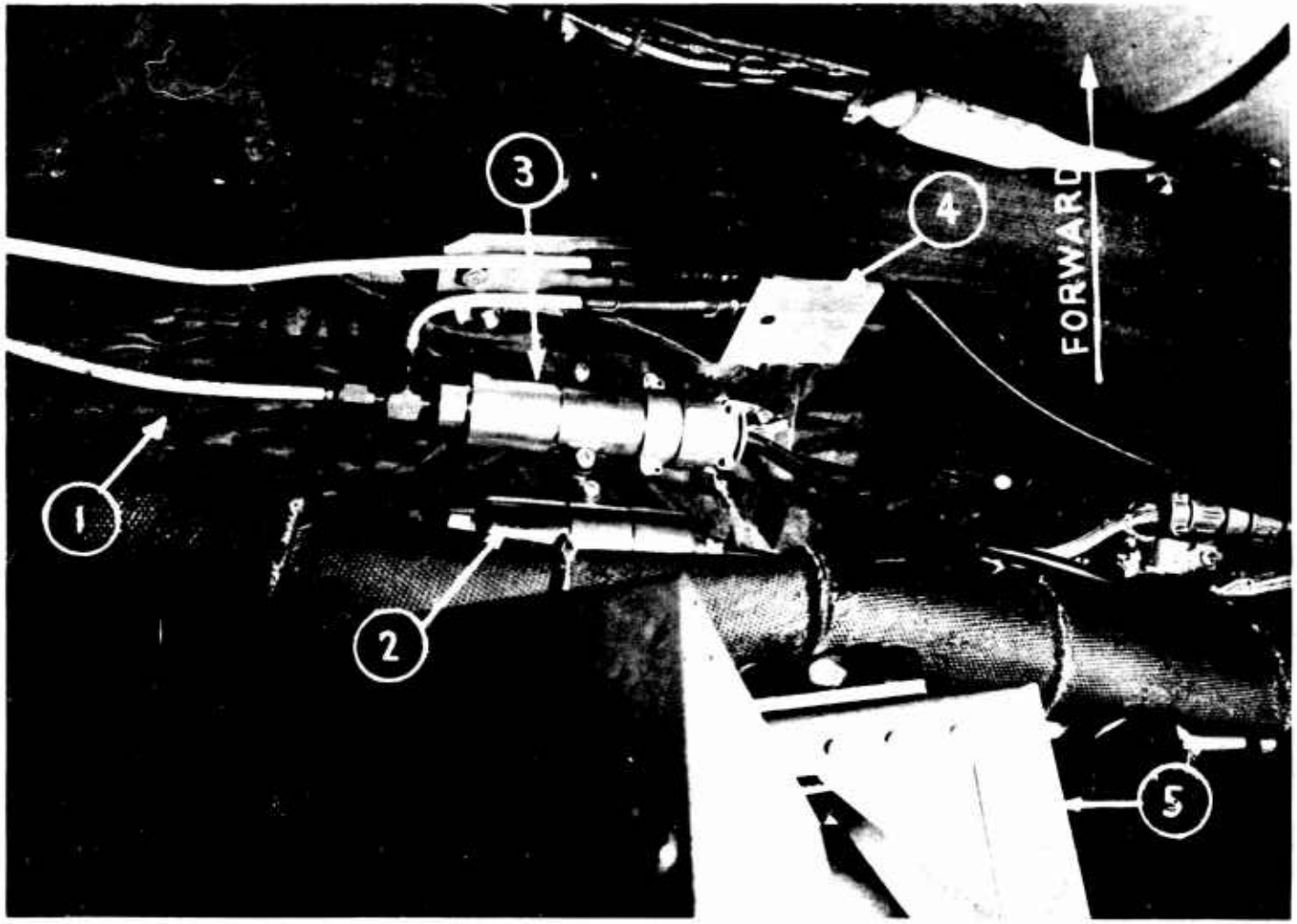

Fig. 2.5 Location of the Statham Transducers

(1) Former, station 706 (ref.)
(2) Pressure transducer (manifold) P10-40G-180
(3) Pressure transducer (altitude) P24-15A-180
(4) Pressure transducer (air speed) P64-2D-180
(5) Rack assembly, electrometer 51J2034 (ref.)

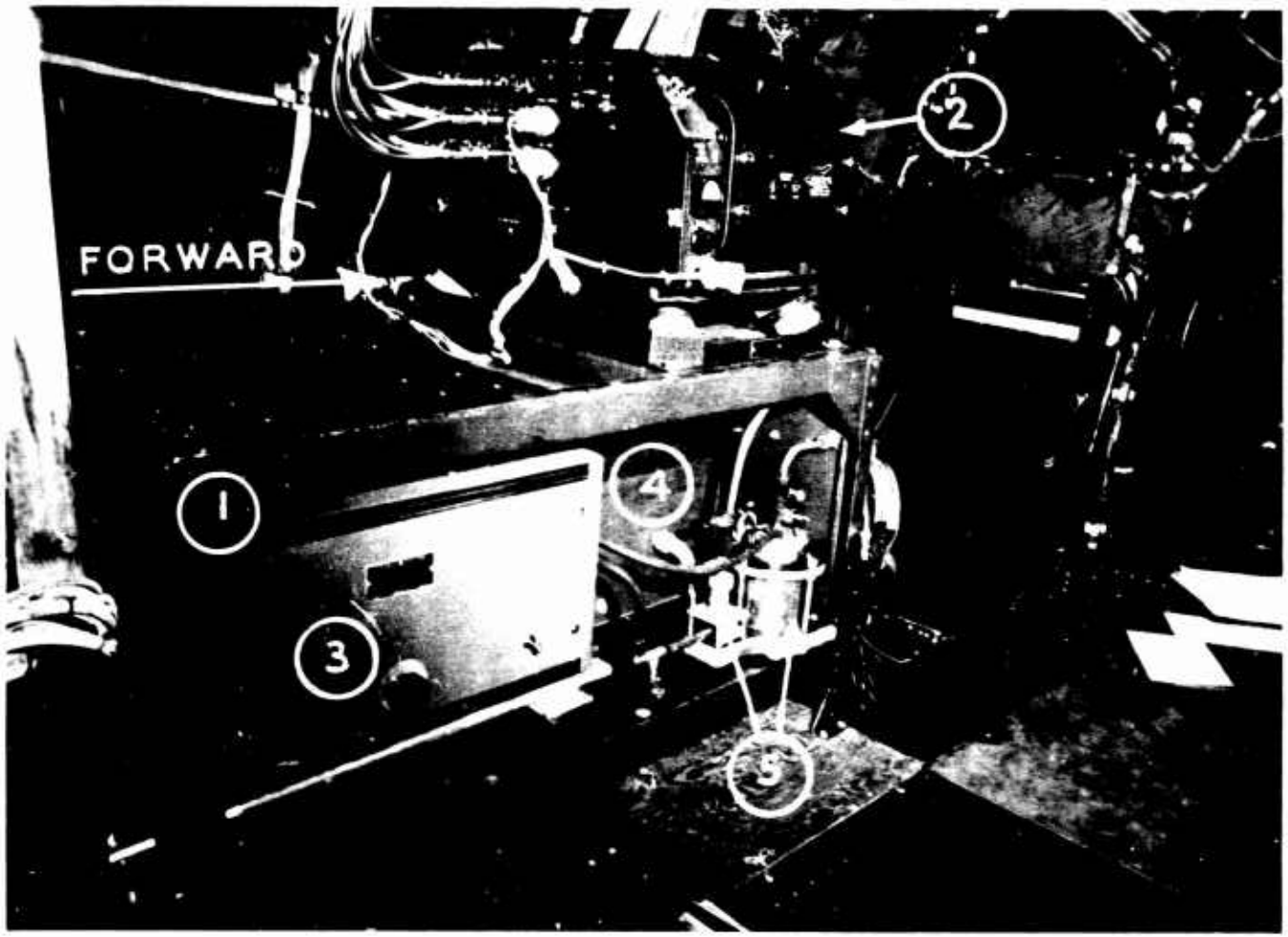

Fig. 2.6 The Consolidated Recording Oscillograph

(1) Recording-oscillograph equipment rack
(2) Recording oscillograph
(3) Electronics unit, part of nuclei condensation detector
(4) Low-voltage battery-box assembly 51D2143
(5) Fiberglas filter assembly and humidifier, part of nuclei condensation detector

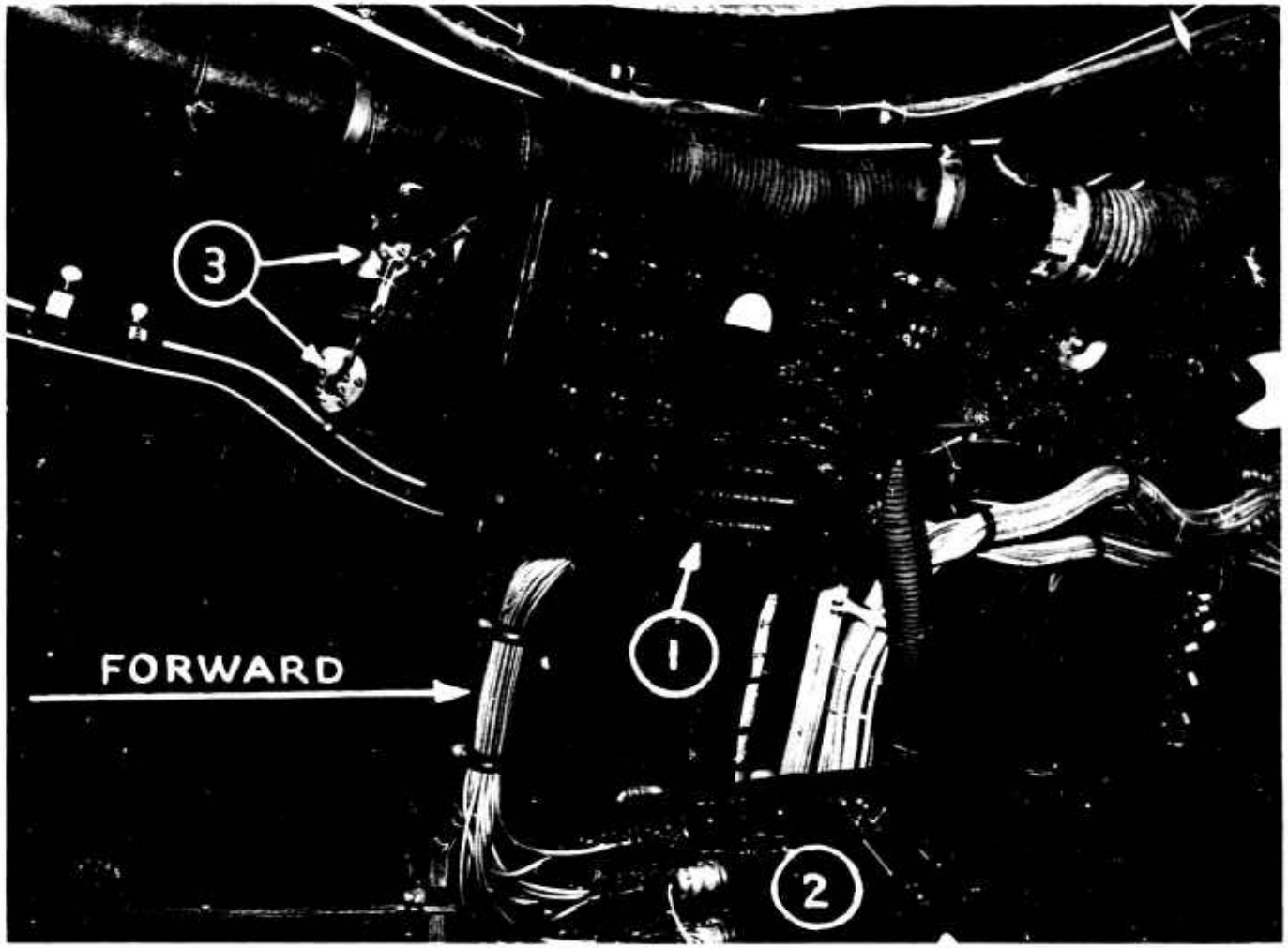

Fig. 2.7 Junction Box for the Consolidated Recorder

(1) Aft junction box 51F2100
(2) Recording oscillograph (ref.)
(3) Probe assembly, thermometer, part No. 177746, two required

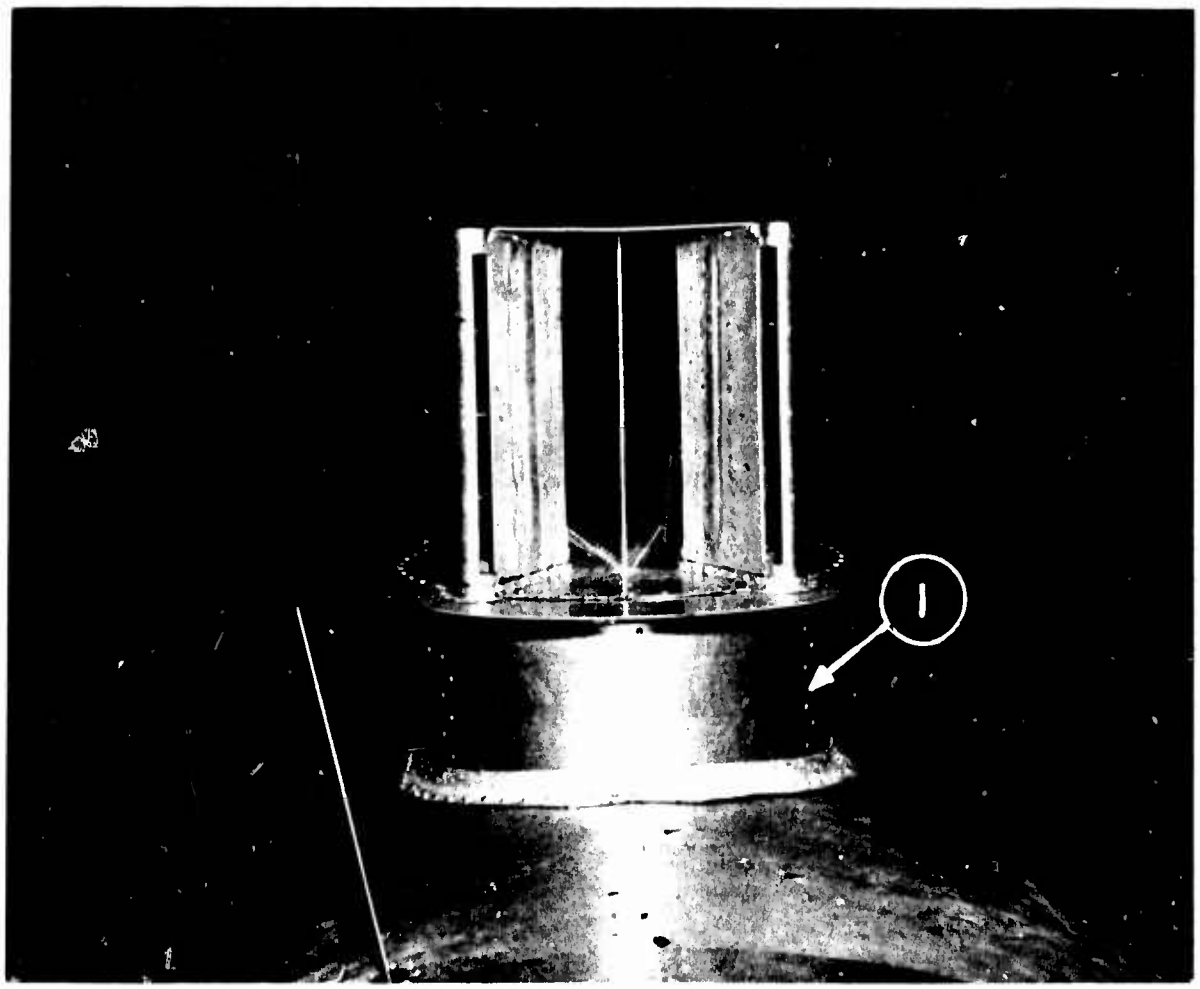

Fig. 2.8 Particle Filter
(1) W. 26 foil, entrance

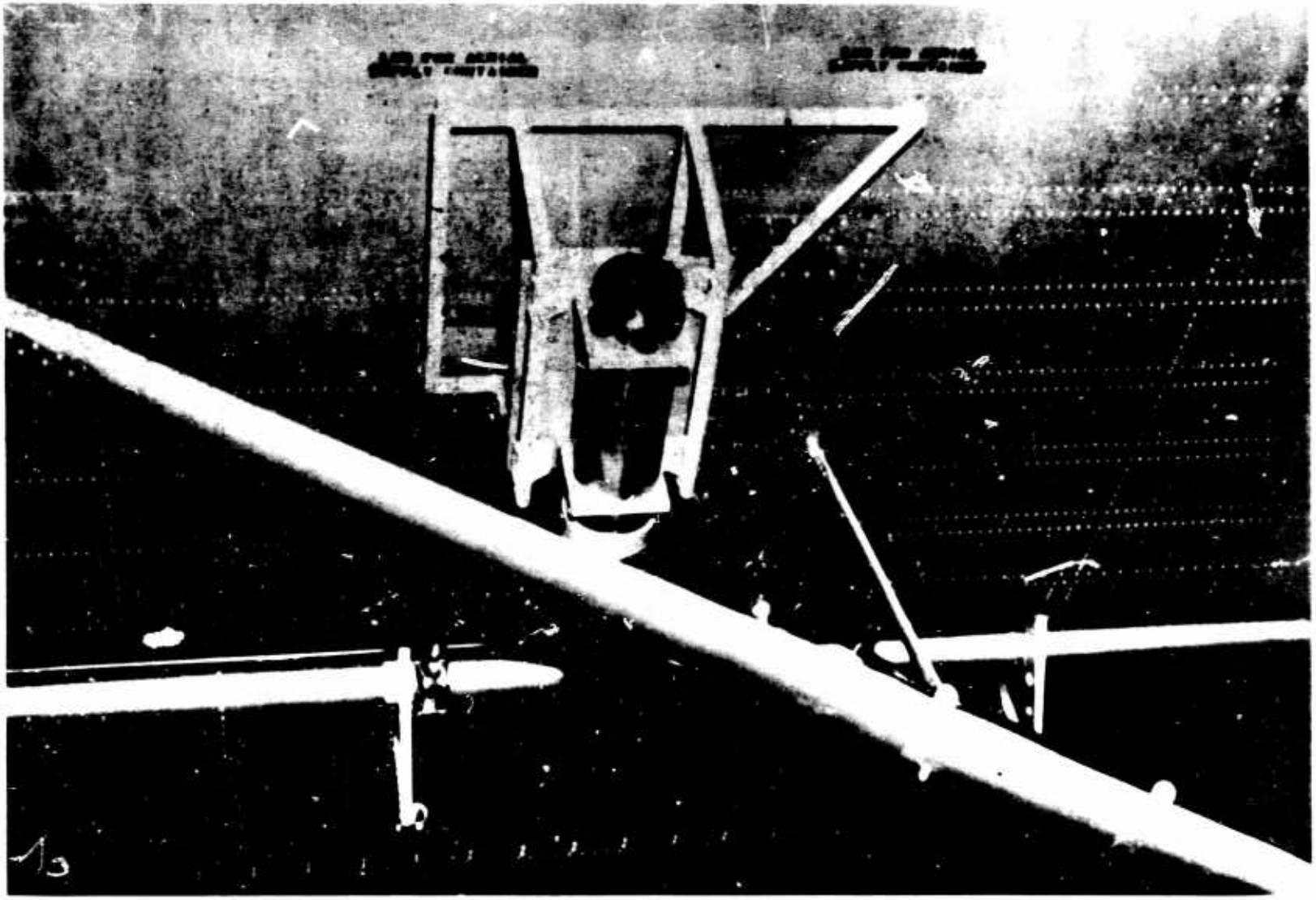

Fig. 2.9 L-13 Conductivity Chamber

[redacted]

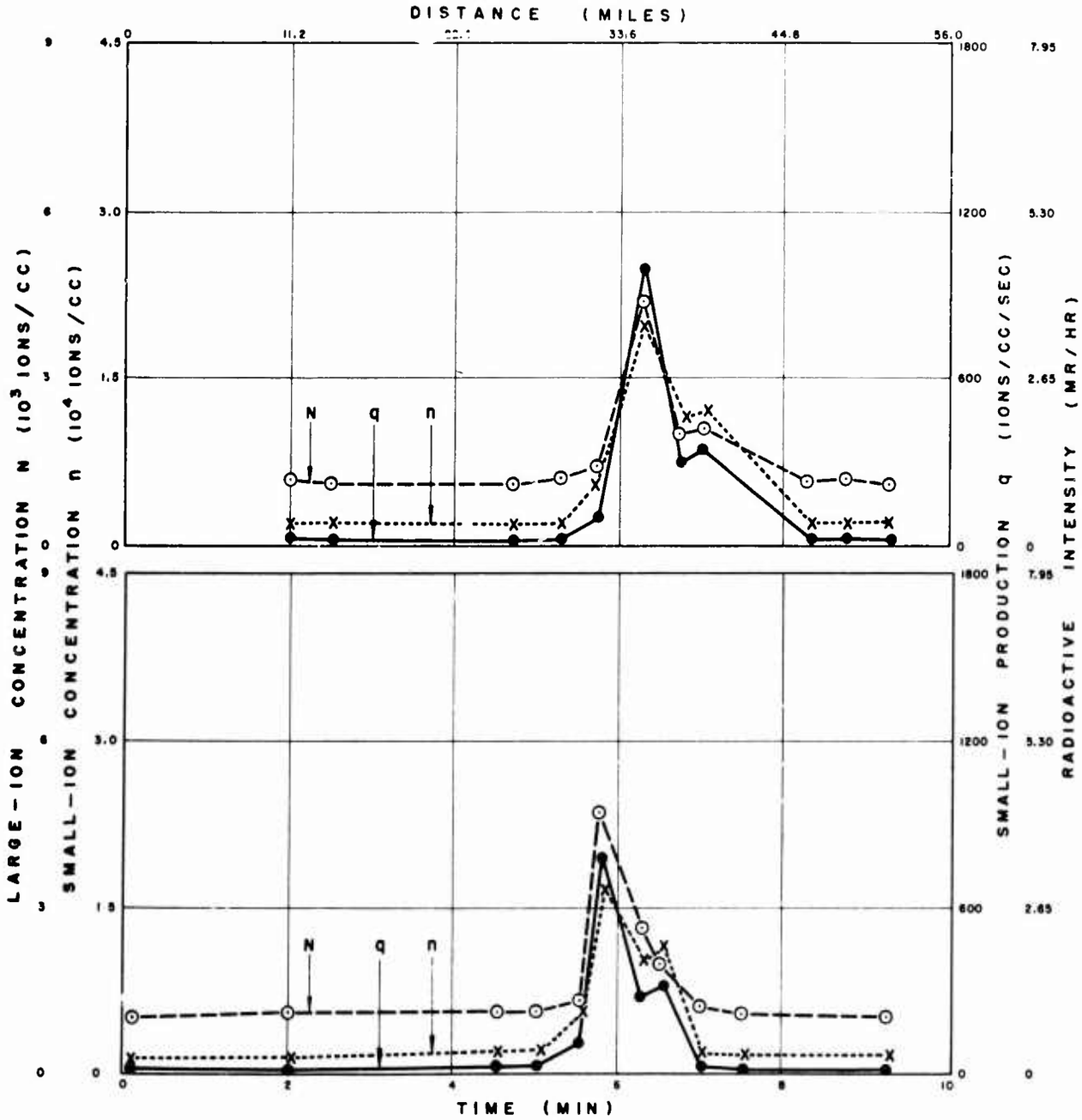

Fig. 3.1 Measured Values of Large Ions per Cubic Centimeter, N; Small Ions per Cubic Centimeter, n; and Calculated Values of Ions per Cubic Centimeter per Second, q. Before, during, and after encountering the atomic cloud (Easy Shot, 21 Apr. 51). Top, from 1031 to 1041 hours; bottom, from 1026 to 1036 hours.

[redacted]

[redacted]

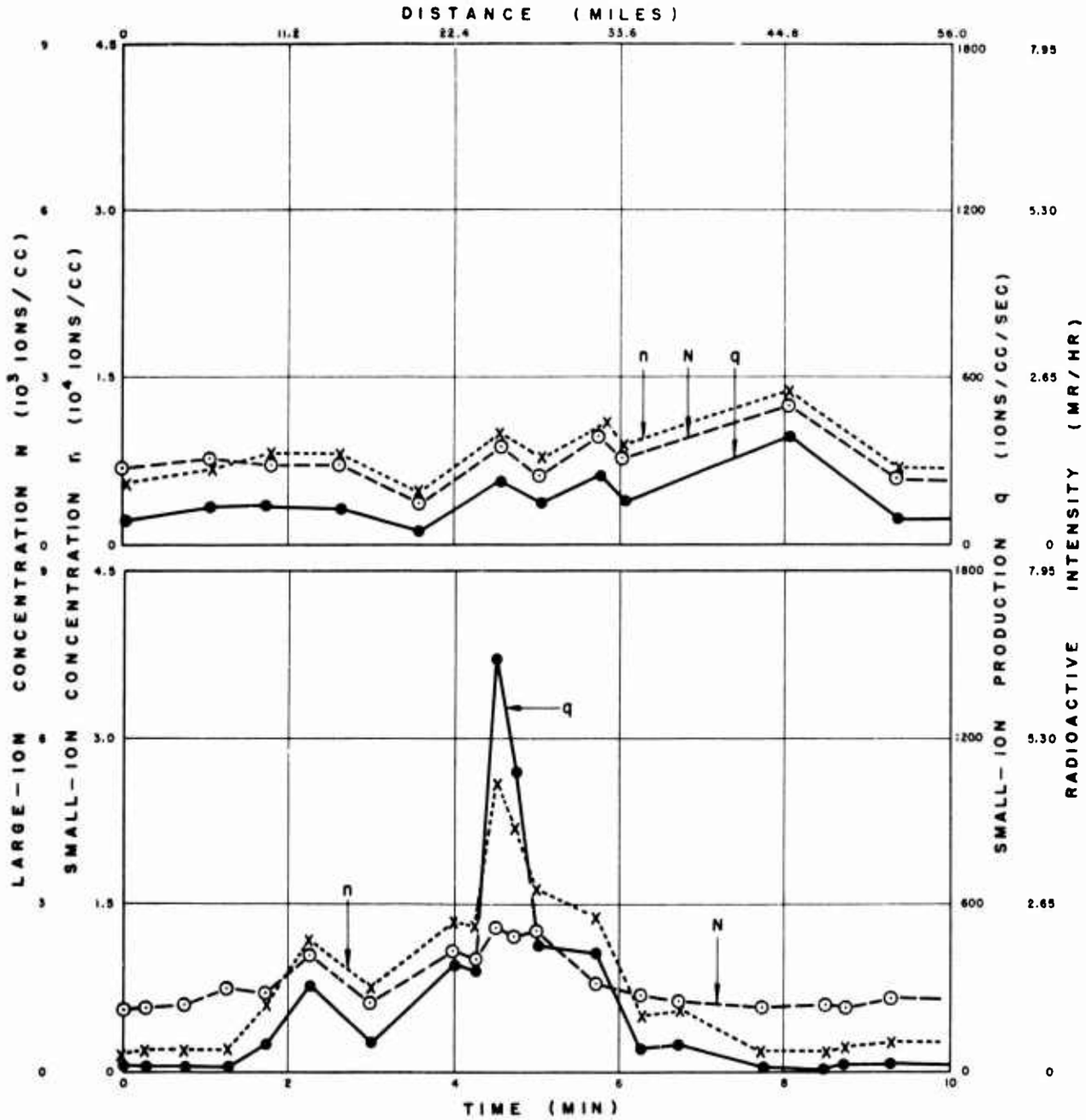

Fig. 3.2 Measured Values of Large Ions per Cubic Centimeter, N; Small Ions per Cubic Centimeter, n; and Calculated Values of Ions per Cubic Centimeter per Second, q. Before, during, and after encountering the atomic cloud (Easy Shot, 21 Apr. 51). Top, from 1049 to 1059 hours; bottom, from 1039 to 1049 hours.

[redacted]

[redacted]

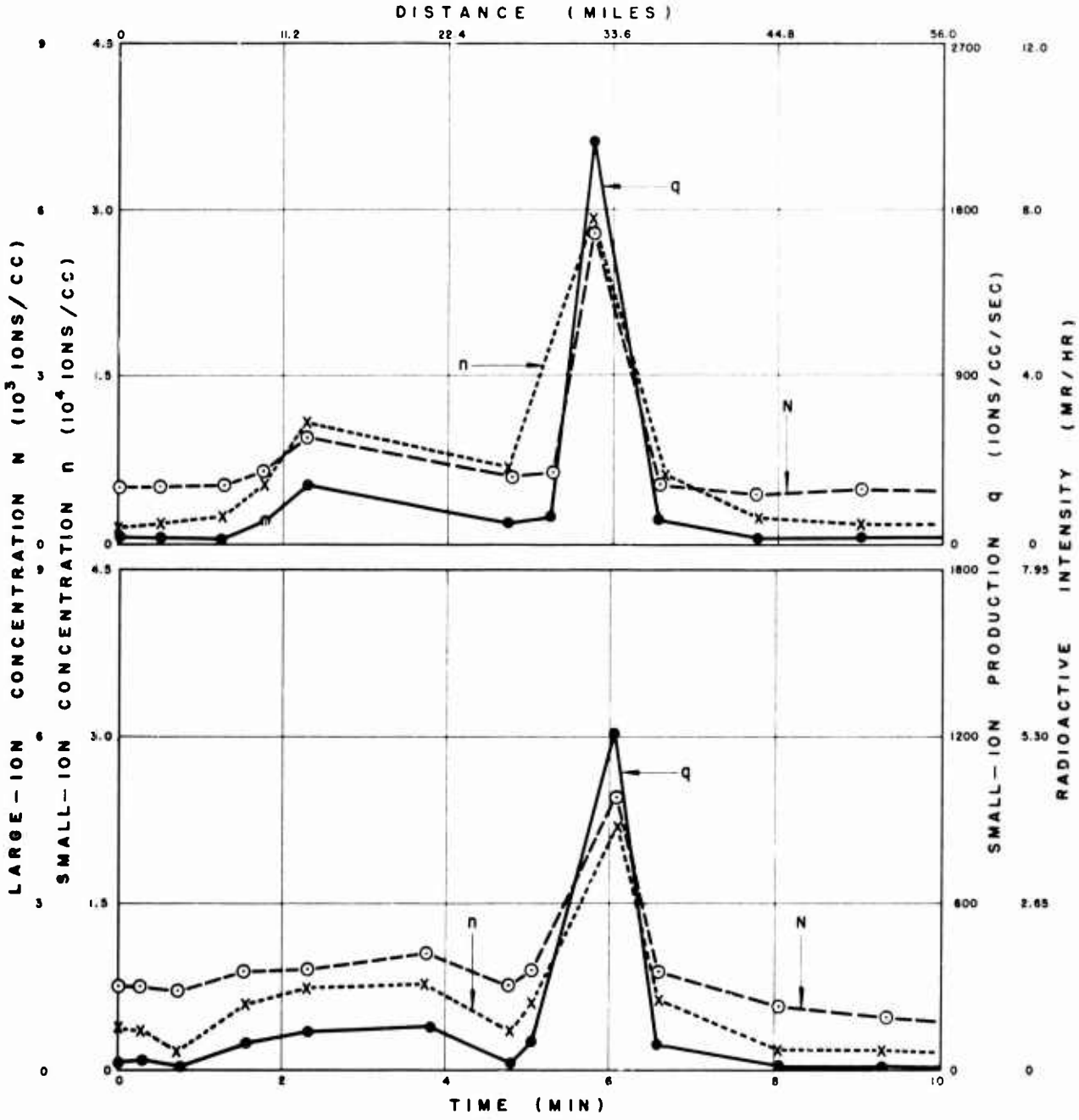

Fig. 3.3 Measured Values of Large Ions per Cubic Centimeter, N; Small Ions per Cubic Centimeter, n; and Calculated Values of Ions per Cubic Centimeter per Second, q. Before, during, and after encountering the atomic cloud (Easy Shot, 21 Apr. 51). Top, from 1149 to 1159 hours; bottom, from 1124 to 1134 hours.

[redacted]

[redacted]

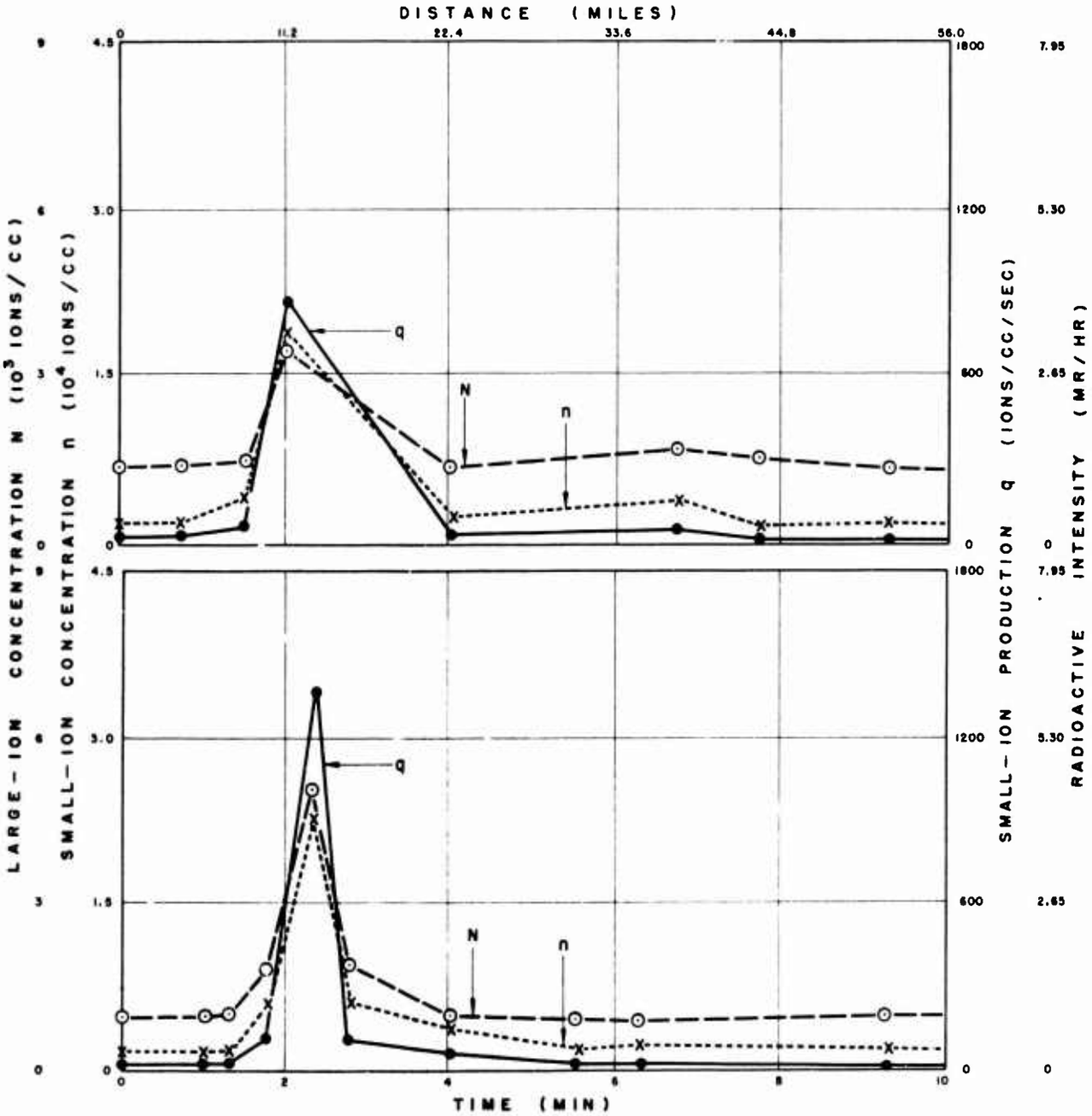

Fig. 3.4 Measured Values of Large Ions per Cubic Centimeter, N; Small Ions per Cubic Centimeter, n; and Calculated Values of Ions per Cubic Centimeter per Second, q. Before, during, and after encountering the atomic cloud (Easy Shot, 21 Apr. 51). Top, from 1346 to 1356 hours; bottom, from 1208 to 1218 hours.

[redacted]

[redacted]

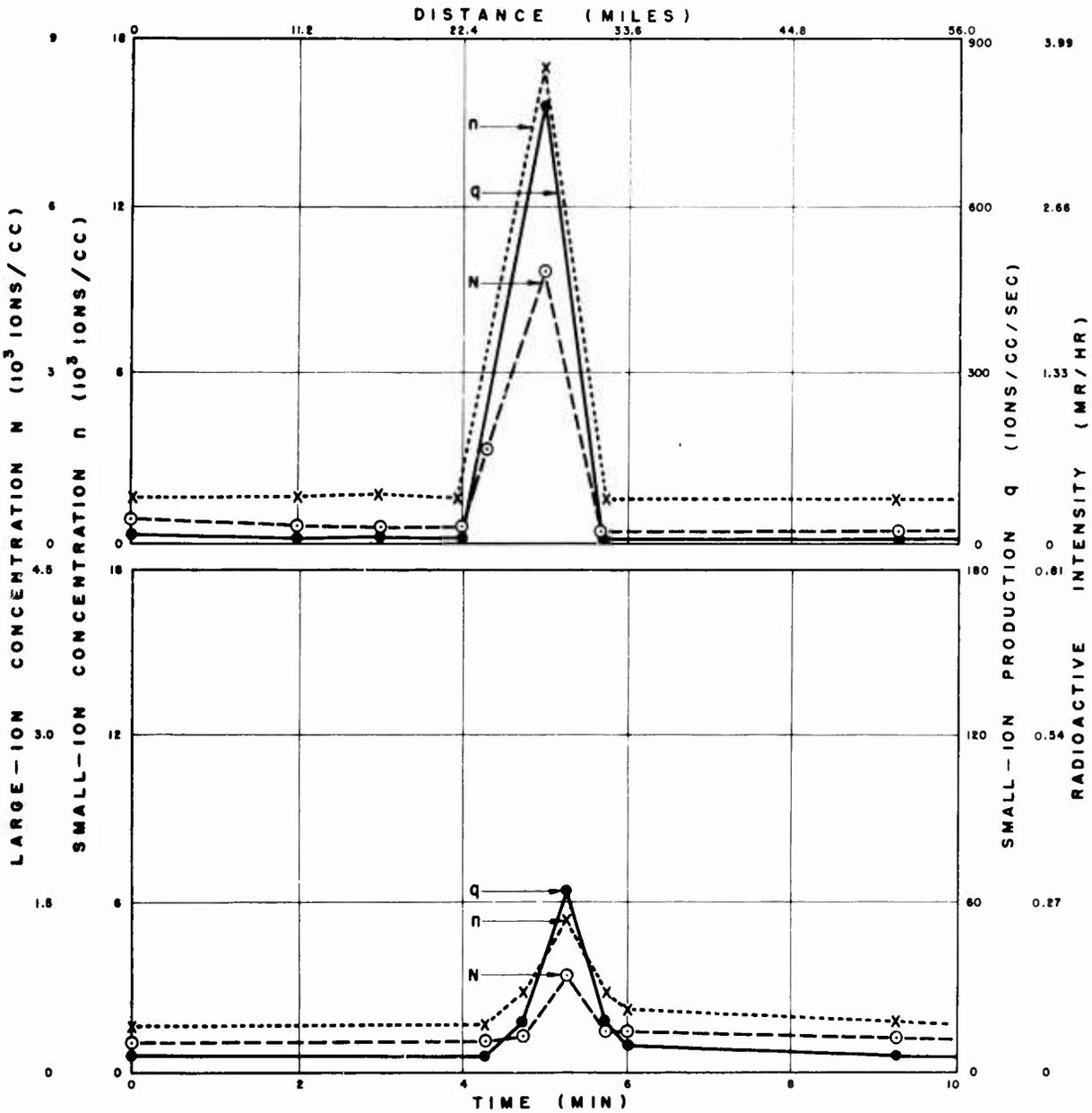

Fig. 3.5 Measured Values of Large Ions per Cubic Centimeter, N; Small Ions per Cubic Centimeter, n; and Calculated Values of Ions per Cubic Centimeter per Second, q. Before, during, and after encountering the atomic cloud (Dog Shot, 8 Apr. 51). Top, from 1109 to 1119 hours; bottom, from 1130 to 1140 hours.

[redacted]

[redacted]

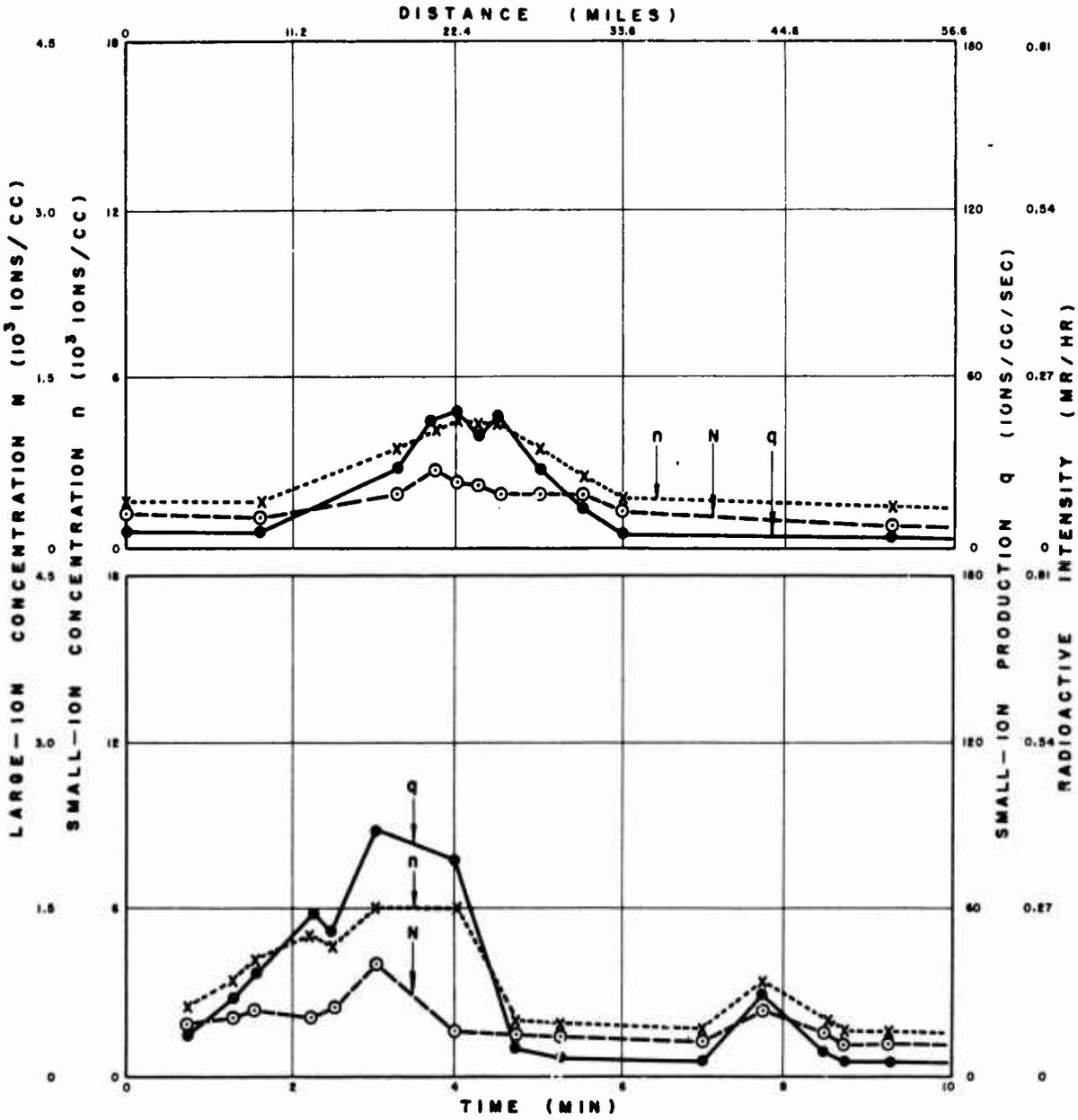

Fig. 3.6 Measured Values of Large Ions per Cubic Centimeter, N; Small Ions per Cubic Centimeter, n; and Calculated Values of Ions per Cubic Centimeter per Second, q. Before, during, and after encountering the atomic cloud (Dog Shot, 8 Apr. 51). Top, from 1142 to 1152 hours; bottom, from 1221 to 1231 hours.

[redacted]

[redacted]

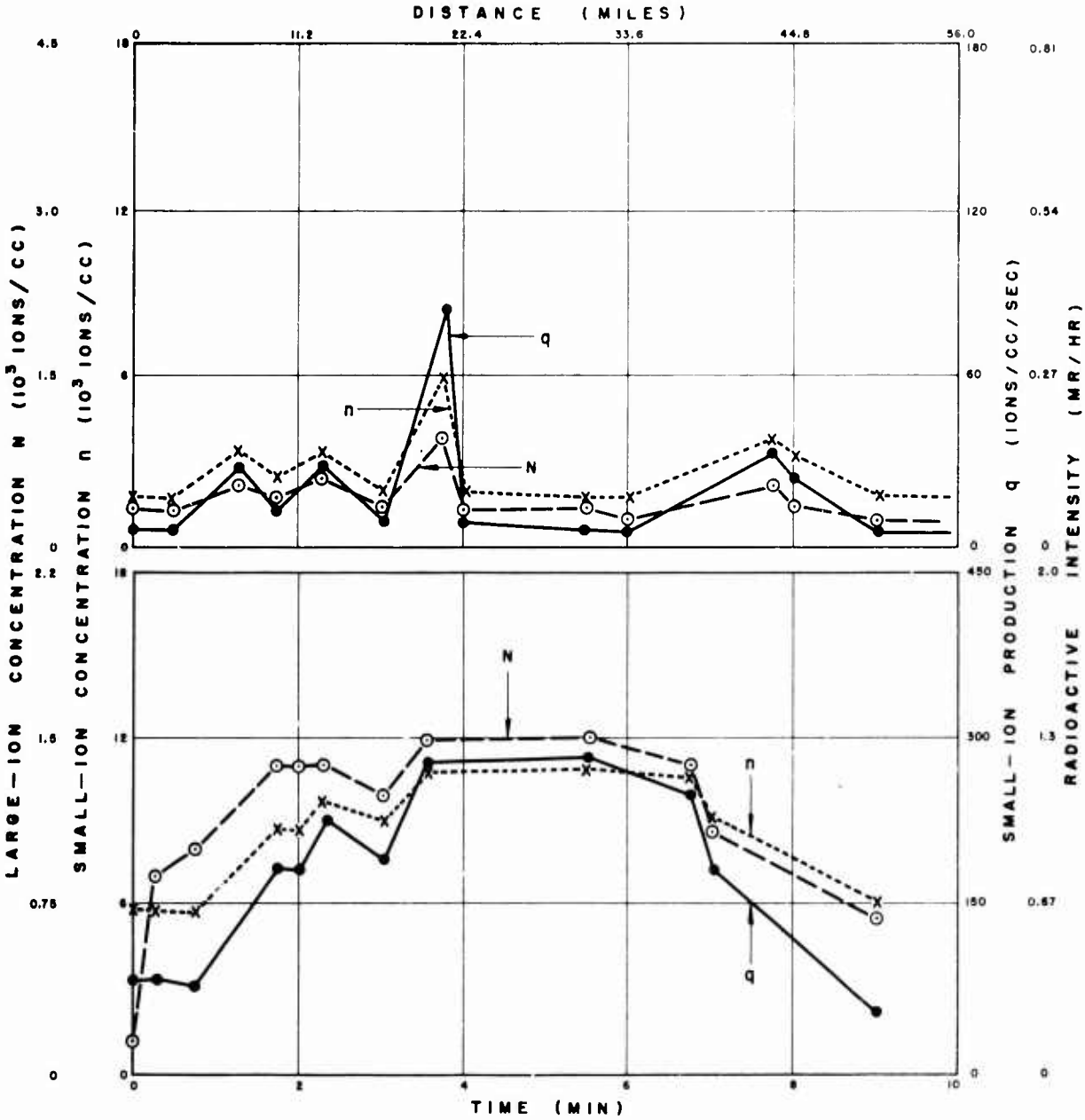

Fig. 3.7 Measured Values of Large Ions per Cubic Centimeter, N; Small Ions per Cubic Centimeter, n; and Calculated Values of Ions per Cubic Centimeter per Second, q. Before, during, and after encountering the atomic cloud (Dog Shot, 8 Apr. 51). Top, from 1230 to 1240 hours; bottom, from 1258 to 1308 hours.

[redacted]

[redacted]

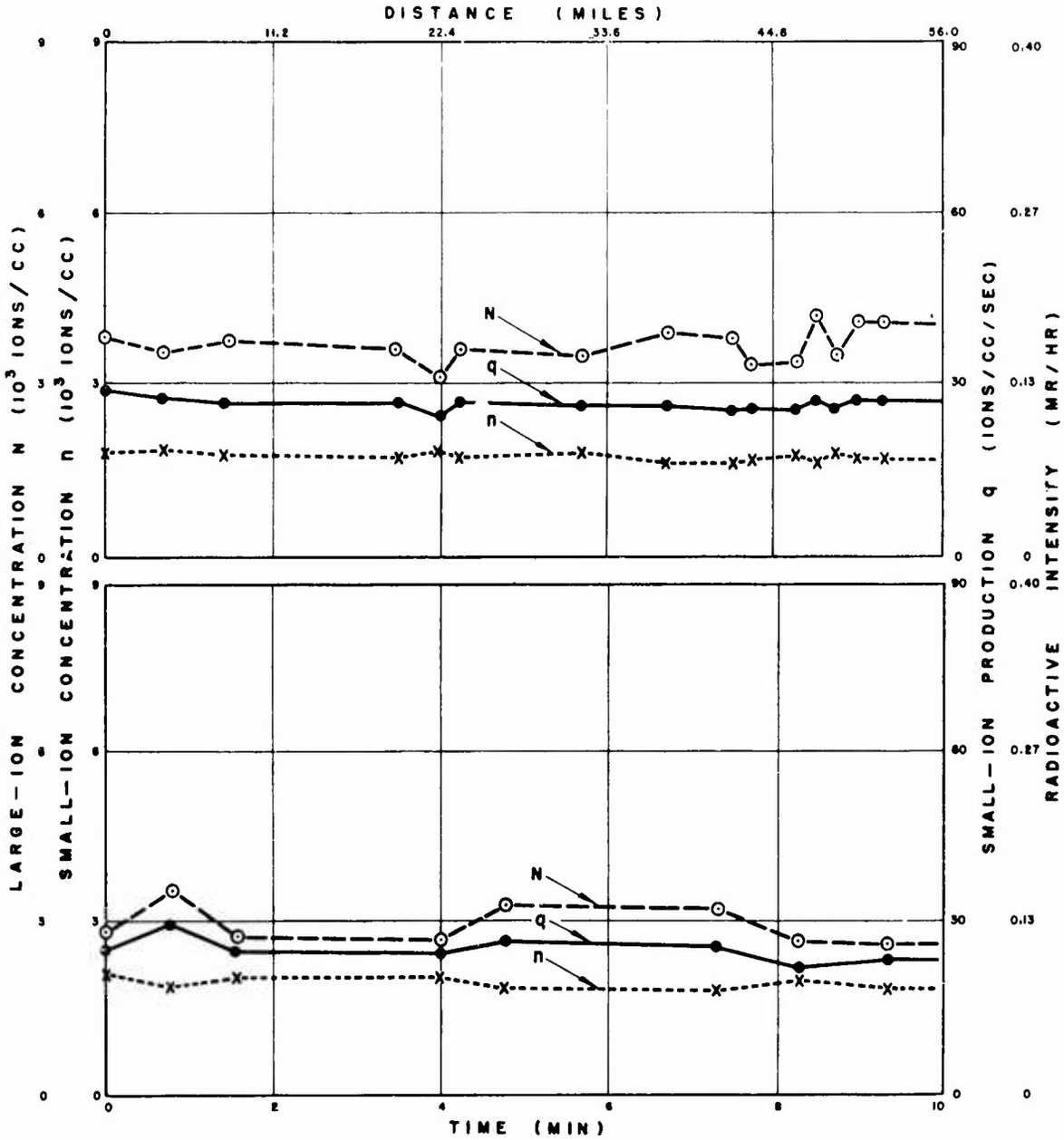

Fig. 3.8 Measured Values of Large Ions per Cubic Centimeter, N; Small Ions per Cubic Centimeter, n; and Calculated Values of Ions per Cubic Centimeter per Second, q. Before, during, and after encountering the atomic cloud (Dog Shot, 10 Apr. 51). Top, from 1502 to 1512 hours; bottom, from 1521 to 1531 hours.

[redacted]

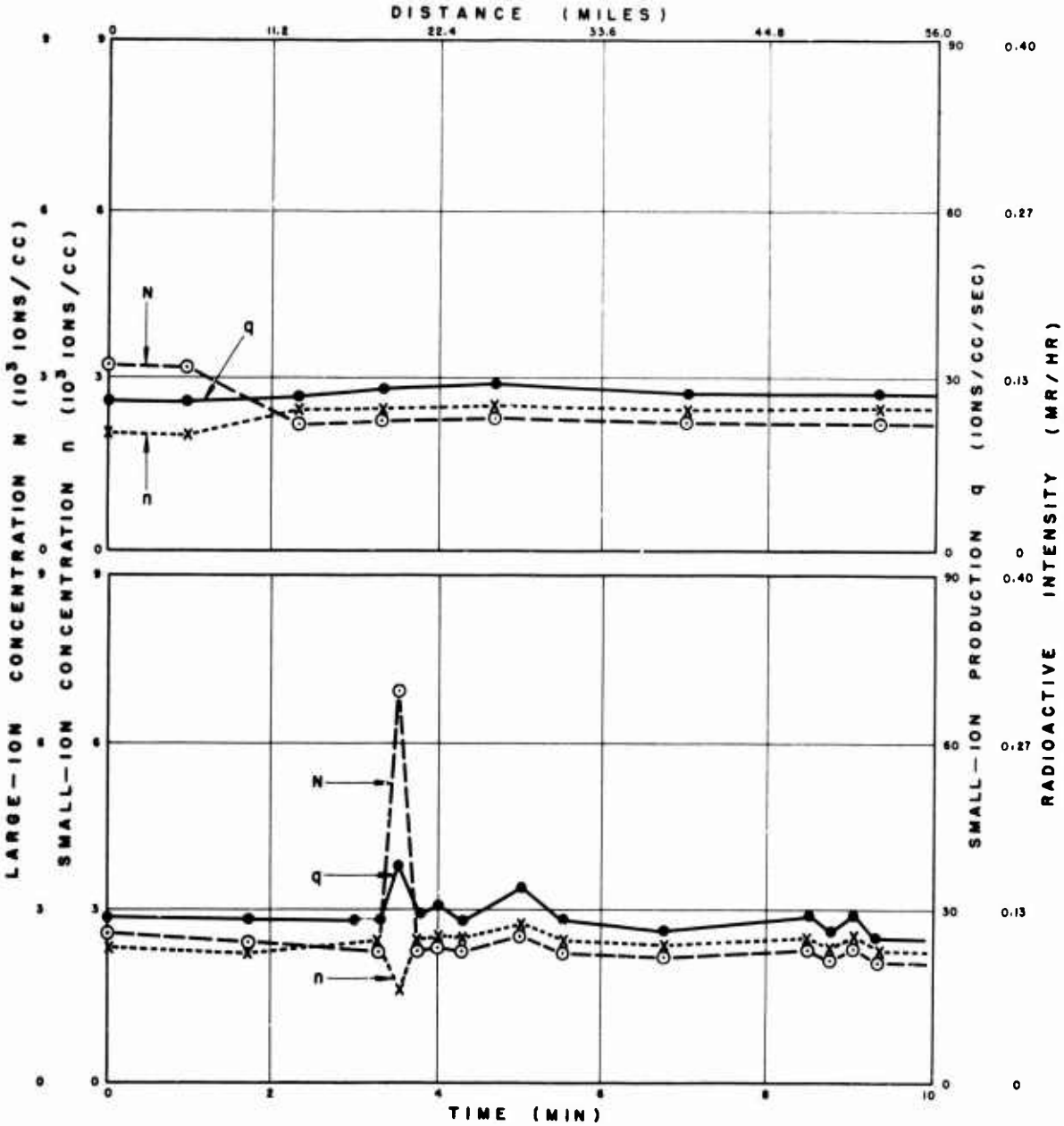

Fig. 3.9 Measured Values of Large Ions per Cubic Centimeter, N; Small Ions per Cubic Centimeter, n; and Calculated Values of Ions per Cubic Centimeter per Second, q. Before, during, and after encountering the atomic cloud (Dog Shot, 10 Apr. 51). Top, from 1608 to 1618 hours; bottom, from 1617 to 1627 hours.

[redacted]

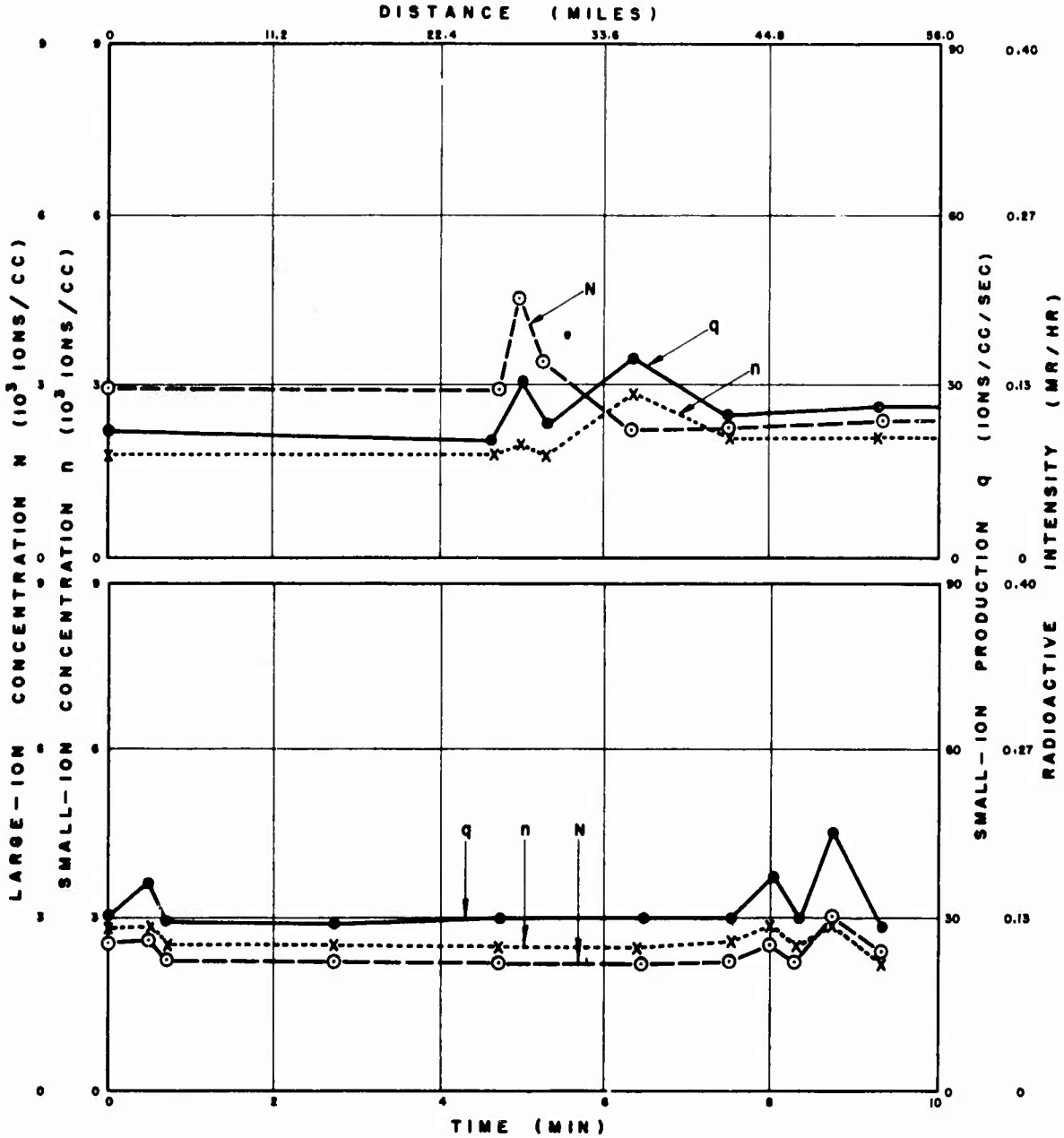

Fig. 3.10 Measured Values of Large Ions per Cubic Centimeter, N; Small Ions per Cubic Centimeter, n; and Calculated Values of Ions per Cubic Centimeter per Second, q. Before, during, and after encountering the atomic cloud (Dog Shot, 10 Apr. 51). Top, from 1242 to 1252 hours; bottom, from 1354 to 1404 hours.

[redacted]

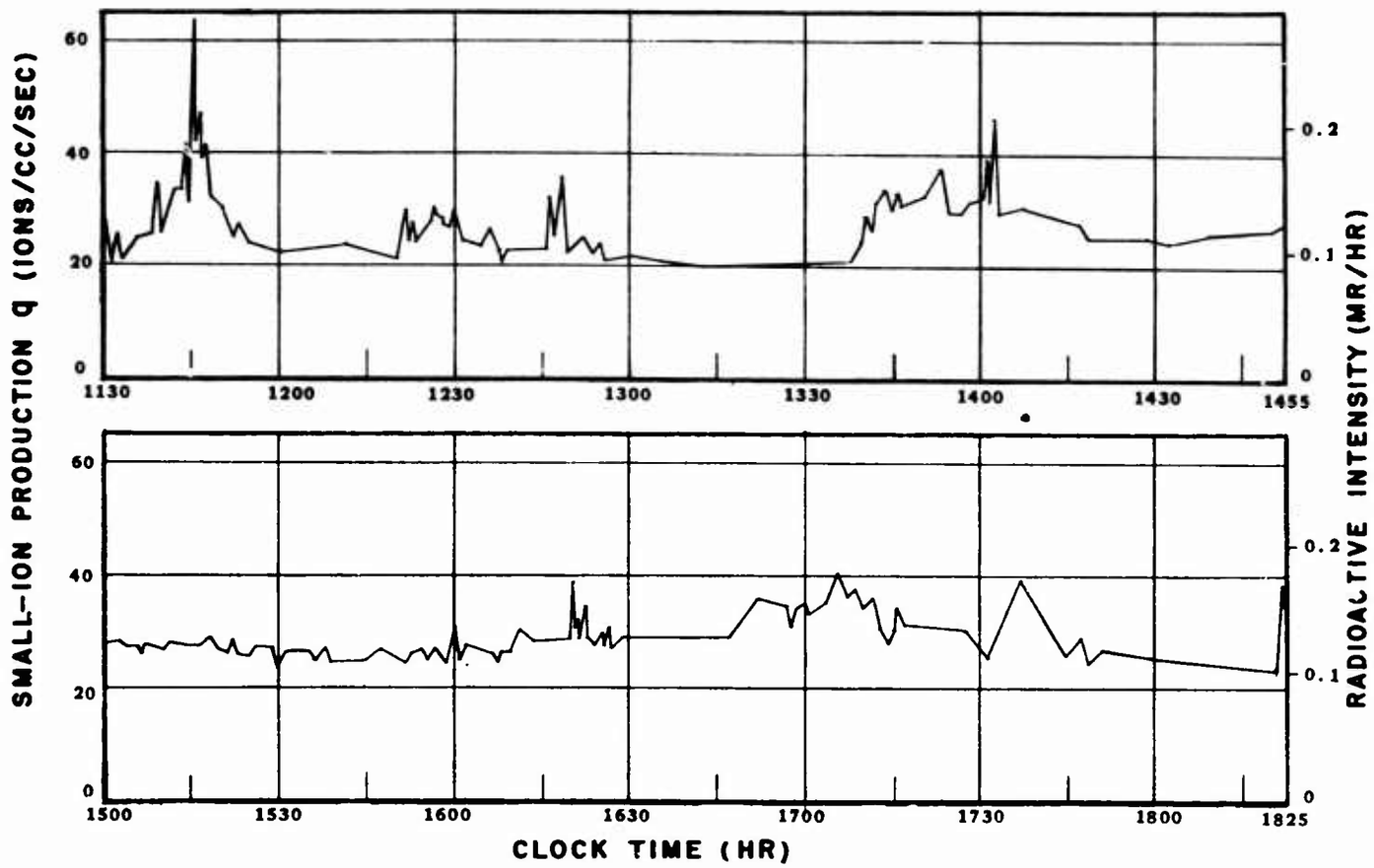

Fig. 3.11 Calculated Values of Ions per Cubic Centimeter per Second, q, vs Time (Dog Shot, H+52 to H+60)

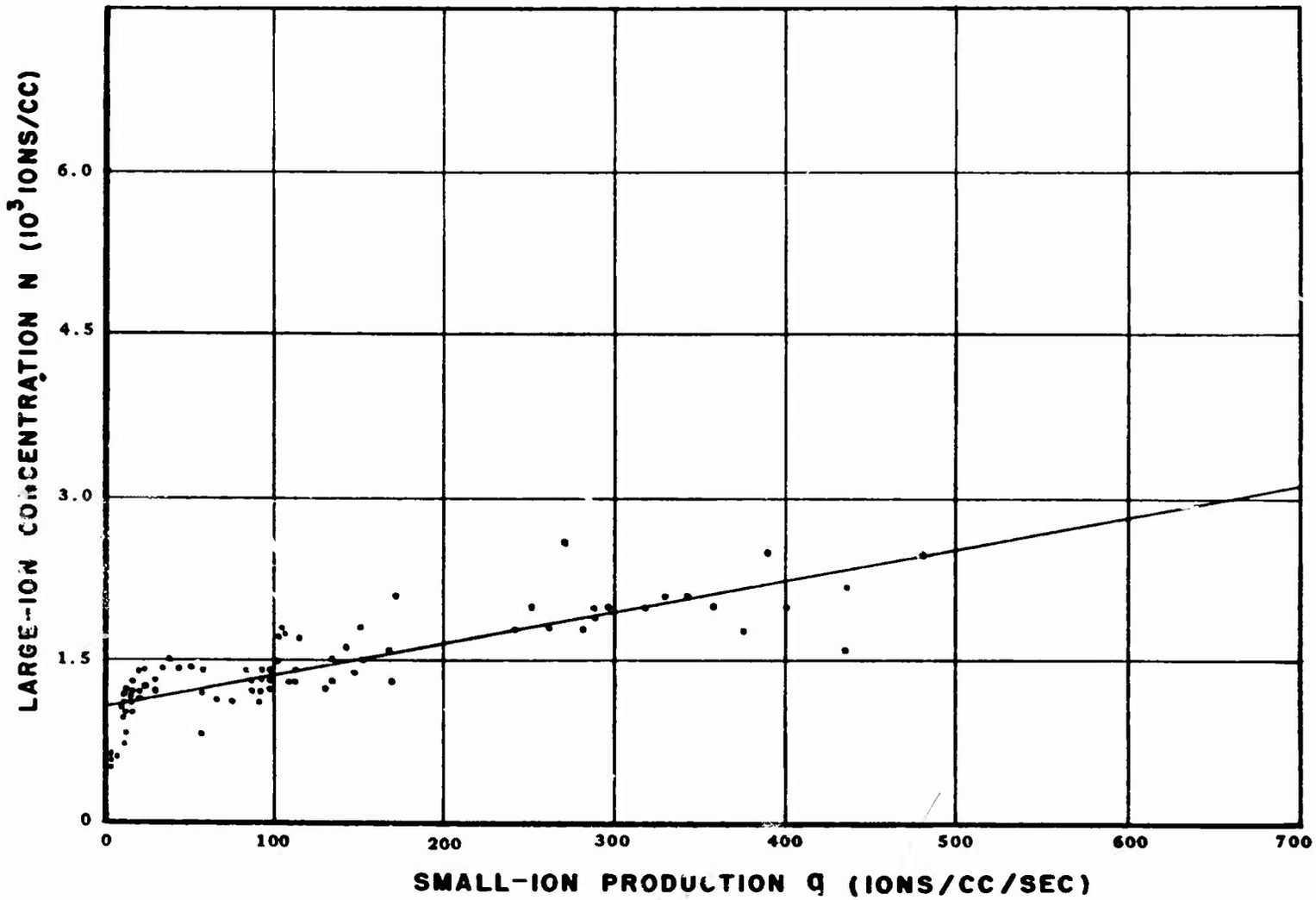

Fig. 3.12 Plot for Obtaining K, the Quantity of Radioactive Matter per Large-ion Particle, from the Relation $KN = \alpha n^2 + 2\eta Nn = q$ (Easy Shot, 21 Apr. 51)

[redacted]

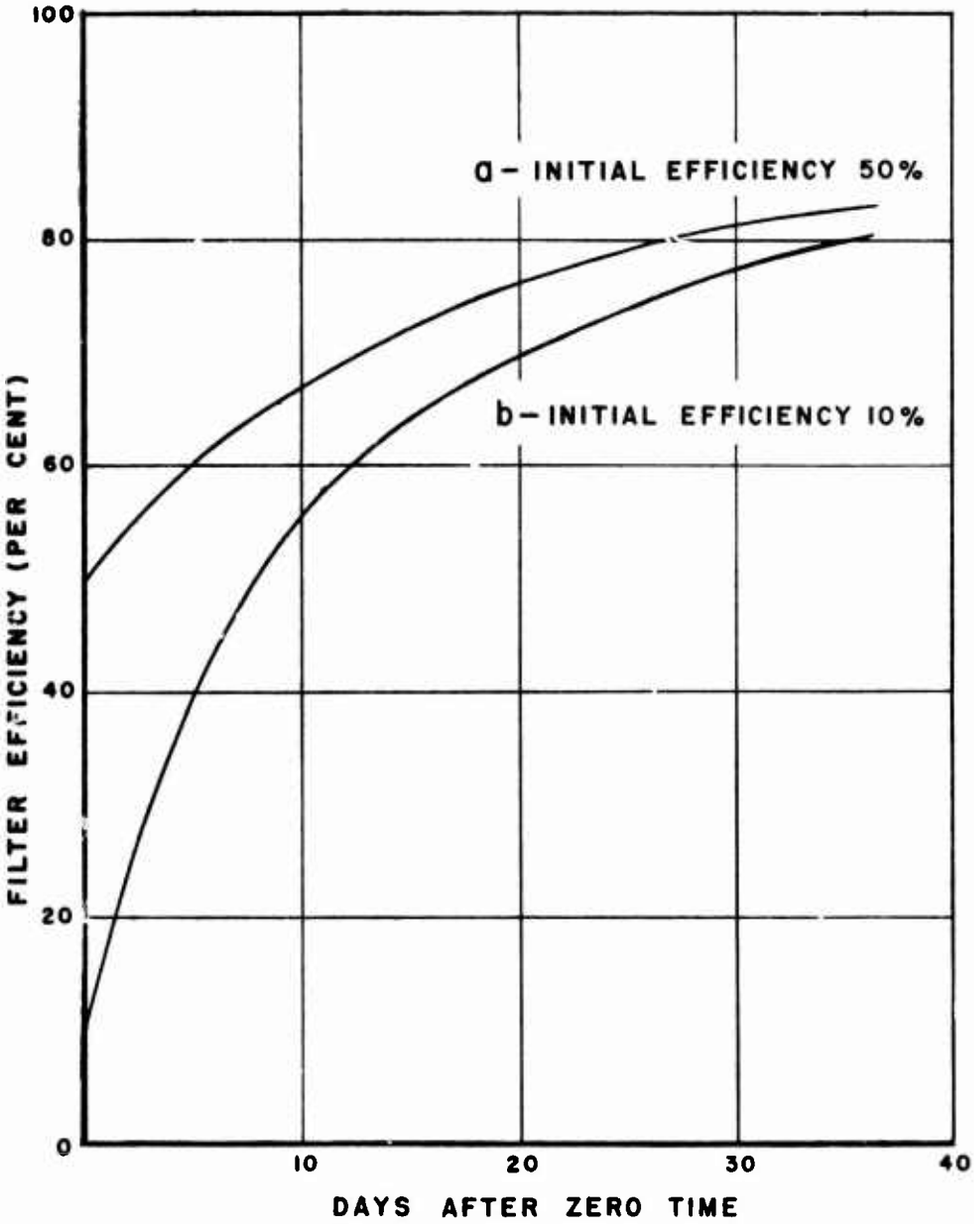

Fig. 3.13 Variation with Time of Filter Efficiency Due to Agglomeration between Radioactive Particles of Micron Size and Large-ion Size

[redacted]

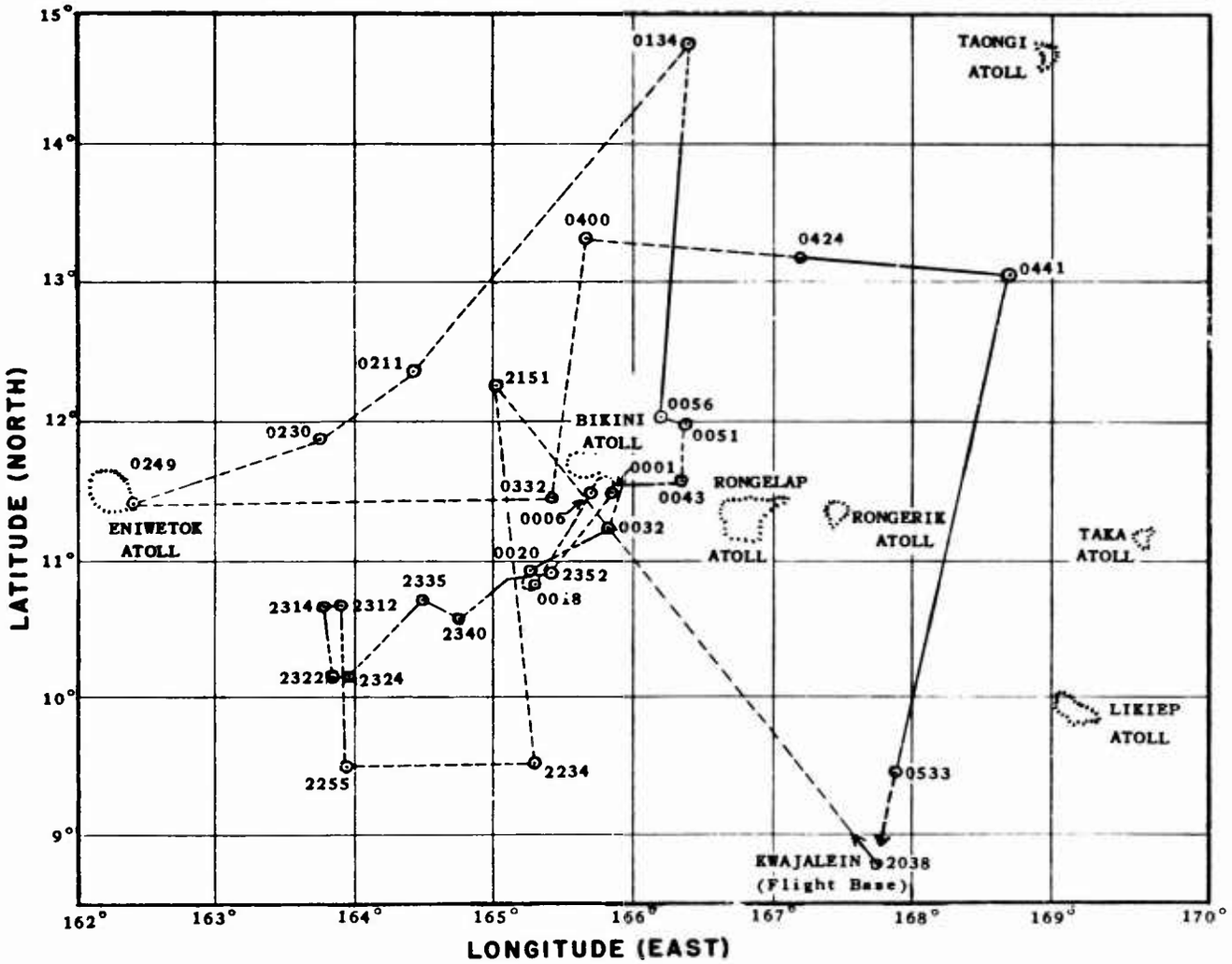

Fig. 3.14 Flight Path for Dog Shot, H+2 to H+11 Hr

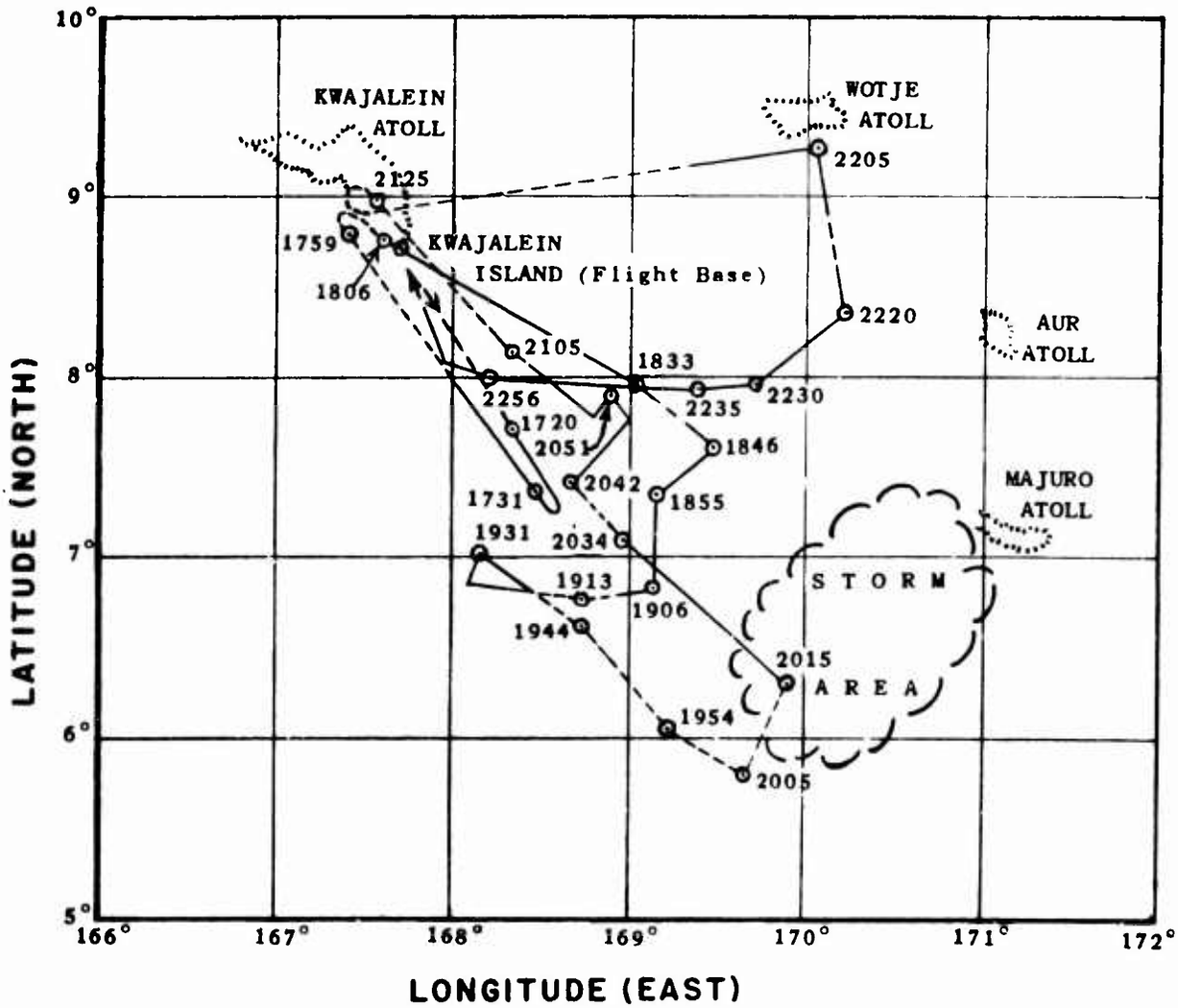

Fig. 3.15 Flight Path for Dog Shot, H+24 to H+30 Hr

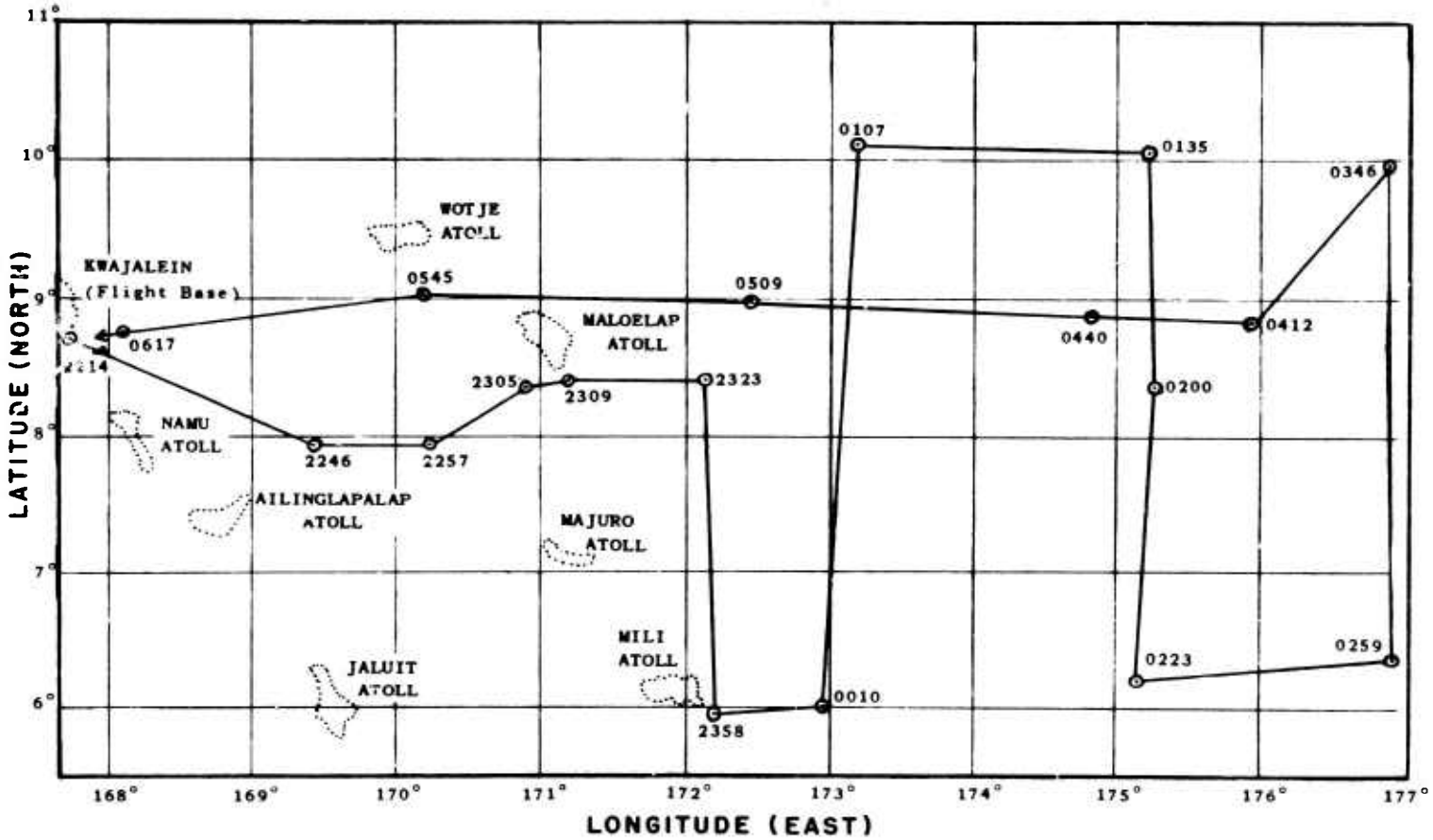

Fig. 3.16 Flight Path for Dog Shot, H+52 to H+60 Hr

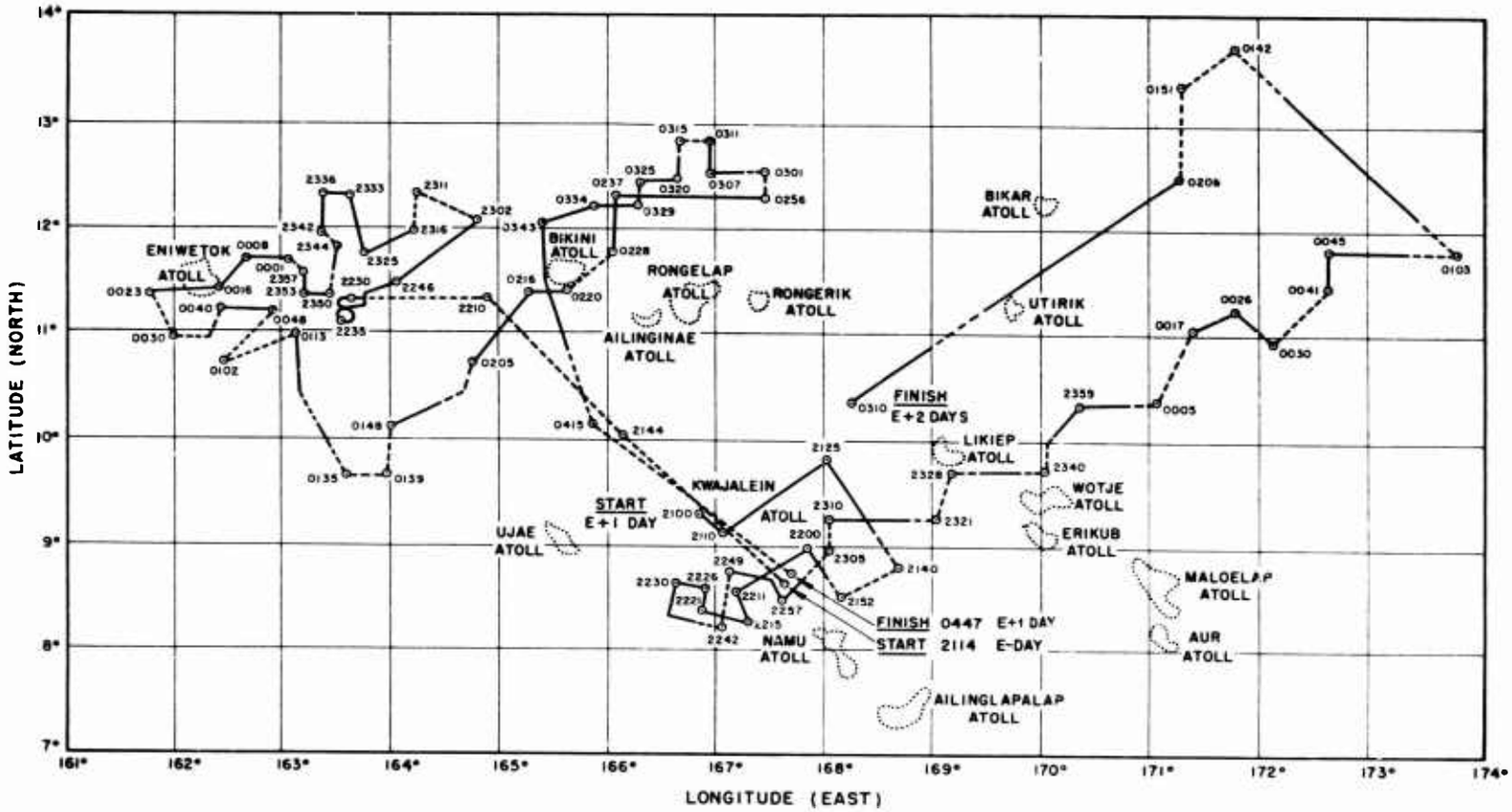

Fig. 3.17 Flight Paths for Easy Shot. Left, H+2 to H+9 hr; right, H+26 to H+32 hr.

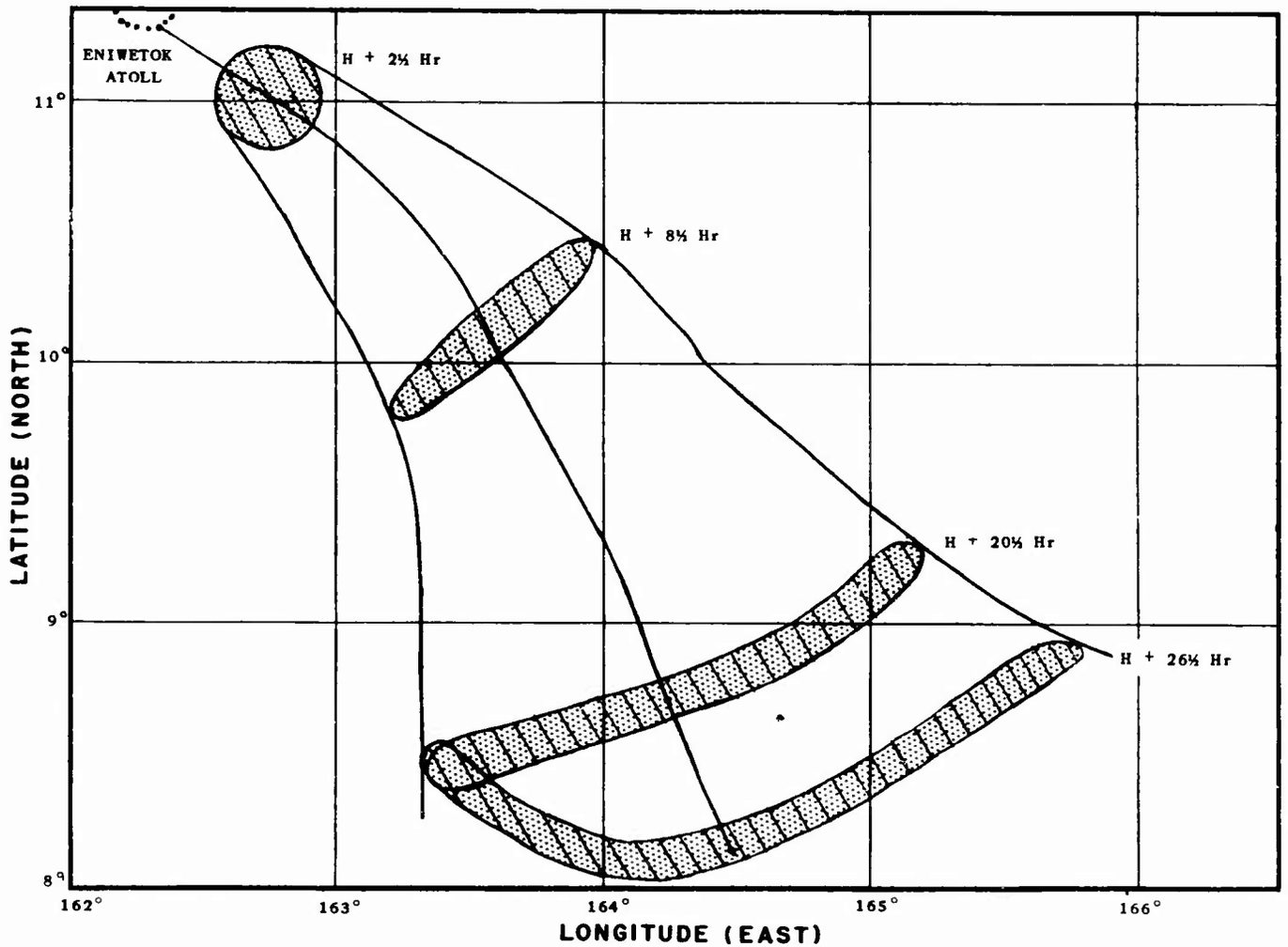

Fig. 3.18 Cloud Positions at 25,000 Ft Predicted from Observed Winds at That Altitude (Easy Shot)

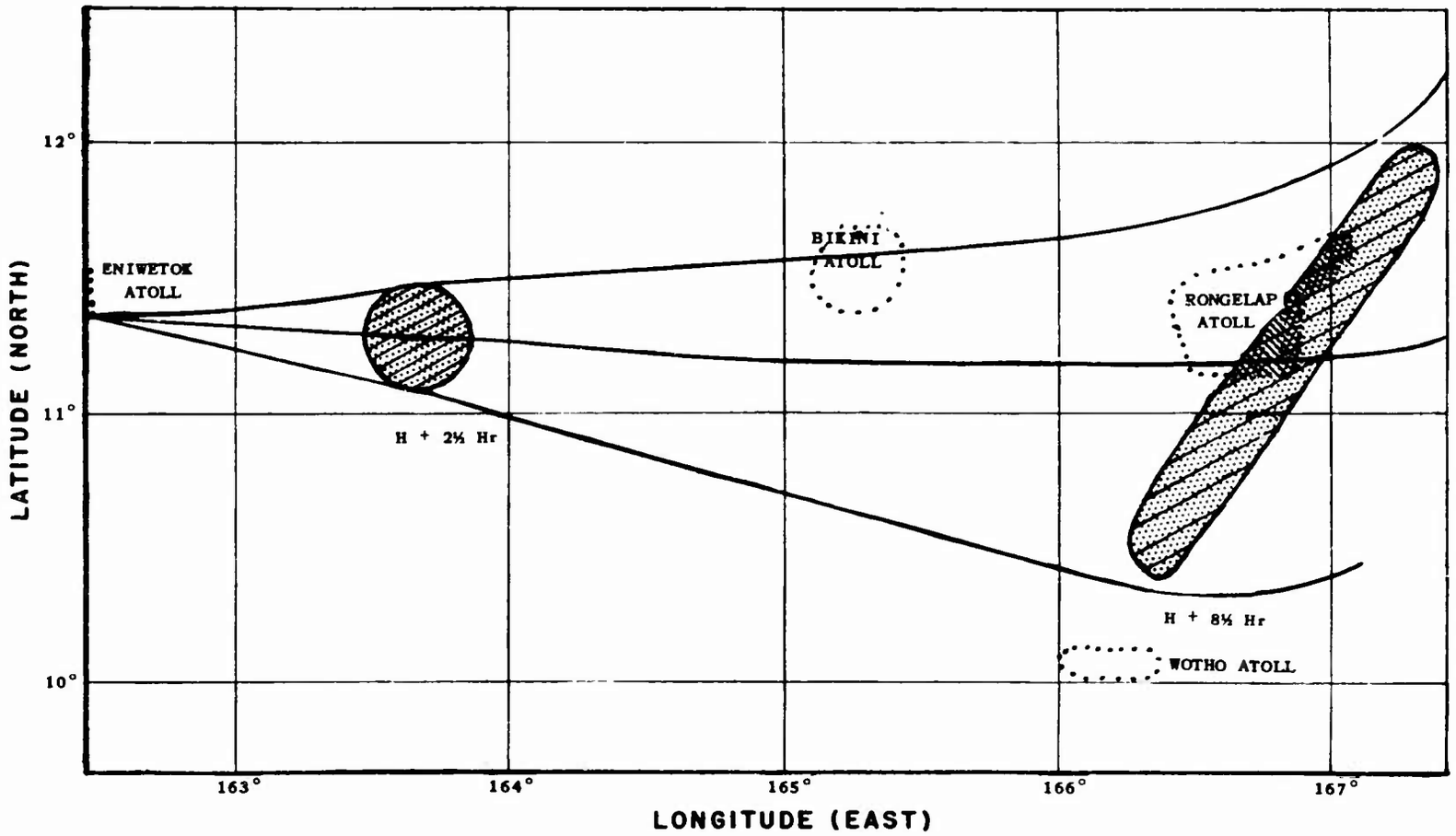

Fig. 3.19 Cloud Positions at 35,000 Ft Predicted from Observed Winds at That Altitude (Easy Shot)

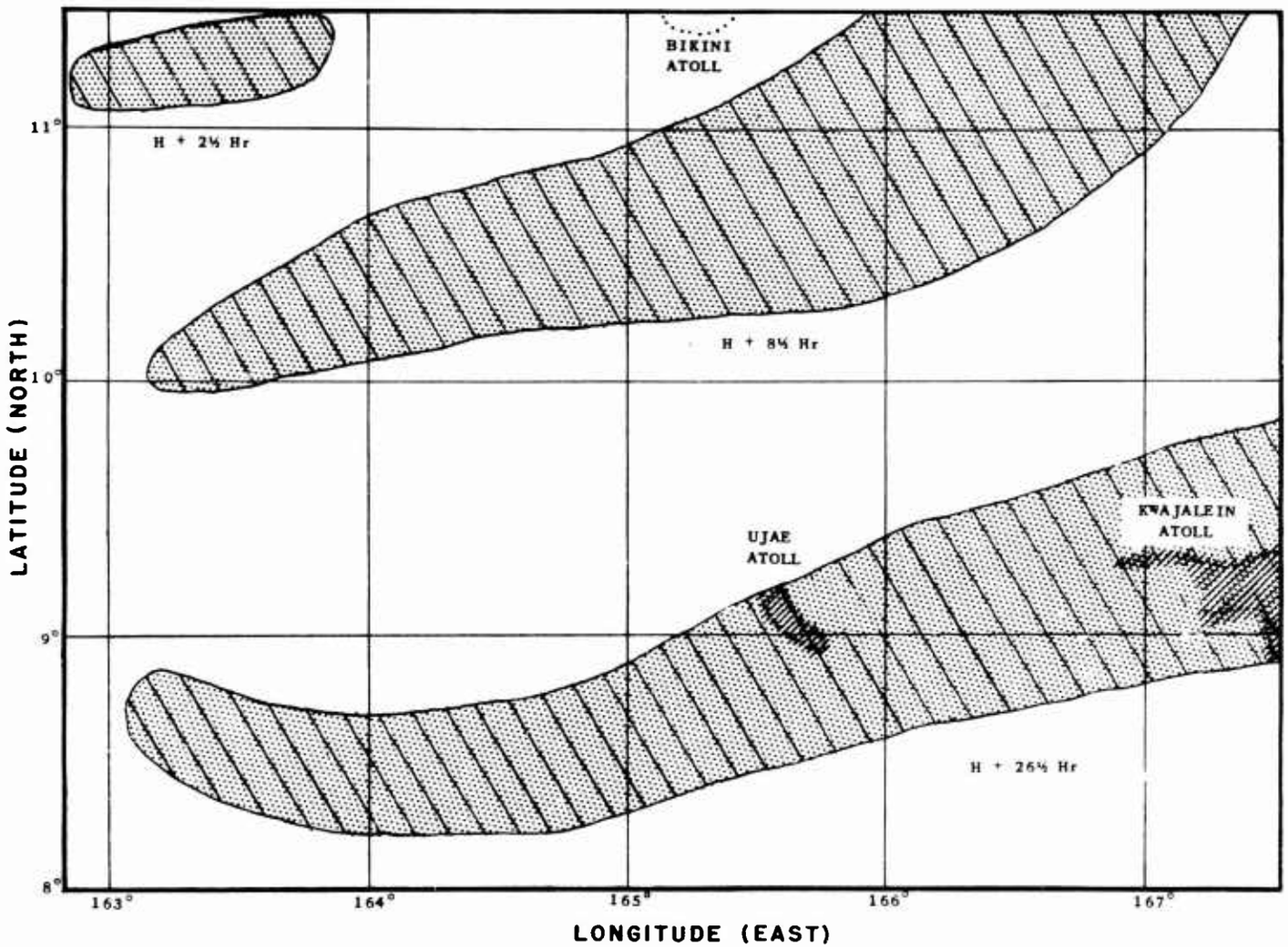

Fig. 3.20 Predicted Cloud Positions at 25,000 Ft Assuming That Vertical Mixing Occurs within the Layer between 25,000 and 40,000 Ft (Easy Shot)

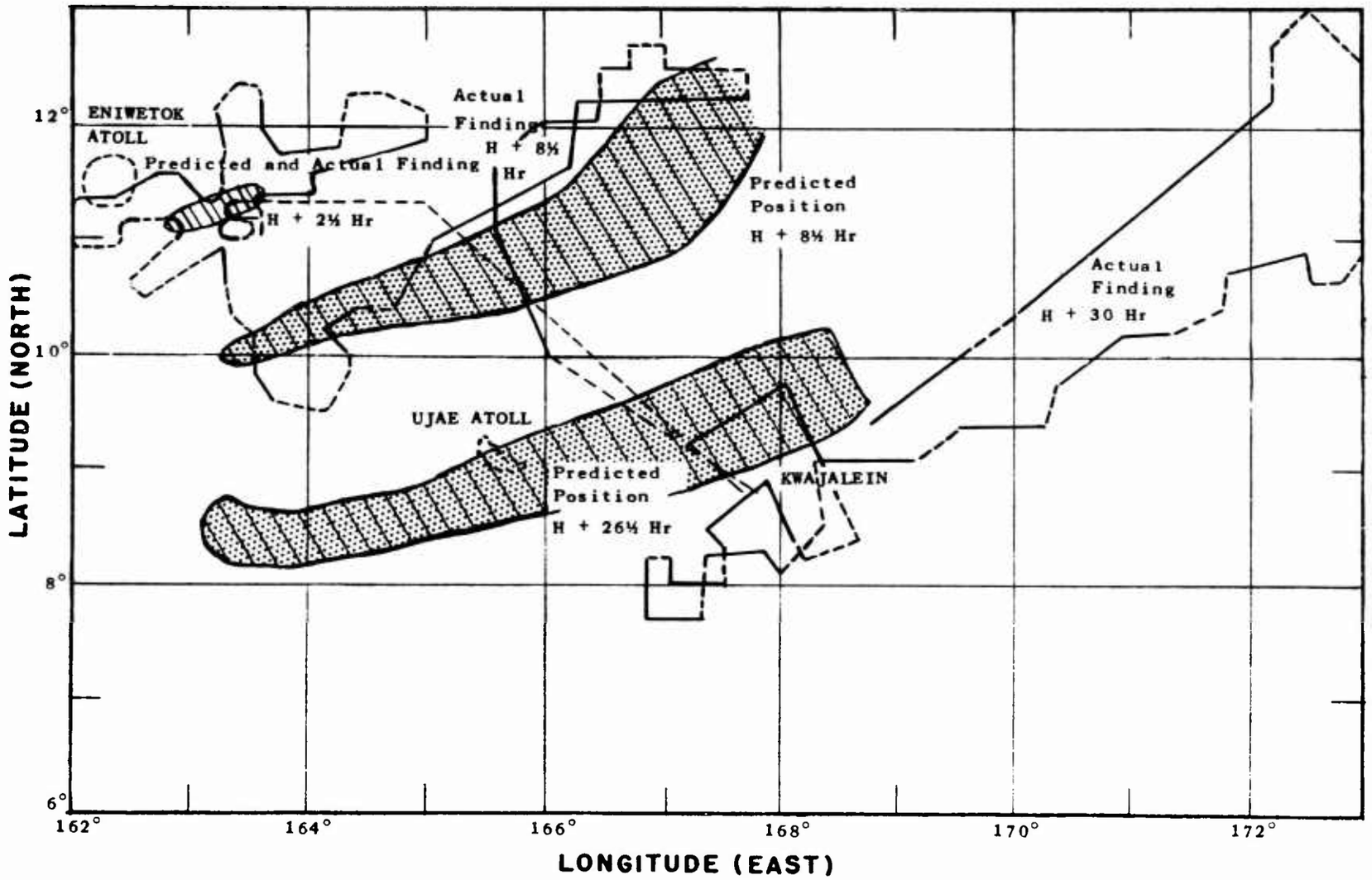

Fig. 3.21 Predicted and Actual Cloud Positions at 25,000 Ft (Easy Shot). ▨, predicted; ----, actual.

[redacted]

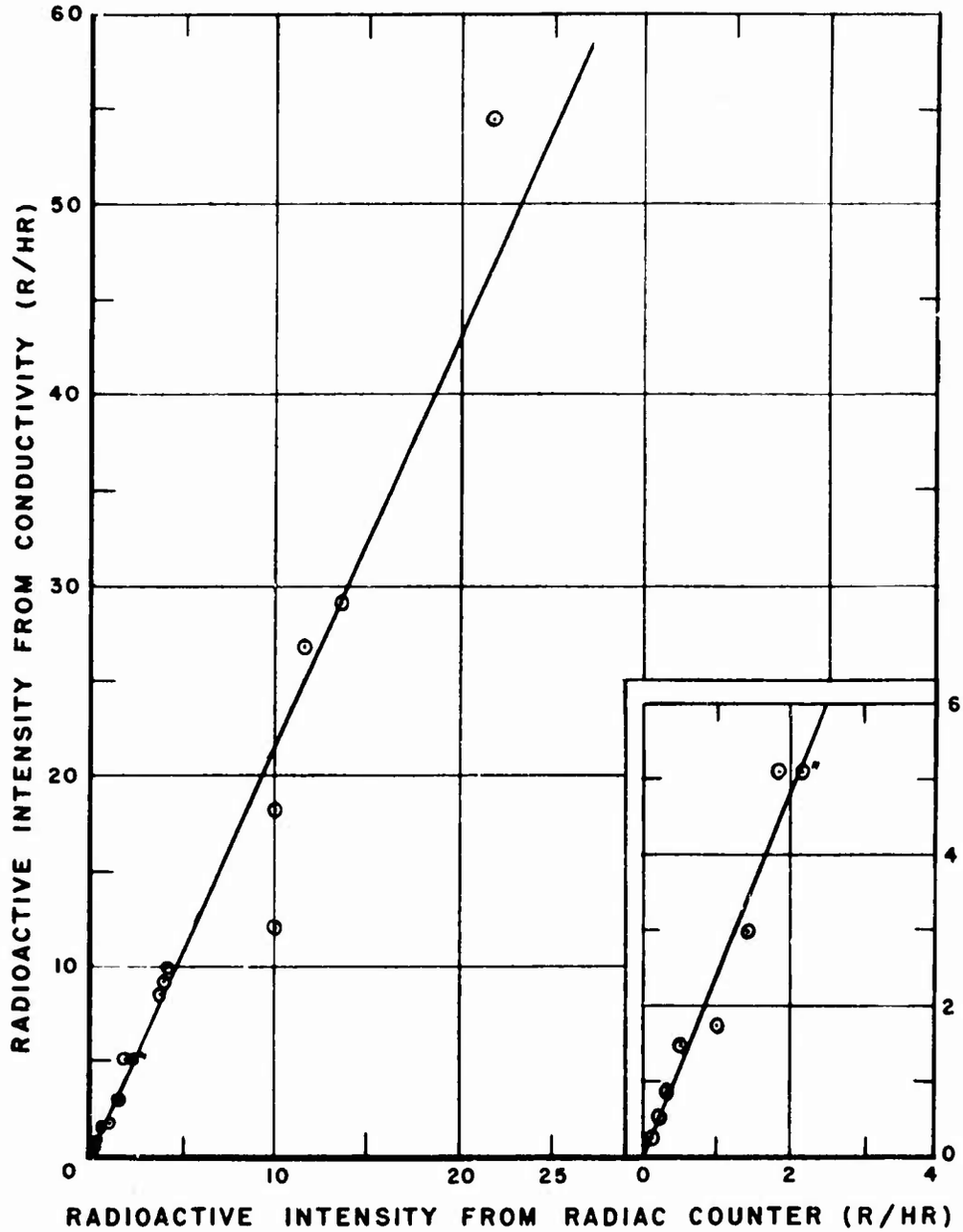

Fig. 3.22 Comparison of Conductivity and Radiac AN/PDR-T1B Counter Readings in Roentgens per Hour for George Shot. Insert: scale expanded. Data were obtained at various altitudes from 100 to 3000 ft on G to G+7 days.

[redacted]

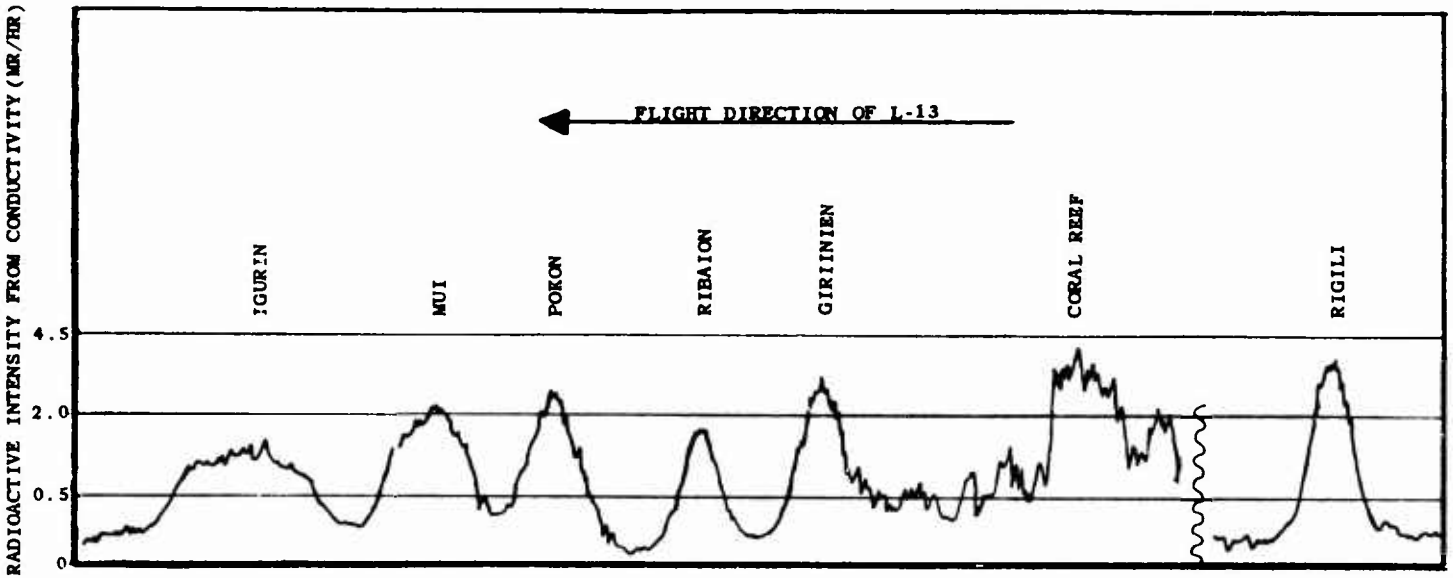

Fig. 3.23 Fall-out, Dog Shot, H+10 Hr, Altitude 1000 Ft

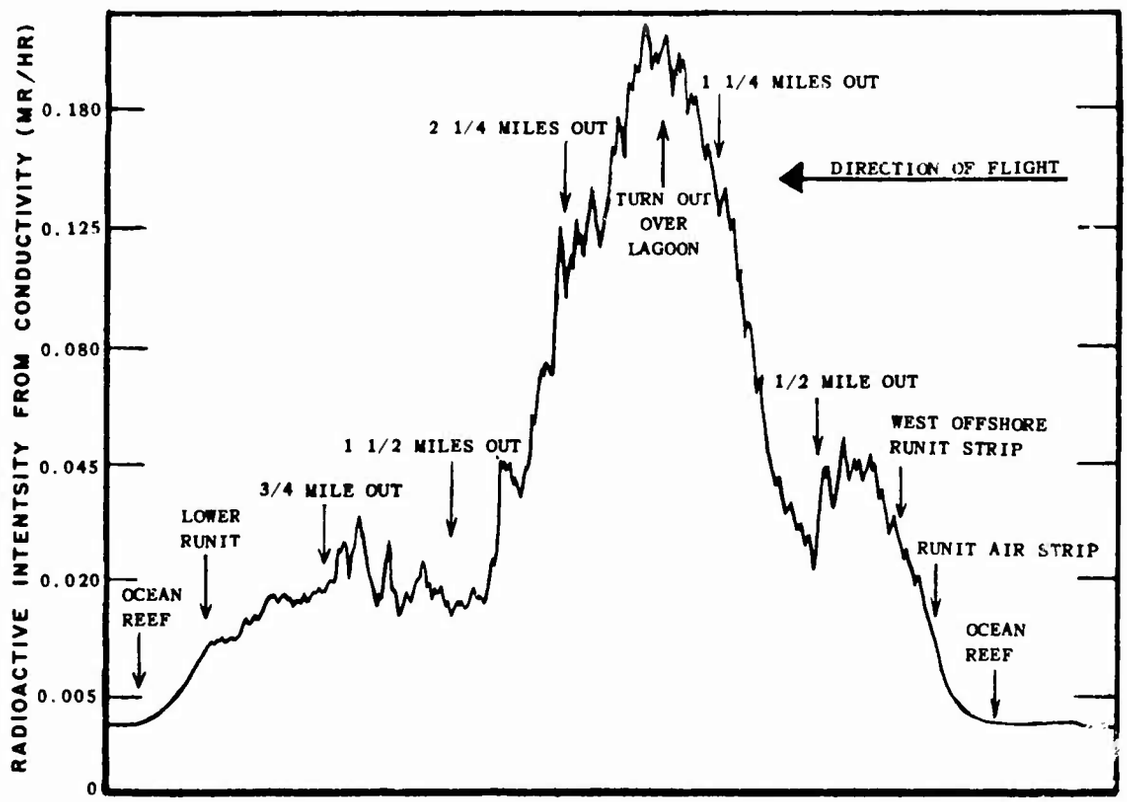

Fig. 3.24 Example of Fall-out on Pinnacle near Runit Shot Island at an Altitude of 500 Ft on D+3 Days

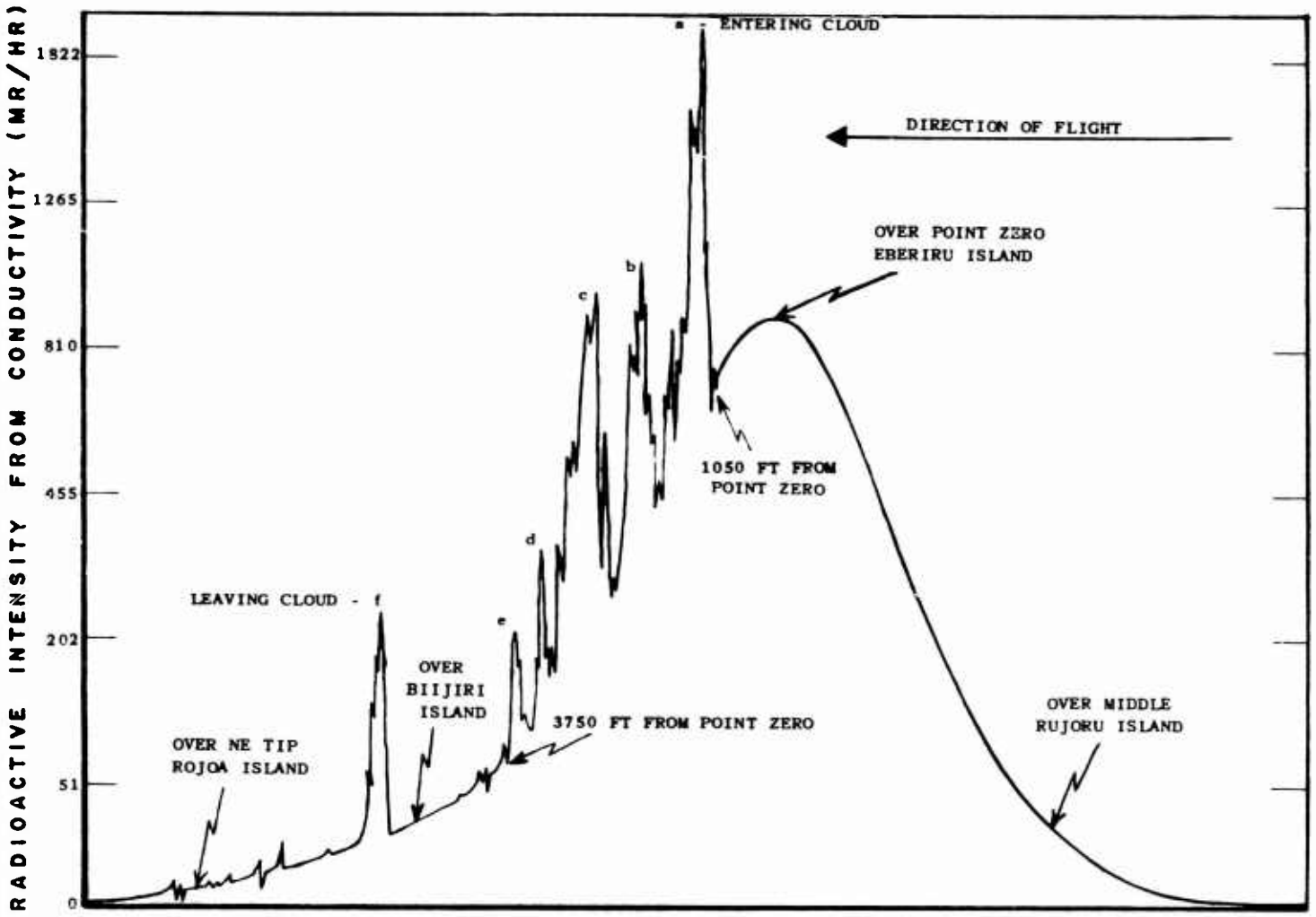

Fig. 3.25 Pass through Building Cumulus Cloud, Base 1500 Ft, Height 4500 Ft, near George Shot Island at an Altitude of 3000 Ft on G-Day, H+6 Hr

[redacted]

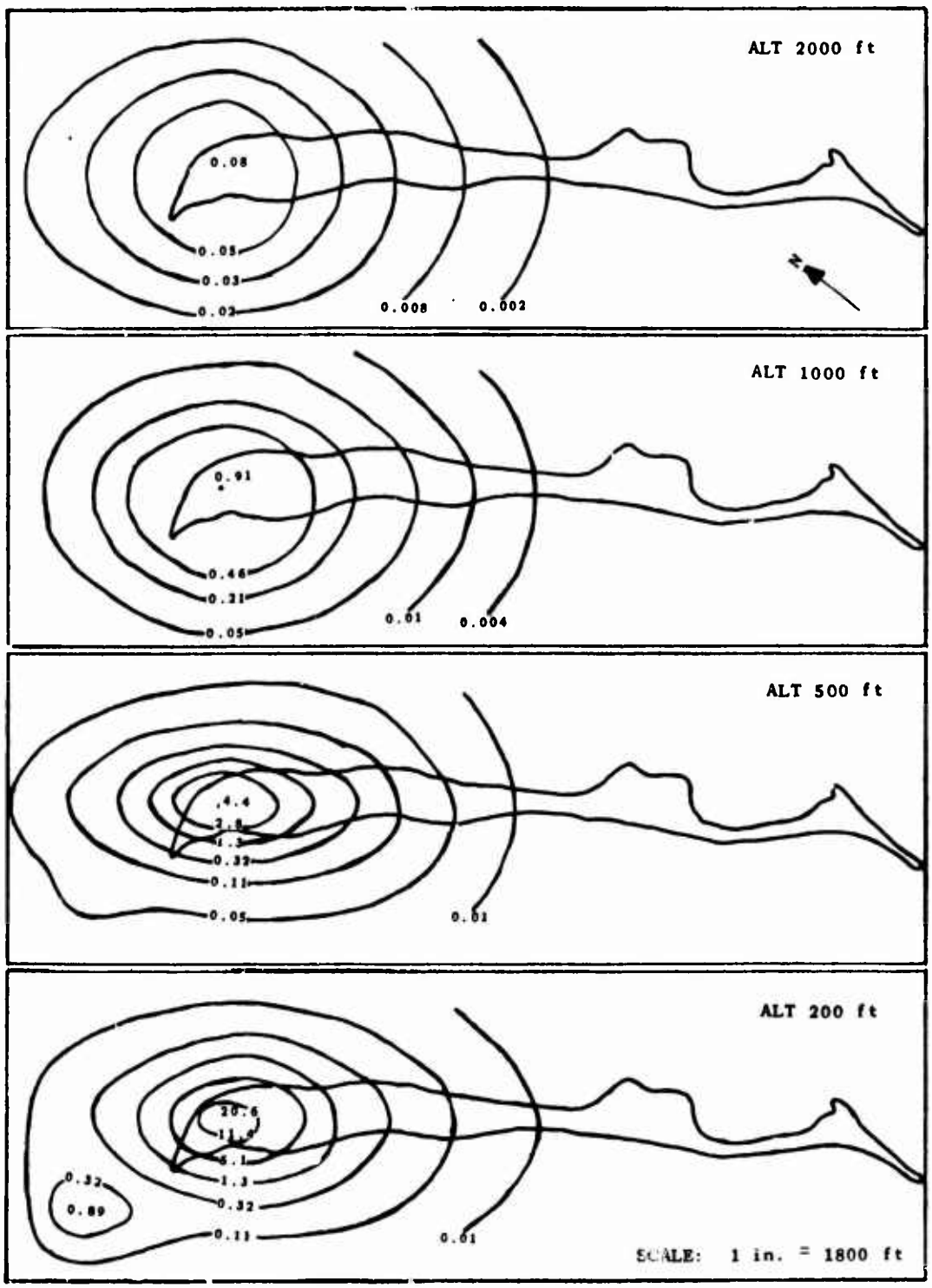

Fig. 3.26 Contour Maps of Radioactivity over Runit Shot Island at Various Altitudes on D+3 Days. Contour lines are expressed in roentgens per hour.

[redacted]

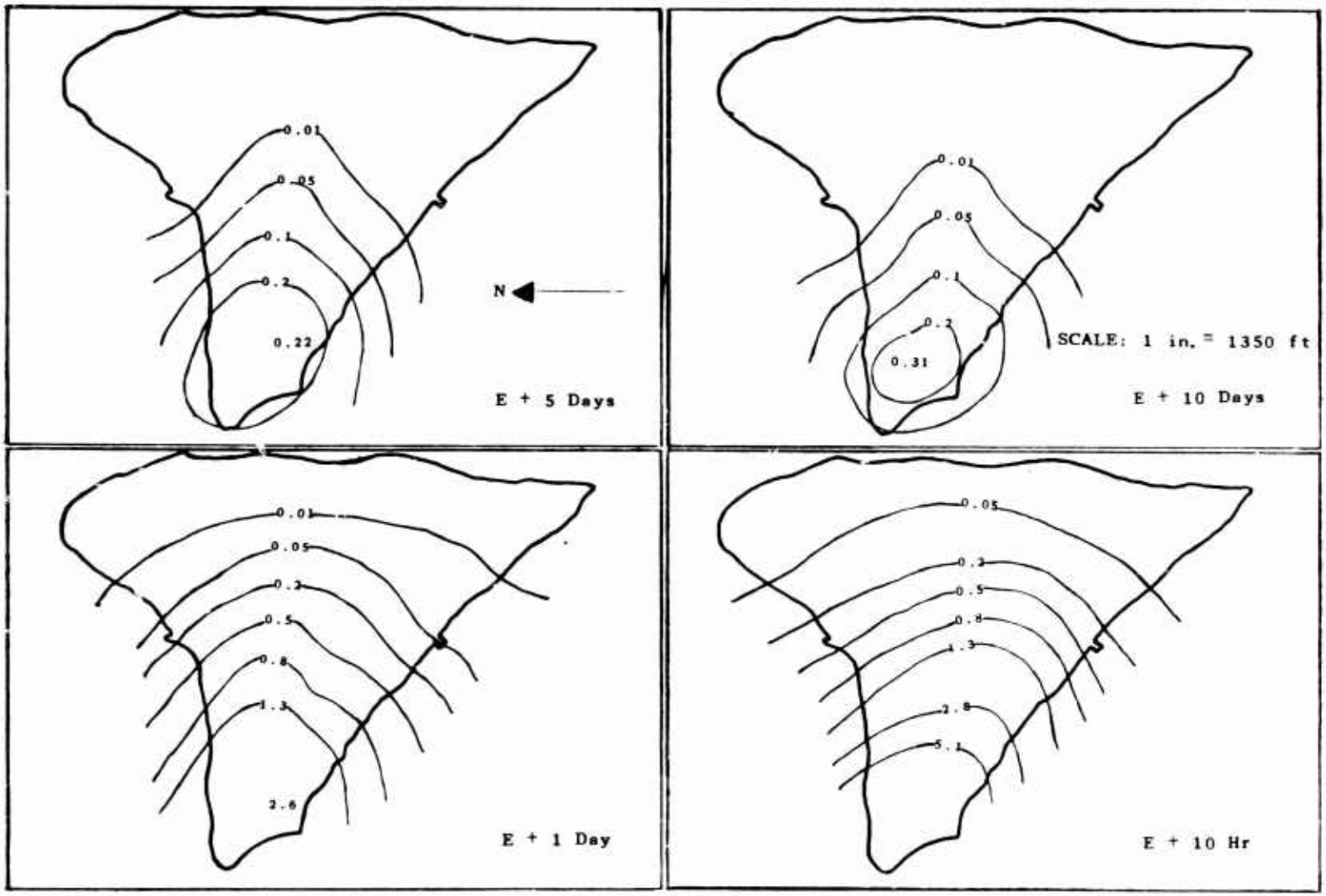

Fig. 3.27 Contour Maps of Radioactivity over Engebi Shot Island at Altitude of 500 Ft for Different Times. Contour lines are expressed in roentgens per hour.

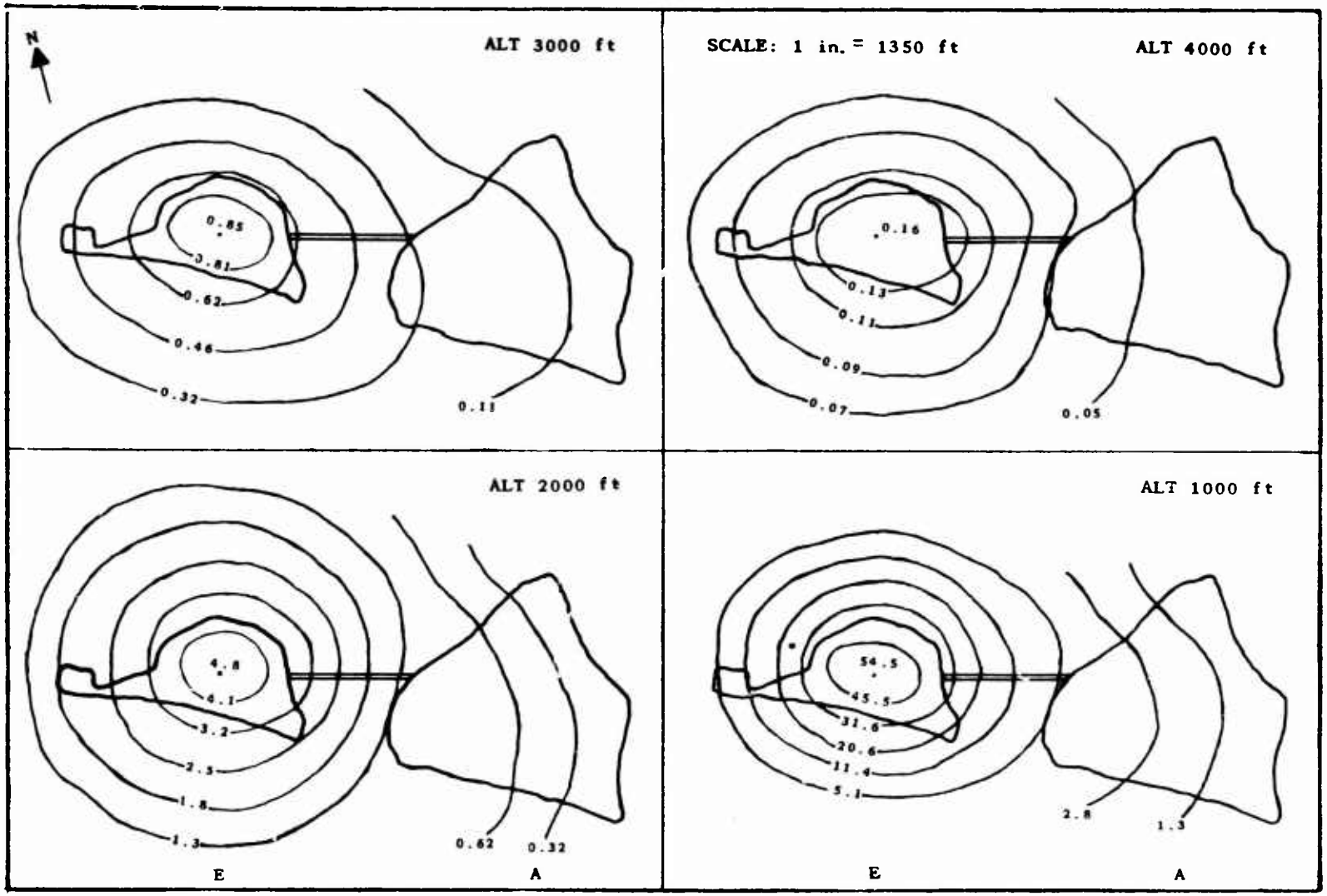

Fig. 3.28 Contour Maps of Radioactivity over Shot Island at Various Altitudes on G-Day, H+6 Hr. Contour lines are expressed in roentgens per hour. E, Eberiru Island; A, Aomon Island.

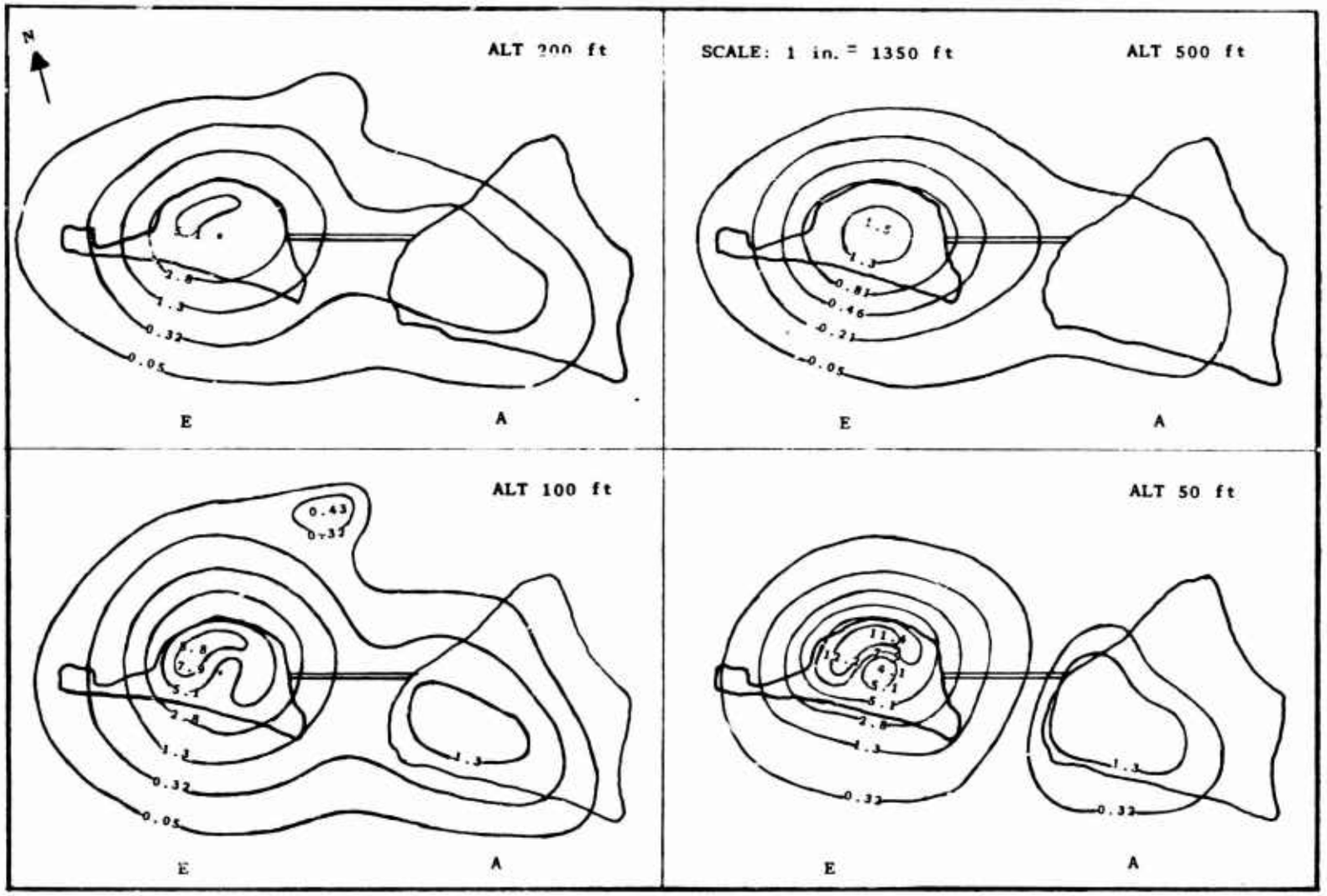

Fig. 3.29 Contour Maps of Radioactivity over Shot Island at Lower Altitudes on G+7 Days. Contour lines are expressed in roentgens per hour. E, Eberiru Island; A, Aomon Island.

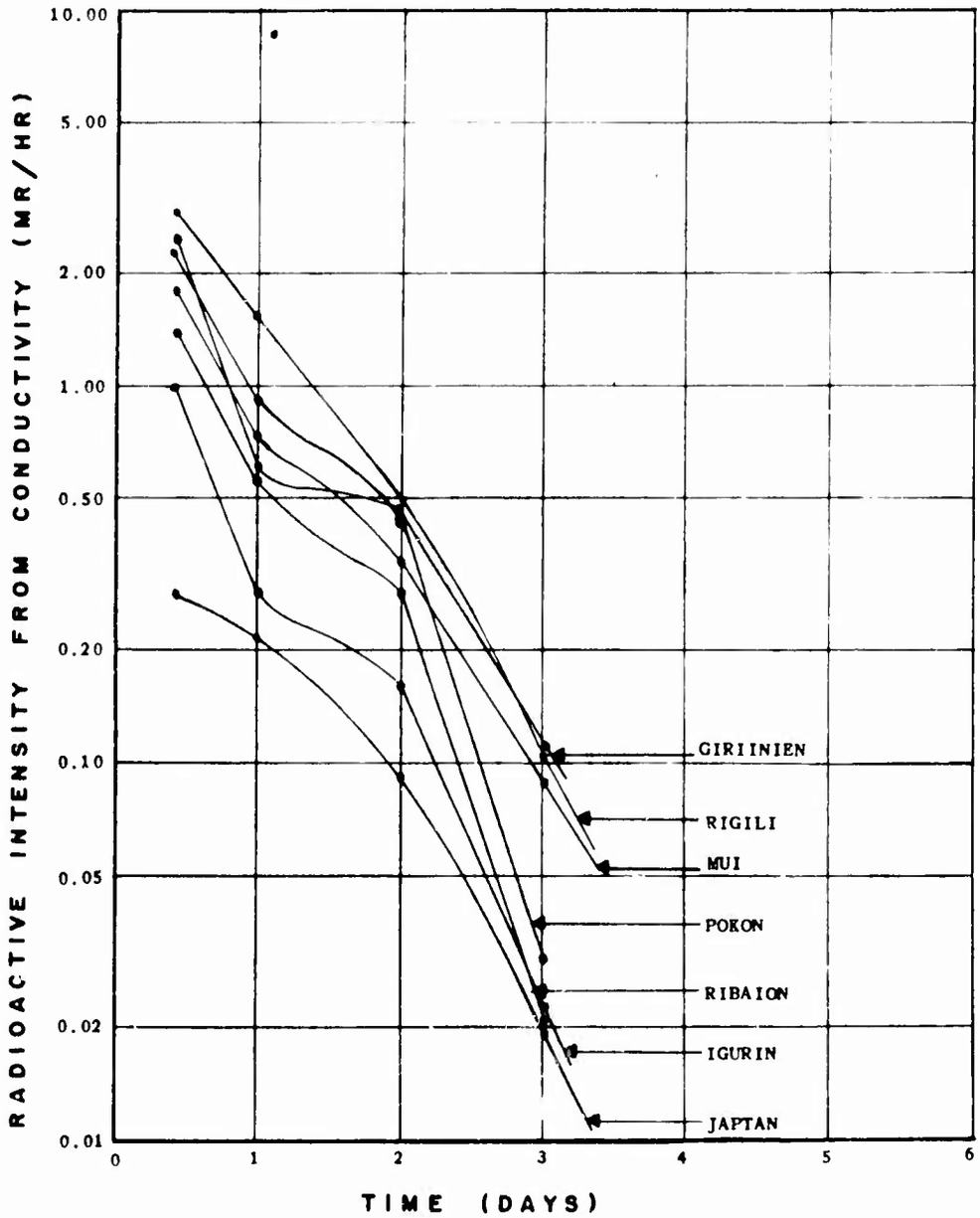

Fig. 3.30 Decline in Activity Due to Decay of Induced Radiation and Fall-out Material from Conductivity Measurements at Certain Fixed Altitudes over Shot and Adjacent Islands (Dog Shot, 1000 Ft)

[redacted]

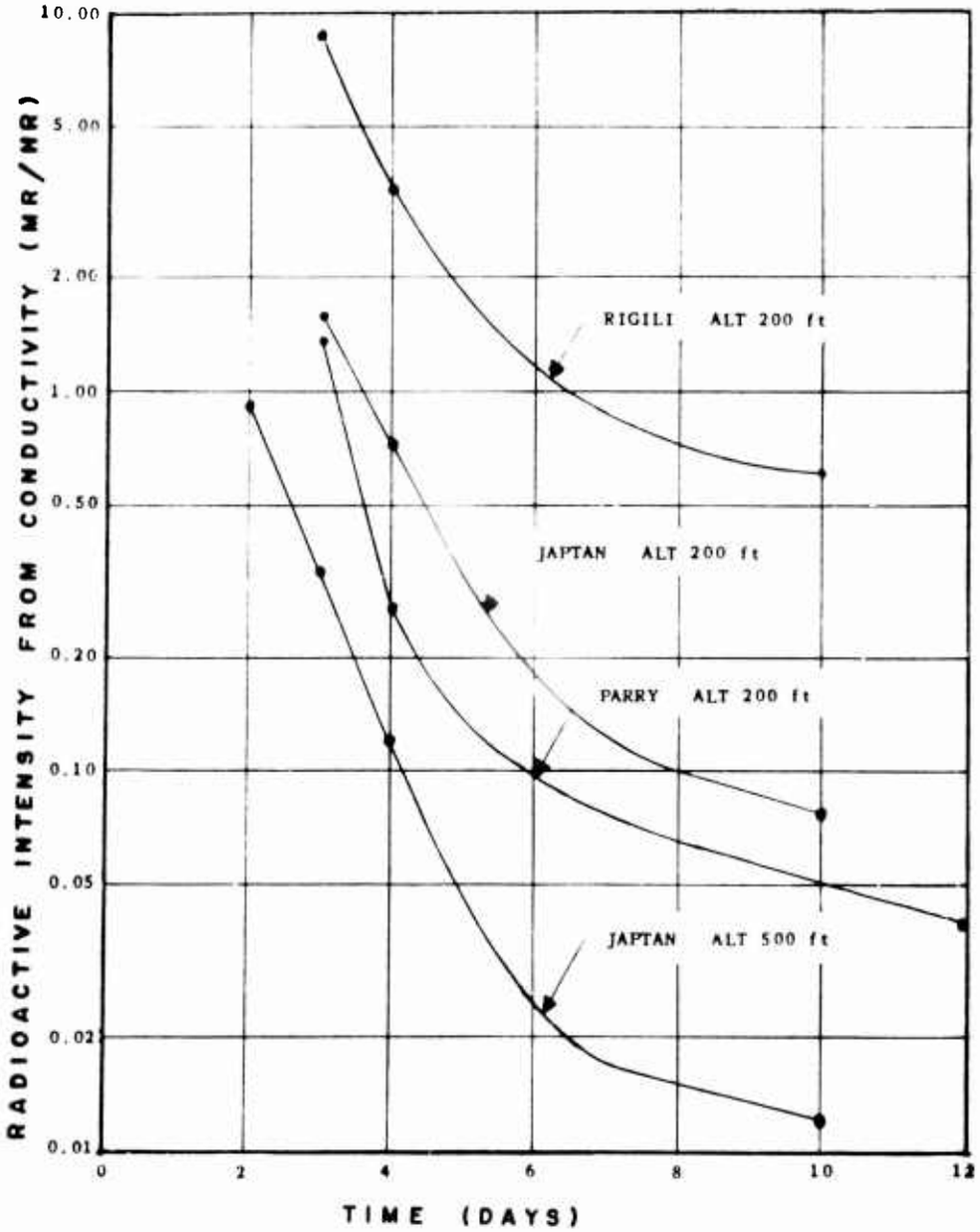

Fig. 3.31 Decline in Activity Due to Decay of Induced Radiation and Fall-out Material from Conductivity Measurements at Certain Fixed Altitudes over Shot and Adjacent Islands (Dog Shot)

[redacted]

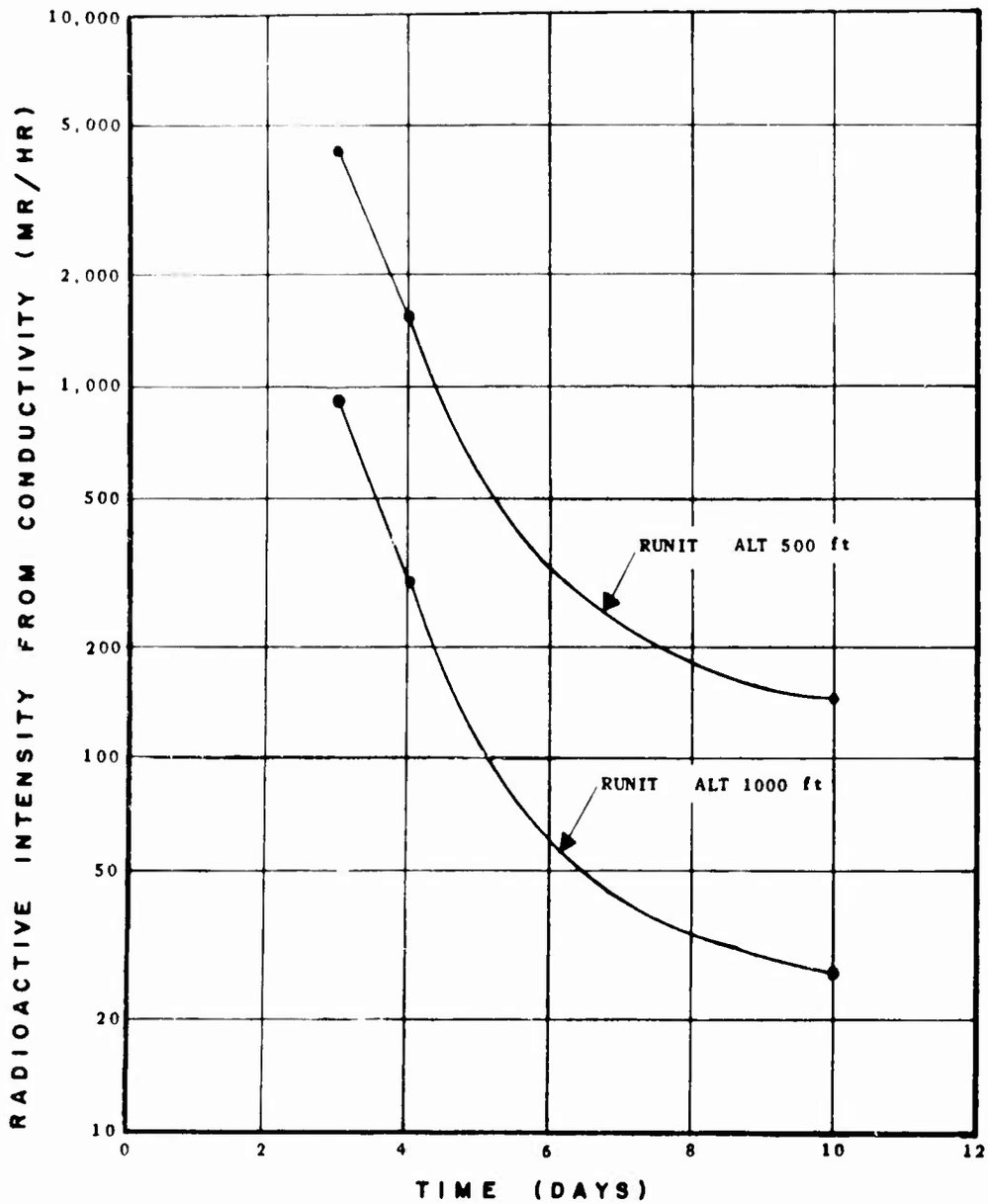

Fig. 3.32 Decline in Activity Due to Decay of Induced Radiation and Fall-out Material from Conductivity Measurements at Certain Fixed Altitudes over Shot and Adjacent Islands (Dog Shot)

[redacted]

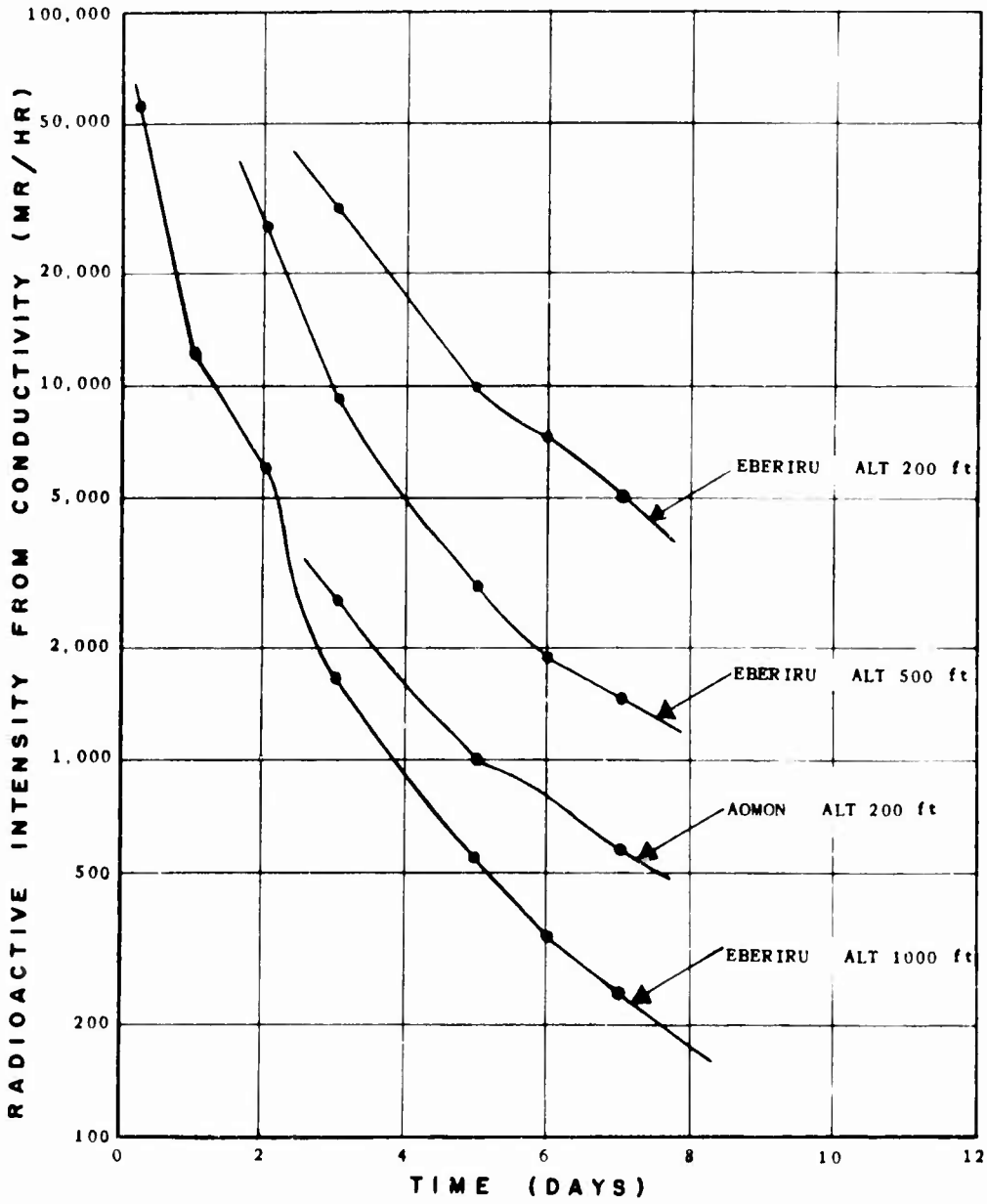

Fig. 3.33 Decline in Activity Due to Decay of Induced Radiation and Fall-out Material from Conductivity Measurements at Certain Fixed Altitudes over Shot and Adjacent Islands (George Shot)

[redacted]

[redacted]

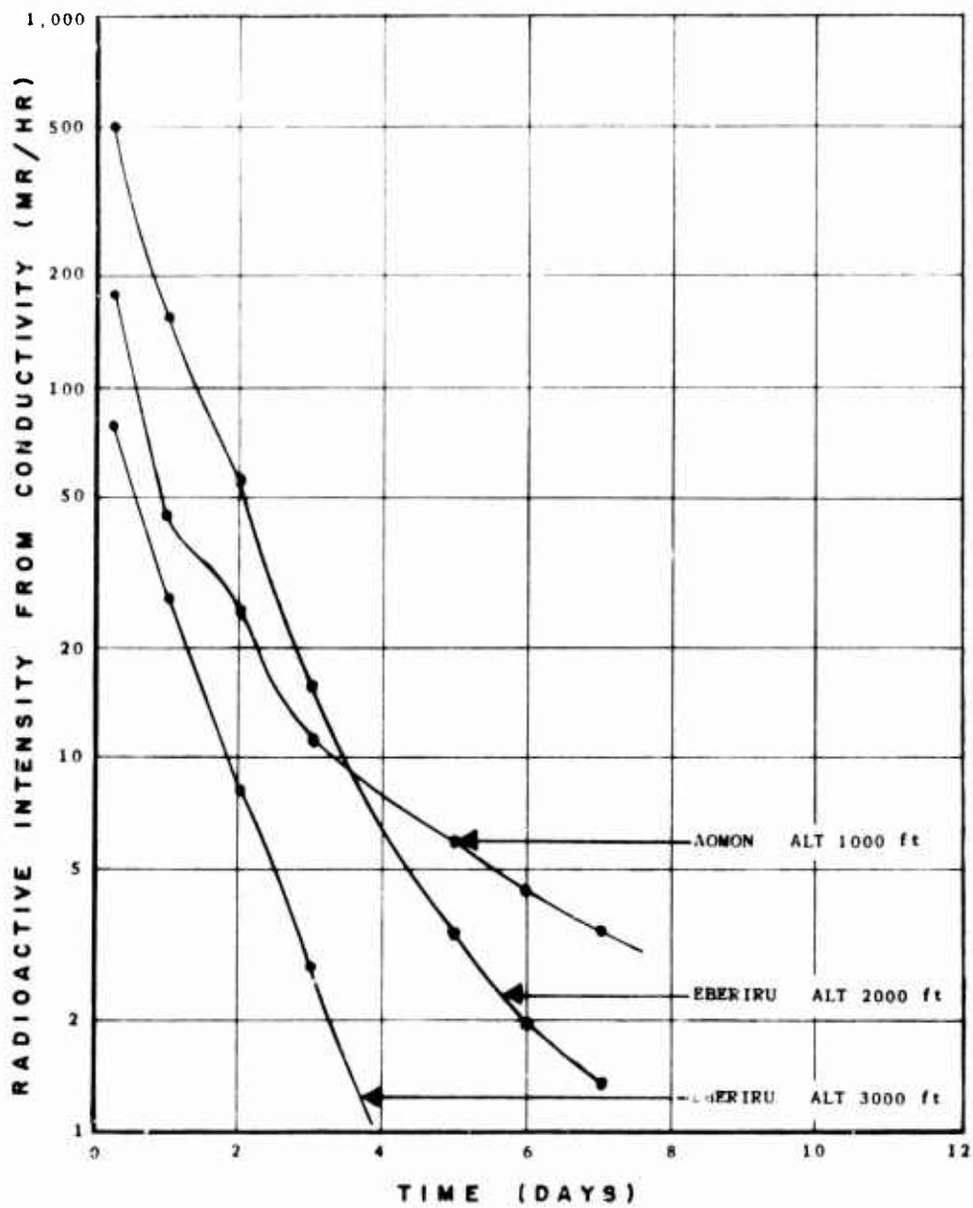

Fig. 3.34 Decline in Activity Due to Decay of Induced Radiation and Fall-out Material from Conductivity Measurements at Certain Fixed Altitudes over Shot and Adjacent Islands (George Shot)

[redacted]

[redacted]

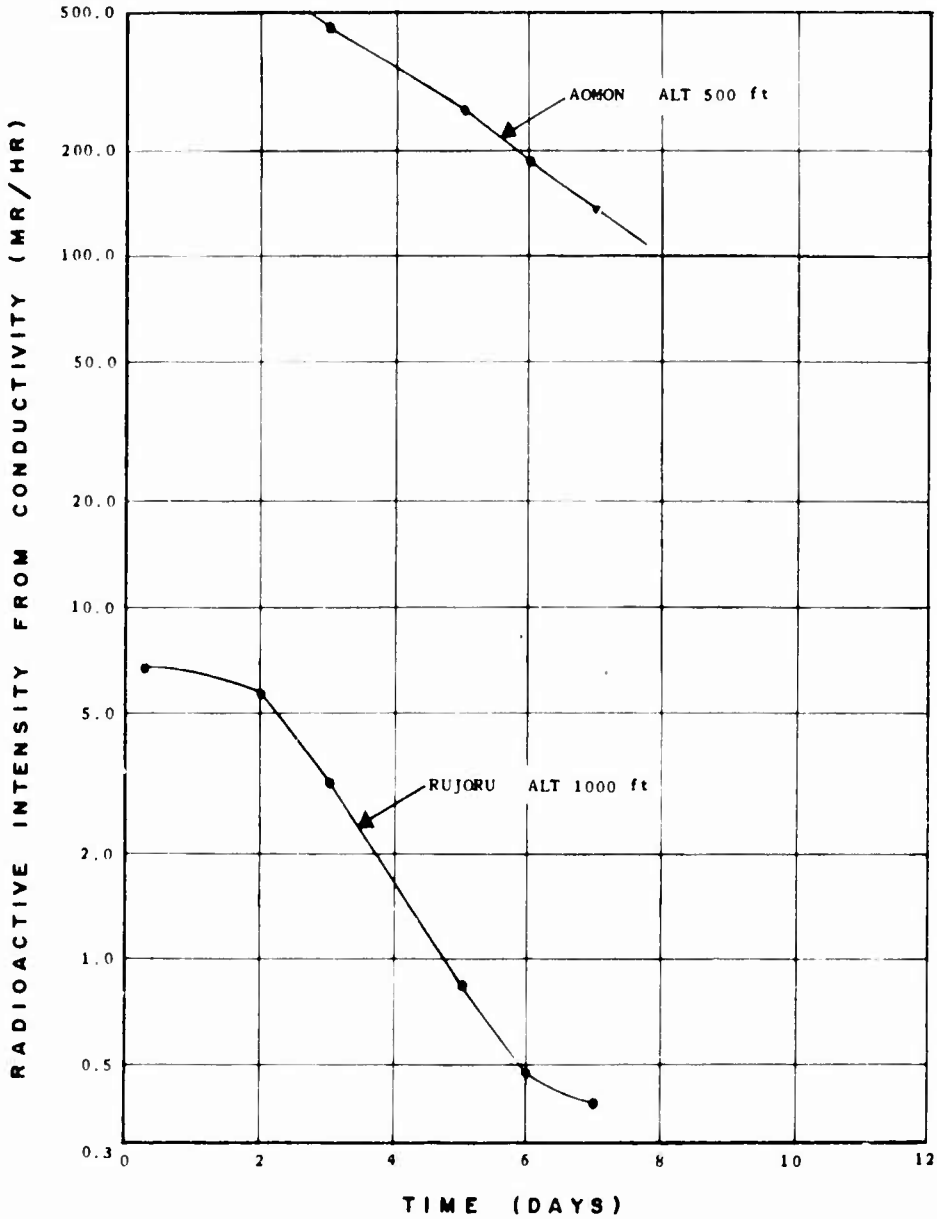

Fig. 3.35 Decline in Activity Due to Decay of Induced Radiation and Fall-out Material from Conductivity Measurements at Certain Fixed Altitudes over Shot and Adjacent Islands (George Shot)

[redacted]

[redacted]

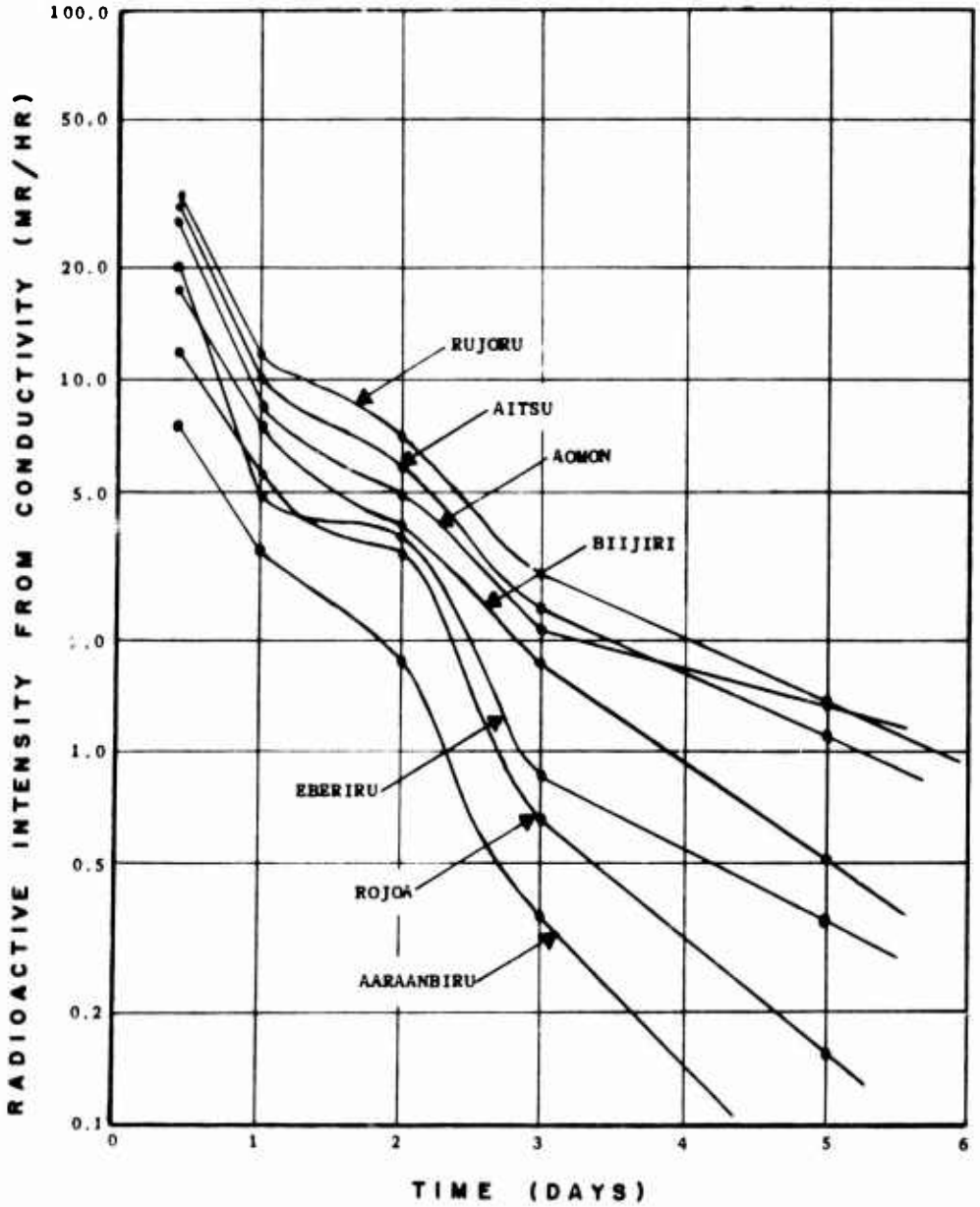

Fig. 3.36 Decline in Activity Due to Decay of Induced Radiation and Fall-out Material from Conductivity Measurements at Certain Fixed Altitudes over Shot and Adjacent Islands (Easy Shot, 500 Ft)

[redacted]

[redacted]

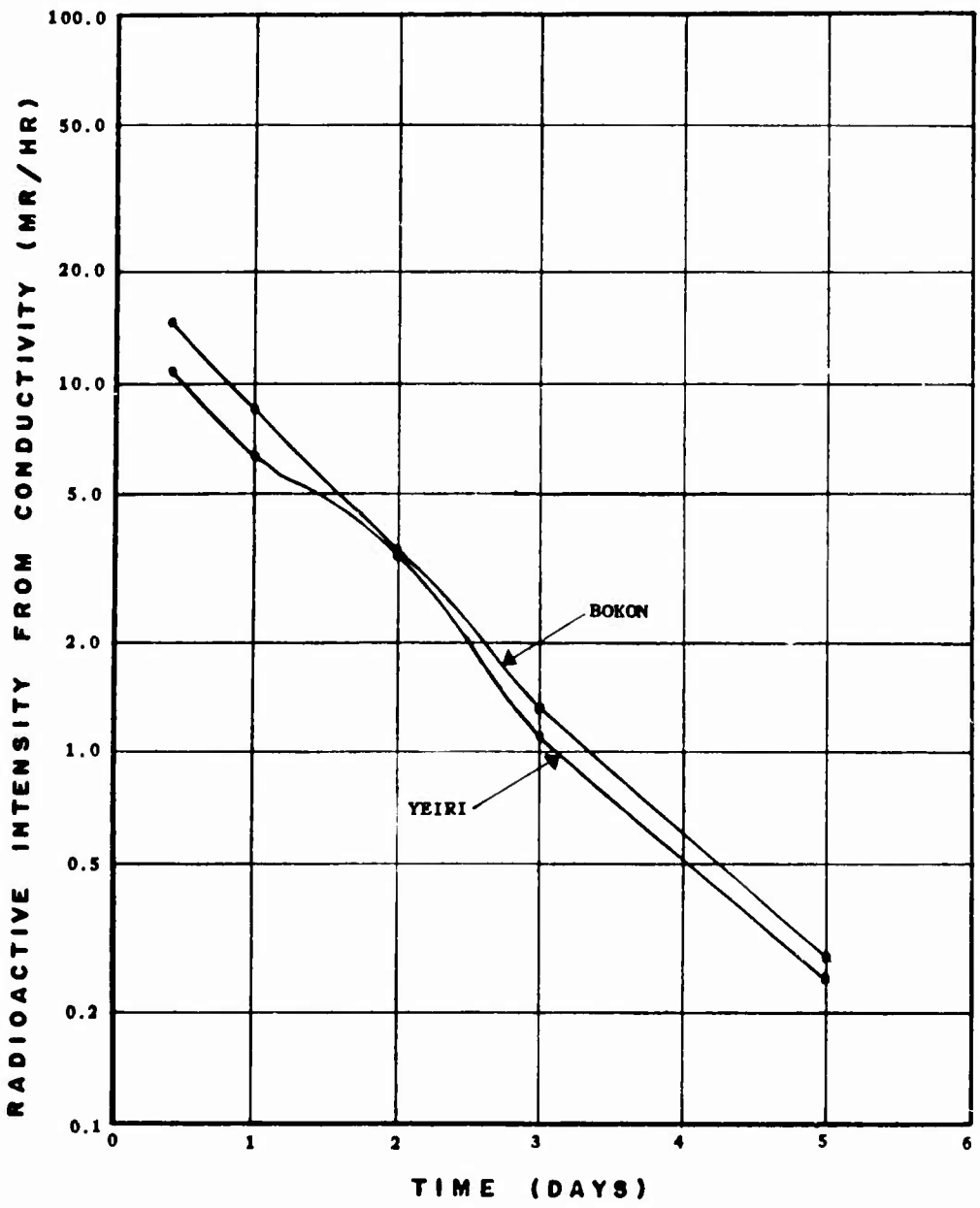

Fig. 3.37 Decline in Activity Due to Decay of Induced Radiation and Fall-out Material from Conductivity Measurements at Certain Fixed Altitudes over Shot and Adjacent Islands (Easy Shot, 500 Ft)

[redacted]

[redacted]

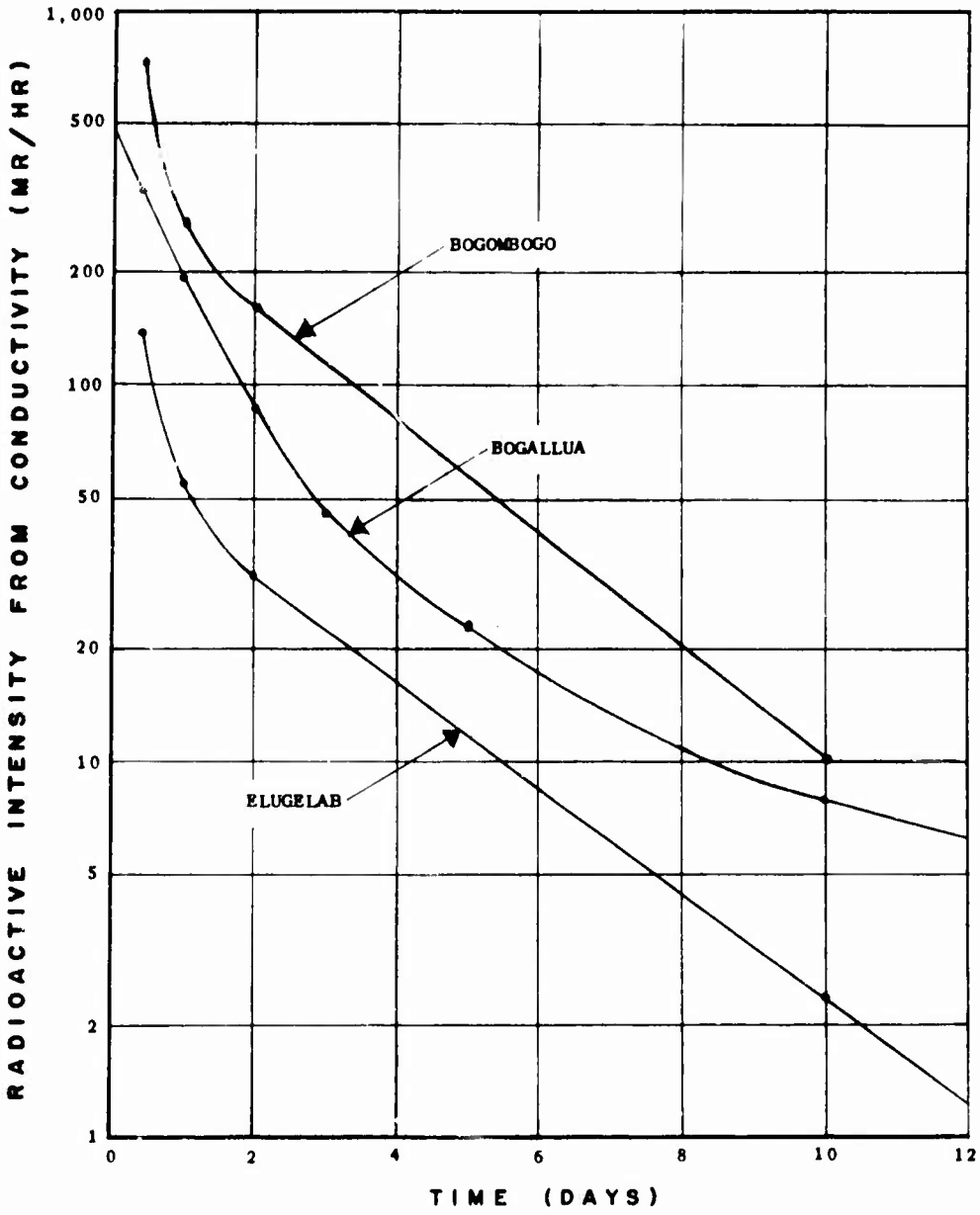

Fig. 3.38 Decline in Activity Due to Decay of Induced Radiation and Fall-out Material from Conductivity Measurements at Certain Fixed Altitudes over Shot and Adjacent Islands (Easy Shot, 500 Ft)

[redacted]

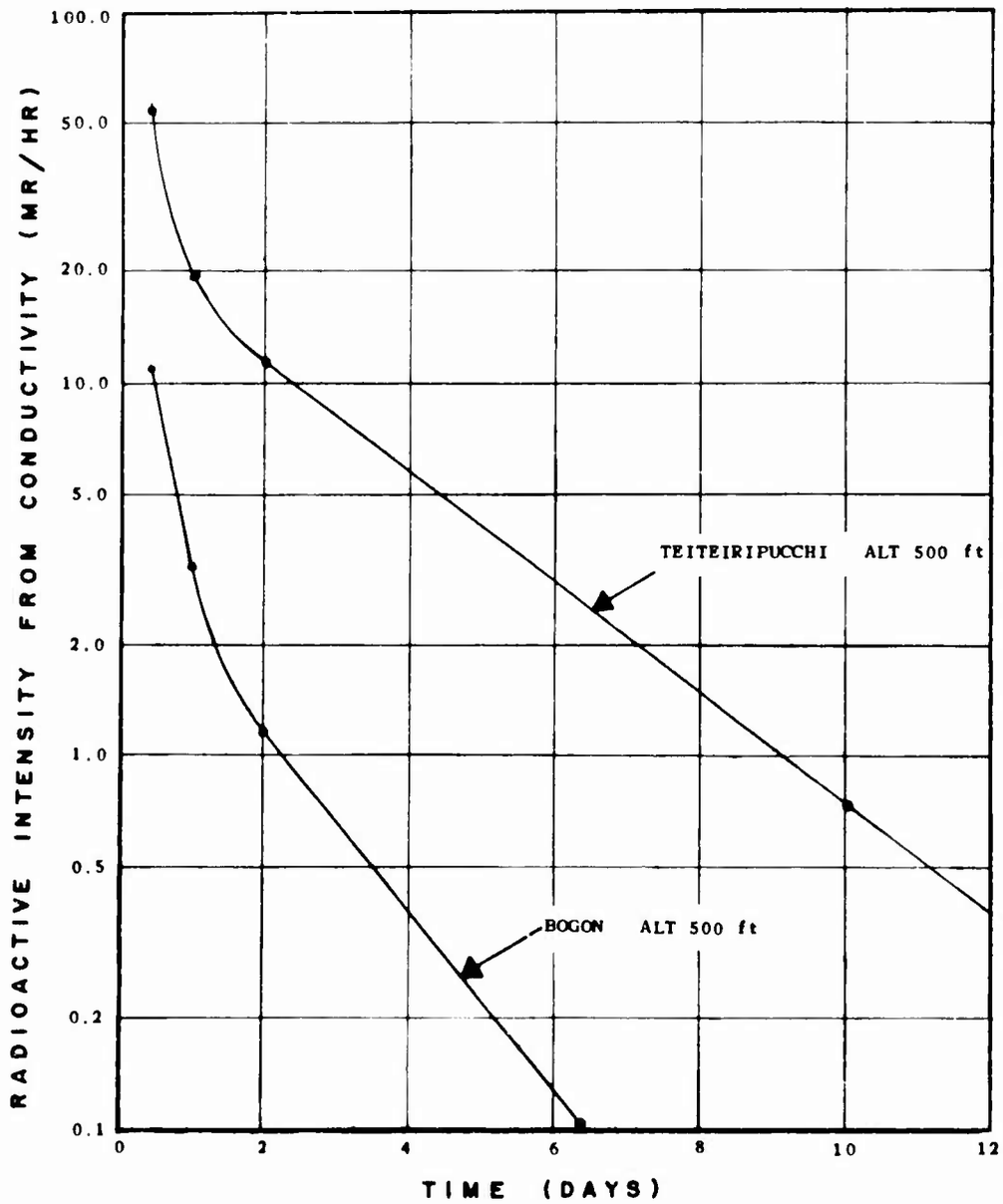

Fig. 3.39 Decline in Activity Due to Decay of Induced Radiation and Fall-out Material from Conductivity Measurements at Certain Fixed Altitudes over Shot and Adjacent Islands (Easy Shot)

[redacted]

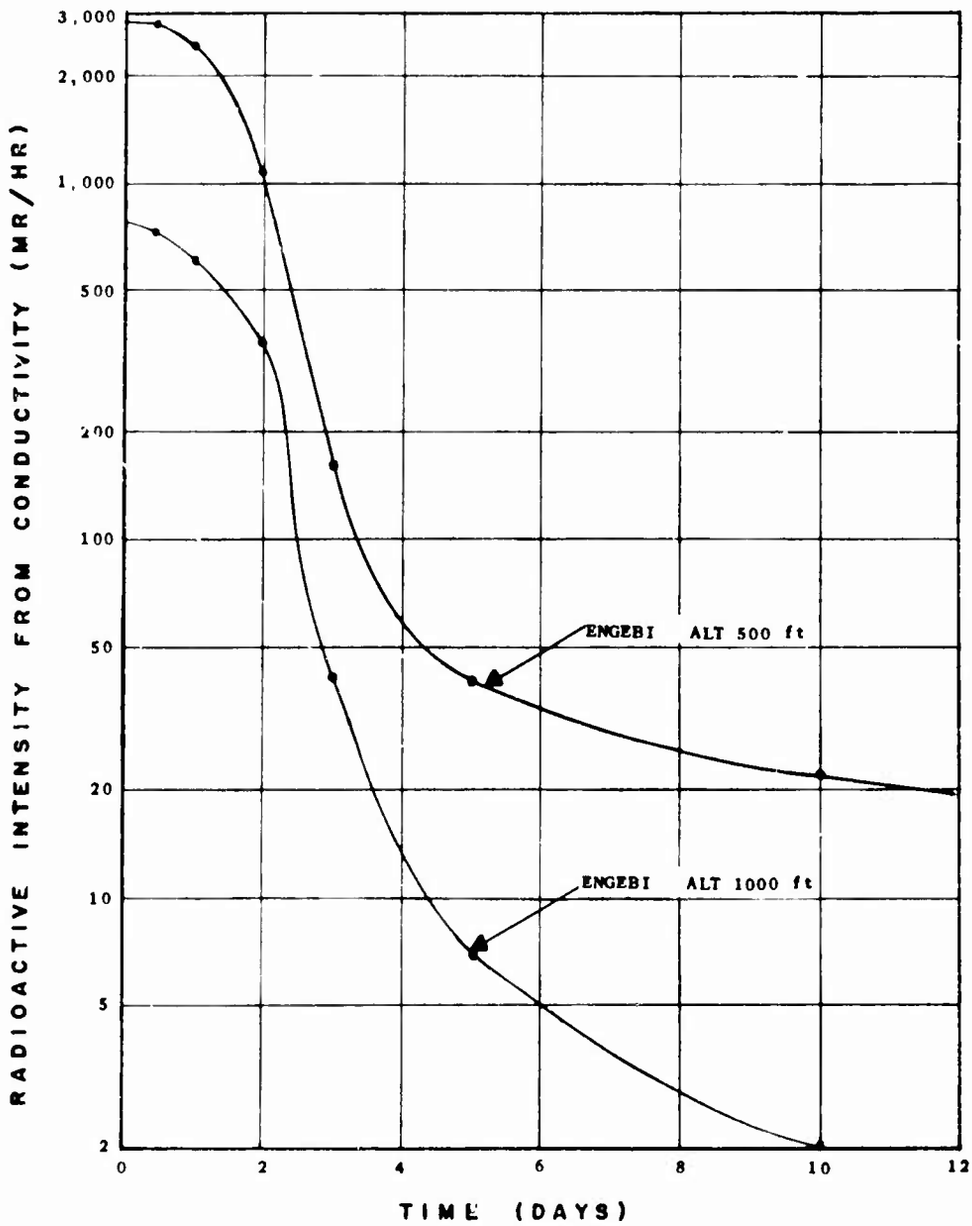

Fig. 3.40 Decline in Activity Due to Decay of Induced Radiation and Fall-out Material from Conductivity Measurements at Certain Fixed Altitudes over Shot and Adjacent Islands (Easy Shot)

UNCLASSIFIED

[redacted]

Inventoried: Date 9 Mar 79

By [illegible]

UNCLASSIFIED

[redacted]